STUDIES ON THE COMPOUND EYE OF THE COCKROACH *PERIPLANETA AMERICANA*

by

Richard Gordon Butler

Department of Neurobiology
Research School of Biological Sciences

A thesis submitted for the degree of
Doctor of Philosophy
in the Australian National University
1971

STATEMENT

I declare that all the results of the investigations which are reported in this thesis are my own original work. Comparisons and references to the work of others is duly acknowledged.

Richard Butler

Richard Butler

NOTE: Parts of CHAPTER III and CHAPTER V have been published prior to submission of this thesis (Butler, 1971a), and in accordance with University Regulations are included herein. A Golgi study on the optic lobes of Periplaneta americana is not sufficiently complete to include in the thesis, although the new method developed for the study has recently been published (Butler, 1971b).

ACKNOWLEDGEMENTS

It is a pleasure to thank my supervisor, Professor G.A. Horridge, for the opportunity to work in his laboratory, for his encouragement, and criticism and for conveying the notion of relevance as applied to scientific investigations.

I must also thank several others for help. Dr B. Walcott, Dr D. Sandeman and especially Mr A. Ioannides, kindly read and criticised various chapters of the thesis, and I have benefitted from many discussions and advice from them. Mr V.B. Meyer-Rochow kindly led me through the intricacies of the German language on many occasions. Mrs Caroline Giddings provided patient instruction on the use of the interference microscope and printed the final copies of the figures.

Finally, I must thank my wife Joyce, for her help and encouragement, for typing the drafts, and mostly for her patient tolerance of her status as a 'laboratory widow', especially during this last year.

The investigations were started at the Gatty Marine Laboratory, University of St Andrew's, Scotland. The bulk of the work was completed in the Department of Neurobiology of the Research School of Biological Sciences during the tenure of an Australian National University Research Scholarship.

TABLE OF CONTENTS

SUMMARY

1. The structure and function of the compound eyes of the cockroach, Periplaneta americana L. were studied using standard histological and electrophysiological techniques.
2. Four pairs of cells, each lying in the ventral, anterior, dorsal and posterior quadrants, form the eight retinular cells of each ommatidium. All cells contribute to the rhabdom. The spatial geometry within each ommatidium is fixed, predictable and consistent across the retina. The receptor pattern of the left eye is mirror-imaged in the right eye, about a dorsal-ventral axis. In serial sections, cells appear in a predictable sequence, and this provided a convenient way of numbering the cells (1 to 8).
3. A map of the interommatidial angles across the retina shows general trends, with vertical angles decreasing and horizontal angles increasing, from the anterior to posterior direction. There is extensive overlapping in the anterior, dorsal and posterior composite fields of view.
4. The fine structure of the retina reveals that Periplaneta has a typical fused-rhabdomere, apposition compound eye of the eucone variety.

The eye of the first instar is very similar to the adult. Generally, the rhabdomeric lamellae tend to be orthogonal in adjacent pairs of cells.

5. A significant difference occurs between light- and dark-adapted eyes. In the dark, cisternae of the endoplasmic reticulum develop, congregating adjacent to the rhabdom, forming the palisade.

6. The intracellularly recorded depolarizing responses from the retinula cells are similar to those found in other arthropods, with (initial) transient and (later) plateau phases. The magnitude of the response is graded with respect to stimulus intensity.

7. Measurements from receptor responses show that Periplaneta's photoreceptor membrane fits the theoretical electrical analogue model reasonably well.

8. Angular sensitivity (angles of acceptance) and hence acuity, changes upon light/dark adaptation. The angles of acceptance are: 2.4° ± 0.9° (horizontal plane) and 2.3° ± 0.6° (vertical plane) for the light-adapted state; and 6.7° ± 1.8° (horizontal) and 6.0° ± 1.3° (vertical) for the dark-adapted state. The palisade is the only anatomical change found which could account for this difference.

9. There is a large spread in absolute sensitivity among light- and dark-adapted cells. Generally the DA group is about one log unit more sensitive than the LA group for the same stimulus intensity.
10. Retinula cells are highly sensitive to polarized light, with a maximum: minimum response ratio of 5:1. Two groups exist with PL maxima 90° apart. These peaks occur when the e-vector is parallel to the two sets of orthogonal lamellae of the rhabdom.
11. Two spectral types of cells exist, one sensitive to ultra-violet (UV) light and the other to green light. They both occur in the same ommatidium, in the ratio 3 UV : 5 green. The position of each type is also fixed within each ommatidium, with cells 1, 5, 7 (both ventral cells and the posterior-dorsal cell) being the UV group, and cells, 2, 3, 4, 6, 8 constituting the green group.
12. Inter-retinal transfer of light/dark adaptation effects does not exist.
13. The degree to which the palisade forms in the dark-adapted state is related to the amount of rhabdomere immediately adjacent. This also applies to the rate at which the palisade forms. It is suggested that the formation of the palisade depends on the state of the

rhabdomere as related to its resting potential.

14. The rhabdomeres are not of uniform diameter over their entire length, but constrict and bulge over their retinal depth.

CHAPTER I: INTRODUCTION

Much of the work which has been done on compound eyes has been involved with the four theories of insect vision. The oldest of these is the Müller and Exner mosaic theory for apposition and superposition eyes (which is now being questioned) (Exner, 1891). The other major one, the diffraction image theory (Burtt and Catton, 1962; Rogers, 1962) was formulated to explain unexpectedly high acuity levels in the compound eye which cannot be accounted for by the mosaic theory. The remaining two theories are attempts to explain visual processing through patterns of neural organization and are (1) lateral inhibition (for Limulus) and (2) cybernetic theories (eg. McCann and MacGinitie, 1965).

One of the more serious objections raised against the mosaic theory was the fact that the field of sensitivity of a single apposition eye ommatidium was found to be larger than the interommatidial angle (eg. Burtt and Catton, 1954). These results appeared almost at the same time as microelectrodes and intracellular recording techniques and stimulated studies on the angular sensitivity of individual receptor cells. These measurements have been shown to directly reflect

the acuity of individual receptors, and hence the whole eye (Horridge, 1968).

The flying insects which rely heavily on vision (flies, bees, locusts, dragonflies) have, understandably, received the most attention, not only for angular sensitivity, but also for spectral sensitivity.

Studies of the effect of light- and dark-adaptation on angular sensitivity (and absolute sensitivity) had only been done on one insect (locust, Tunstall and Horridge, 1967) when the work reported in this thesis was started. Most other angle studies have been done only on dark-adapted cells, to benefit from increased sensitivity. The anatomical basis for a functional difference as related to state of adaptation in locust (ie. the palisade) had been established two years previously, with the physiological results correctly predicted (Horridge and Barnard, 1965). Since then, a complete anatomical and physiological study of angular and absolute sensitivity changes in the predacious water bug Lethocerus upon light/dark adaptation has appeared (Walcott, 1971a, b). The interesting result here is that in both cases, angular and absolute sensitivity increase by about three-fold, but each achieves the result through an entirely different mechanism (a palisade in the locust; cell movement in Lethocerus). There has been no work at the single cell level on angular

sensitivities (or any other aspect of retinal physiology) and related anatomical changes on any insect with an almost completely terrestrial mode of life. Studies on an insect of this nature was the next obvious step in the series of investigations which will hopefully lead to the ability to predict the receptor physiology from a knowledge of the retinal anatomy.

The availability and universality of the common cockroach, Periplaneta americana L. made it a most suitable preparation for such a study. For the purposes of this thesis, as complete a study as possible was made on the retina of the one species. The results are presented in CHAPTERS III, IV and V, and concern the anatomy, electrophysiology and identification of spectral cell types within the retina.

Such studies on Periplaneta were desirable from another standpoint. It is regarded as being a very ancient form of insect, apparently little changed since the Carboniferous (Borradaile, 1958; Guthrie and Tindall, 1968). While the dragonfly is also regarded as being just as ancient, it is a flying form and would present an additional opportunity for comparisons.

A review of the literature on the compound eye of Periplaneta revealed an amazing lack of work for such a common insect. Only six papers on retinal

anatomy (all of which are wrong in one aspect or another), and three on ERG's relevant to this work, were found. During the course of the work, two papers on intracellular recordings from Periplaneta retinula cells have appeared. As a result, I decided to incorporate the relevant literature review in the appropriate chapters.

In addition to specific studies on invertebrate vision per se, the compound eye can be a most useful vehicle for the elucidation of more general problems, and this is invariably due to: (1) the photoreceptor units being relatively large and easy to record from and (2) the anatomy of the visual system being relatively simple with the sets and sub-sets of receptors often extensively and predictably repeated across the retina.

CHAPTER II: MATERIALS AND METHODS

A. Animals

Adult males and females of Periplaneta americana L. were used. A large culture was kept in a constant temperature room (24.5°C) and artificially illuminated by a fixed light cycle (12 h dark/12 h light).

A few first instar larvae were used for anatomical investigations. First instars were obtained by removing oothecae from the main culture and allowing them to hatch. Animals which were not used on the day of hatching were checked by the methods of Gier (1947) to ensure that they had not moulted.

B. Anatomical Methods

1. Light Microscopy

(i) Wax Embedded Tissue

Adults were selected while their cuticle was still soft after the final moult. The retina and optic lobes in isolated heads were fixed in situ in either Carnoy's (Davenport, 1970) or Duboscq-Brasil fixative (Pantin, 1946). Fixation was facilitated by removing the posterior cuticle, cephalic musculature and jaws before fixation. Fixation (2 h), dehydration in graded alcohols, and embedding in either paraffin or ester wax was completed within 12 h.

Frontal, coronal and sagittal serial sections were made through oriented heads of adults and first instars, using a Leitz rotary microtome. Several series of each were made at thicknesses of 5, 10, 15 and 20 μm. A few series were stained with Hansen's iron trioxyhaematin and Mallory's triple stain (Pantin, 1946), and the remainder with Holmes' reduced silver stain (Blest, 1961).

(ii) Epoxy Resin Embedded Tissue

Retinae and optic lobes of both adults and first instars were fixed and embedded as for electron microscopy (see section B2). Random and serial sections (transverse and longitudinal to the ommatidia) of 1 μm thickness were cut on either a Porter-Blum MT 1 or a Cambridge Huxley ultramicrotome. Sections of this thickness give good resolution with minimal confusion when viewed with a light microscope.

Sections, cut transverse to the ommatidia, were mounted serially, using an eyelash, on drops of water on slides (Horridge and Meinertzhagen, 1970a). After drying on a 50°C hot plate, they were stained (on the hot plate) with 1 per cent aqueous toluidine blue in a borax/boric acid buffer (pH about 10) (Trump et al., 1961).

Sections which stained poorly could have their contrast increased by etching with NaOH in ethanol (at room temperature) and then restaining (Berkowitz et al., 1968). The sections were then mounted in

Permount under glass coverslips.

2. Electron Microscopy

The compound eyes of adults were excised from isolated heads by cutting well below the basement membrane and further subdivided by cutting longitudinally with respect to the ommatidia. The heads of first instars were fixed whole. Where optic lobes were involved, heads were cut by frontal sections behind the eyes, the cephalic musculature dissected out and the lobes and retina fixed *in situ*.

Many fixatives, often with several variations of each, were tried, with mediocre results in most cases. Finally, standard use was made of three variations which are described below. All electron micrographs presented are from tissue fixed in one of these three ways.

The first involved buffered acrolein fixative (Luft, 1959). Primary fixation with acrolein (acryl aldehyde) in Millonig's (1961) phosphate buffer at

pH 7.4 and 4°C was followed by several washings in buffer. Secondary fixation was in one per cent OsO_4 in the same buffer at 4°C. In each case, the times involved were 1 - 2 h. An alternative method was the buffered gluteraldehyde fixative (Sabatini et al., 1963). Tissue was fixed in five per cent gluteraldehyde in phosphate buffer (pH 7.4) for 2 h at 4°C. After washing for 0.5 h in buffer, post-fixation was in phosphate buffered one per cent OsO_4 for 2 h at 4°C. Finally, the method used by Perrelet (1970) on drone bee retina was adopted. Tissue was fixed for 4 h at room temperature in four per cent gluteraldehyde in 0.1 M phosphate buffer (pH 7.4) (Sabatini et al., 1963). After a brief rinse in this buffer, post-fixation was for 1.5 h in two per cent OsO_4 in Millonig's (1961) phosphate buffer (pH 7.4), again at room temperature.

For all cases, dehydrations were in either graded acetones or alcohols and embeddings in Araldite, Epikote-812 (Epon) or a mixture of the two. After curing, the blocks were mounted in known orientation on stubs with hard sealing wax and thin sections (silver to gold in colour) were cut on either a Reichert Om U2 or Cambridge Huxley ultramicrotome. Sections were picked up on 100 and 200 mesh copper grids and on formvar coated slot grids, and stained with lead citrate (Reynolds, 1963) and uranyl acetate (three per cent in seventy per cent ethanol). Specimens were examined in an Hitachi HU 11E electron microscope at 75 kV.

C. Selective Adaptations

Live animals were fixed in normal posture to glass slides using insect wax (1 part beeswax : 2 parts violin rosin). Heads were fixed securely, but rotated about the anterior-posterior axis such that either the dorsal or the ventral half of the compound eye was pointing directly laterally. Left and right eyes were used. The eye not to be illuminated was covered with insect wax, and then painted with opaque paint to exclude light. Animals were placed in the experimental box (Fig. 1a, b) and then dark adapted for 2.5 h. The box was designed so that the animal and slide were secured firmly. Lateral to the eye, and close to it (1 cm) was a hole in the box over which was fitted an appropriate interference filter (Balzers). The box was light-tight except for those wavelengths admitted by the filter (Fig. 1c).

A single-peaked UV receptor type with λ_{max} at 365 nm and a single peaked green receptor type with λ_{max} at 507 nm occur in cockroach (Mote and Goldsmith, 1970). Filters were chosen to adapt each type of receptor selectively such that the relative sensitivity of the other type was at least one log unit less sensitive than that for the type of receptor under investigation. To adapt the UV receptors, a filter with peak transmission at 311 nm (lowest λ available) was used. Although the UV receptor would be less sensitive at 311 nm than at

365 nm (its λ_{max}), it would be more sensitive to UV in comparison to the green receptor at 311 nm than it would be at 365 nm. Similarly, the green receptor was selectively adapted with a 536 nm filter.

After dark-adaptation, the box was placed with the eye and filter in direct line with the sun. Exposure times were 3 min in all cases. When the time elapsed, the box was opened in the dark and the whole animal dropped into boiling water for 40 s to stop all cellular activity including pigment migration. Histological preparation followed. Tissue was treated as for electron microscopy.

In a second series of experiments on fully dark-adapted animals the same procedure was followed, omitting selective adaptation. In a final series, the eye was adapted with sunlight through a 1.5 neutral density filter (Kodak Wratten) for 2.5 min.

The time course for each experiment was determined after initial trial runs. Five animals were used in each experiment. All experiments were done at midday ± 0.5 h.

After histological treatment, serial 1 µm transverse sections which give adequate resolution were mounted in order and stained with one per cent toluidine blue. Every fifth section was photographed and used to reconstruct the geometry of ommatidia. Selected areas were photographed at high power for measurements. Twenty-five ommatidia selected from

two to five animals were used in each case. Only those ommatidia from each which were judged to have their central axes most perpendicular to the filter (and hence sun) were considered.

D. Electrophysiological Methods

1. Apparatus

(i) Mechanical Equipment

The apparatus used for the experiments is shown in Fig. 2. The microelectrodes were driven vertically using a Zeiss Jena micromanipulator. The eye preparation sat on a Perspex platform which in turn was supported by a rigid bracket bolted to the manipulator bed to minimize vibrations between electrode and preparation. The preamplifier was also carried on the manipulator, to keep the length of the input lead as short as possible.

The system for illuminating the eye was carried on a modified theodolite. Coarse and fine controls for movements through the vertical and horizontal planes permitted the lamp to move through 90° in each plane with an accuracy of 0.25 - 0.5°. The eye preparation was at the centre of the sphere determined by the vertical and horizontal movements. The manipulator and theodolite were bolted to steel plates and sat on a concrete steady bench.

The light source was a pinhole (0.8 mm) located

10 cm from the eye and subtended an angle of about 0.5° at the eye. Illumination was provided by a 15 watt plane filament, end-viewing tungsten bulb (Zeiss microscope bulb) run from a 6 volt transformer. 100 cycle intensity ripple was ignored as no physiological evidence for effect was found with either stimulus durations (1 s flashes or 50 ms trains). By using a small aperture, the stimulus was effectively a point source.

Daily and seasonal fluctuations in mains voltage were controlled by running the lamp voltage supply from a 240 V constant voltage transformer. This helped maintain operation at a constant colour temperature (constant lamp current) and helped pervent undesirable variations in intensity.

A lens system was not used to direct the stimulus to the eye. The use of such a system would have involved centering the facet of the ommatidium in question at the focus of the stimulus sphere, which was not feasible. A shutter, actuated by an electromagnetic relay interrupted the light path between the aperture and the preparation. The shutter relay was controlled by a simple switching transistor circuit and the transistor base was fed single (1 s duration) or trains (50 ms duration, 10 s interval) of pulses from a series of Tektronix 161 and 162 stimulators. The rise time of the stimulus flash was about 2 ms and the decay time

about 7 ms, as determined by a fast (500 μs) rise time photocell.

To control the light flashes for experimental purposes, the beam was interrupted between the shutter and preparation by two filter wheels. One contained 11 Kodak neutral density (ND) filters (3.5, 3.0, 2.5, 2.0, 1.5, 1.0, 0.8, 0.6, 0.4, 0.2, 0.1) and a blank (ND = 0). The other was a 36 position wheel holding a UV-transmitting polaroid filter. The polaroid was interrupted by three supporting bars on the wheel and one section was removed to permit unpolarized light to pass. This arrangement easily permitted an ND series to be recorded for each cell after an angle of acceptance or polarized light sensitivity was measured.

The stimulating lamp was never set greater than 25° from the horizontal as distortions in horizontal angular measures are more than 10 per cent for greater angles.

(ii) Calibrations

The ND filters were the Kodak Wratten type and similar to those previously used by Shaw (1968a). He checked their transmission and found attenuation flat in the visible region of the spectrum, but rising in the ultraviolet (UV) and falling in the far red.

Light emitted by the tungsten bulb was polarized, and is shown in Fig. 3a. This record was obtained by rotating the polaroid in the light beam and recording

the responses of a flat faced photocell. As suggested by Shaw (1968a), a stack of 6 - 8 coverslips was fixed at an angle in the beam and rotated until the polarization was minimal (Fig. 3b) for several axially rotated positions of the photocell.

It was also desirable to know the energy emission of the lamp. This was measured using an ISCO spectro-radiometer with 6 ft probe at a distance of 11.5 cm from the centre-line of the probe to filament. Readings in $\mu W/cm^2/nm$ were made from 425 - 750 nm in 25 nm increments. Fig. 3c shows the results of this calibration after application of appropriate correction factors. The tungsten source emitted little energy in the violet - UV region, but increased linearly up to the far red.

The two types of receptors in Periplaneta americana have already been mentioned. This calibration was important in that most of the electrophysiological results must be attributed to the green receptors (λmax at 507 nm), as the energy output at the λmax for the UV receptors (365 nm) is negligible. Shaw (1968a) noted that the energy emission curve for a very similar lamp resembled that of a black body at 2200°K (Moon, 1948). This was confirmed for this lamp and a colour temperature of 2200°K assumed.

2. The Eye Preparation

All experiments were performed at room temperature (18 - 25°C) on isolated head preparations. There has been no evidence to suggest that intracellular recordings from eye slices are different from intact animals; in fact, evidence exists that responses are the same (Scholes, 1965a, on locust; Shaw, 1968a, on fly, cf. Burkhardt and Autrum, 1960, on fly). Elimination of respiratory and some cephalic muscle activity facilitated intracellular recording with fine glass microelectrodes by limiting retinal tissue displacements.

After decapitation, the antennae were removed to prevent interference with the light beam and electrodes. Then the jaws and a small corneal cap were sliced off with a razor blade. The planes of these cuts are shown in Fig. 4a. The rest of the head remained intact, thus maintaining physical support for the retina, an intact tracheal system to retard tissue anoxia, as full a compliment of normal physiological fluids as possible and relatively undisturbed neural relations. The handling and positioning of whole heads was easier than if isolated eyes were used. The head stood alone, without additional support, in appropriate orientation on filter paper soaked with saline on a platform provided for the purpose. The filter

paper covered a silver wire which led to the backing-off circuit and 10 mV calibration, and acted as the indifferent electrode. Impalements were made through the open corneal slice and the electrode in position is shown in Fig. 4b.

The exposed retina and filter paper were kept moist with cockroach saline: 210.2 mM NaCl, 3.1 mM KCl, 1.8 mM $CaCl_2$, 0.2 mM NaH_2PO_4, 1.8 mM Na_2HPO_3, pH 7.2 (Hamasaki and Narahashi, 1959).

3. Electrodes and Recording Equipment

Glass microelectrodes (used in all experiments) were made from hard glass (working point about 1000°C) capillary tubing (OD 1.15 mm), supplied by Owens-Illinois (Toledo, Ohio, U.S.A.).

Initially, electrodes were pulled on a home-built, vertical puller (gravity powered), filled with methanol under reduced pressure, transferred to distilled water and later to electrolyte, and were usable after 2 - 3 days. Little success was achieved with these electrodes.

The electrodes used in successful experiments were pulled on a commercially available two stage vertical micropipette puller (David Kopf Instruments, Model 700 C, Tujunga, Calif., U.S.A.), and filled directly with electrolyte using a modification of the fibre method of Tasaki et al., (1968). Prior to

pulling electrodes, pieces from the same batch of glass from which electrodes would be made were heated in a gas flame and rapidly pulled apart, producing thin fibres. These were broken into appropriate lengths and two or three inserted into the bore of the tubing to be pulled. Electrodes, pulled in the normal fashion, had their tips examined at 400x in a light microscope. A rough estimate of tip resistance could be judged by the fuzziness of the tip, as a well defined tip indicated very low resistance and a tip which extended beyond the limit of resolution indicated (usually) a useable electrode (Tomita, 1969). Electrolyte was injected into the electrode using a syringe and 2.5 inch 30G hypodermic needle. Electrodes were ready for use immediately.

Apparently, as the glass is pulled, the tubing and fibre melt but the fibre does not block the electrode tip. It recedes slightly from the tip and conducts electrolyte by capillary action from the shaft, through the shank to the tip. Electrolyte moves well under injection pressure in the relatively broad shaft and by capillary action in the very narrow tip region. Neither work well in the shank. Often the electrode will not fill properly if only one fibre is used. It requires at least two or three fibres to narrow the gap between shank walls to permit sufficient capillary action to pass electrolyte. Electrodes filled in this way have about one-half the

resistance of electrodes filled by the substitution method (Tasaki et al., 1968). Sustained impalements of Periplaneta retinula cells were easier when electrodes of 100 - 150 MΩ resistance (tested in situ: see Fig. 5B), filled by the fibre technique, were used. The assumption here is that the tips were very small (0.1 μm or less).

The electrolyte used was 3.0 M KCl. 4.0 M CH_3COOK and 0.6 M K_2SO_4 (saturated soln.) electrodes were tried, but no improvements over the KCl electrodes were obvious.

Transmembrane voltage changes were recorded with the microelectrode inside a retinula cell and the indifferent electrode outside (the rest of the head was effectively the indifferent electrode). Fig. 5A shows the recording arrangements. A Tektronix 502A oscilloscope was triggered by the shutter of a Nihon Kohden oscilloscope camera. The time base output was inverted and fed to the input of a Tektronix 161 pulse generator as a negative sawtooth. The delay and duration times of the simgle output square pulse were appropriately set to control the shutter of the light stimulus (1 s). Long pulses could be generated by setting the CRO to very slow sweep speeds and by using external capacitors (approx. 1 μF = 1 s) in the duration circuit. Trains of pulses (50 ms duration, 10 s interval) were generated by the Tektronix 162 waveform generator and a second pulse generator.

The backing-off circuit inserted a standing voltage of either polarity between ground and the preparation (indifferent electrode) to neutralize unwanted voltages (e.g. tip potentials). A 10 mV calibration pulse could be manually inserted on top of the neutralization voltage for calibration purposes. The recording electrode was connected to a high impedance preamplifier with a very short input lead, and this in turn was fed to the oscilloscopes (recording and slave) and recorded on a DC mode.

Fig. 5B gives the circuit diagram for the preamplifier. It was based on a battery operated solid state FET operational amplifier (Philbrick/ Nexus Model 1009) and marked a change from the conventional valve cathode followers used in this laboratory (Scholes, 1965a; Shaw, 1968a). It had an input impedance of 10^{11} Ω and a close loop gain of 10. The input featured capacity compensation as well as a circuit for checking electrode resistance in situ. Frequency response was tested with an oscillator and simulated electrode (100 MΩ resistor) and was flat up to 850 Hz, dropping slowly above that. This was adequate for the slow DC nature of receptor potentials, although the relatively rapid rise time may have been affected. Response could be improved with the capacity compensation available, but this advantage was offset by increased noise level due to the positive feedback in the compensation (a considerable problem with 100^{+} MΩ electrodes).

Figure 1

The apparatus for selective adaptation experiments.

a and b. This pair of photographs show the box used for selectively adapting retinula cells to either 536 or 311 nm light. In (a), the 311 nm filter is attached to the outside of the box (sprayed flat black, inside and out) and the box is sealed. In (b), the box has been opened and the cockroach, fixed to the glass slide, is set in place with its left eye in juxtaposition with the hole over which the filter is secured.

The curves in (c) are the percentage transmittance curves for the two filters used. They were determined with a UNICAM SP 800 recording spectrophotometer and traced directly from the data sheets. Note that the abscissae scales are different so that the spread of each curve is about the same.

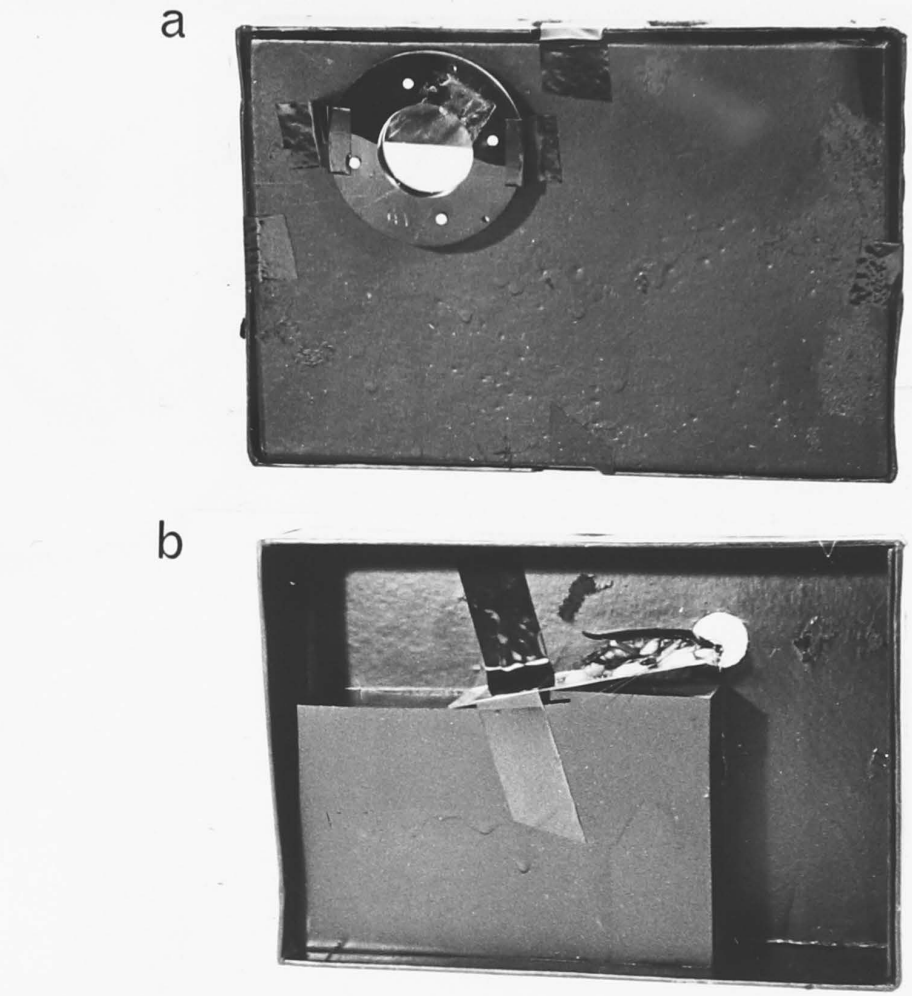
a
b
c
100
10
1
transmittance
536
311
600
500
350
300
λ (nm)

Figure 2

A photograph of the apparatus used to make the electrophysiological recordings.

The bed of the micromanipulator (M) holds a bracket with the preparation platform (P). The preamplifier (PA) and electrode (held in a jig (J)) are both attached to the vertical advance. The output of the preamplifier is fed to recording and slave oscilloscopes (CRO). The modified theodolite with vertical (V) and horizontal (H) traverse controls can move the lamp (L) assembly with shutter (S) and filter wheels (F) with an accuracy of 0.25 - 0.5°.

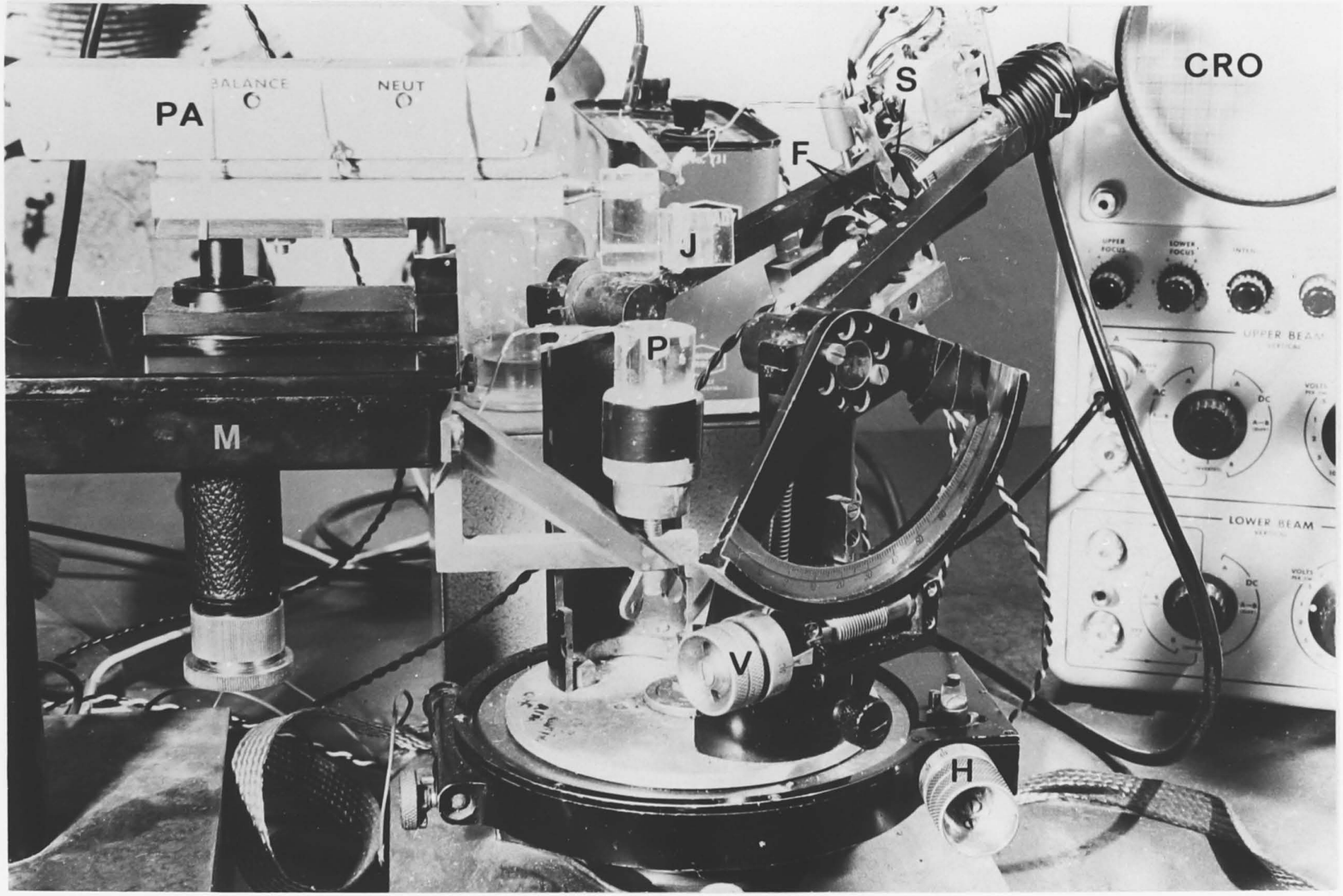
PA
BALANCE
NEUT
CRO
S
L
F
J
P
M
V
H
UPPER BEAM
LOWER BEAM

Figure 3

Calibrations made on the lamp.

The inherent polarization of the bulb can be seen in (a) and (b) shows it correction. In each case, the angular orientation of the horizontal plane of polarization (i.e. the electric or e-vector) is $\psi°$, and increases in 10° increments. Calibrations for each are the respective neutral density (ND) series. The final four responses for each polaroid run show the saturation point for the photocell and indicate that each result arose from unsaturated responses. Aberrant responses (arrows) were caused by interference from the support bars of the wheel. An indication of the degree of source polarization and its correction was the difference between maximum and minimum response heights, converted to equivalent log I. A 50% variation in sensitivity is equivalent to $\Delta \log I = 0.3$, so source polarization was strong and the correction adequate as retinula cell PL sensitivity is high (Fig. 44).

The energy output of the tungsten source with respect to emission wavelength is shown in (c). The relationship is linear over the range measured, with maximal output in the red to far red and little energy being emitted in the UV.

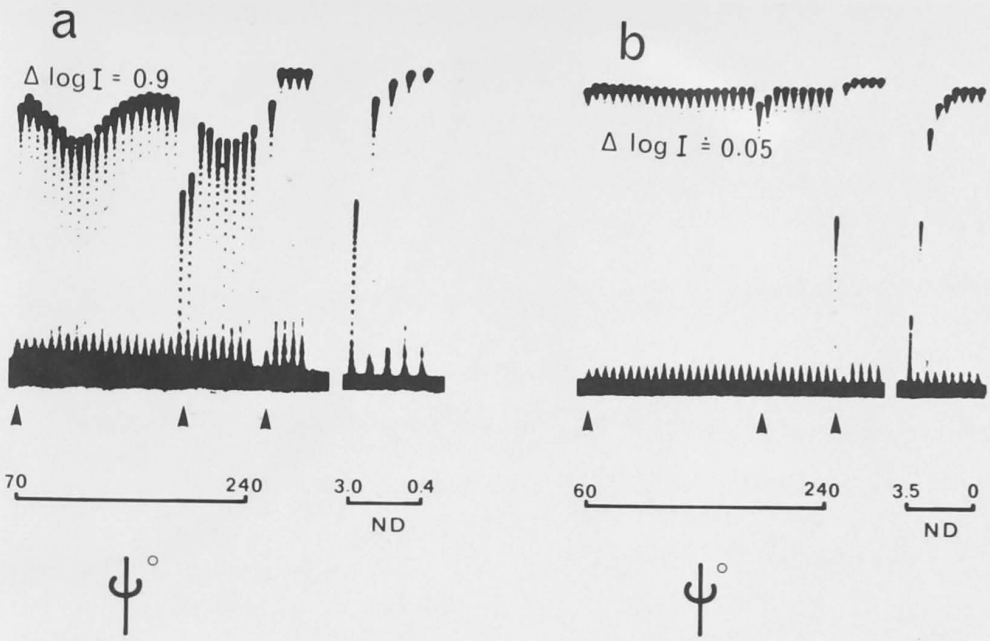
a
Δ log I = 0·9
70
240
3.0
0.4
ND
ψ°
b
Δ log I ≐ 0.05
60
240
3.5
0
ND
ψ°

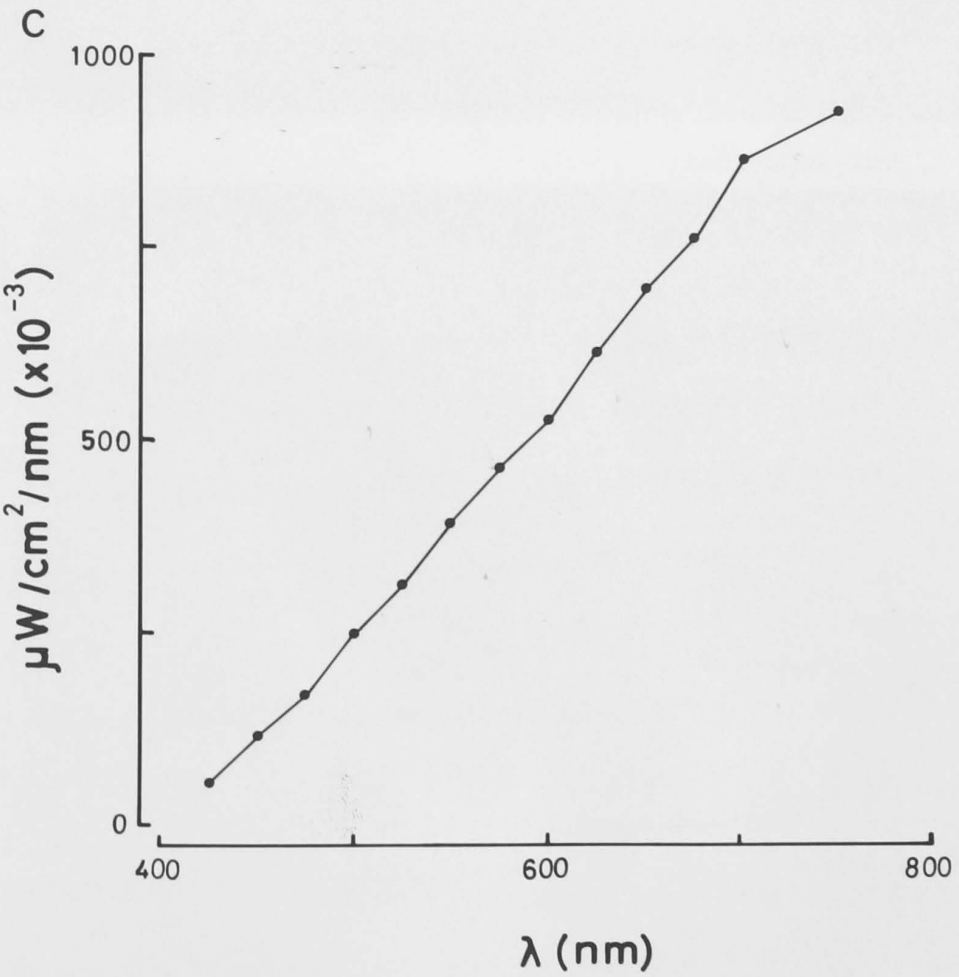
c
1000
500
0
μW/cm²/nm (x10⁻³)
400
600
800
λ (nm)

g. 44).

Figure 4

The eye preparation.

a. A frontal view of the head and compound eyes of Periplaneta americana. The antennae have been removed, leaving the antennal socket (AS). The dotted lines indicate the planes in which the slices (see text section D2) were made. D (dorsal).

b. The preparation in position, sitting on filter paper on the platform (P). The corneal slice is evident, with the glass microelectrode (E) making its vertical traverse through the retina. The arrows indicate the direction of the stimulus.

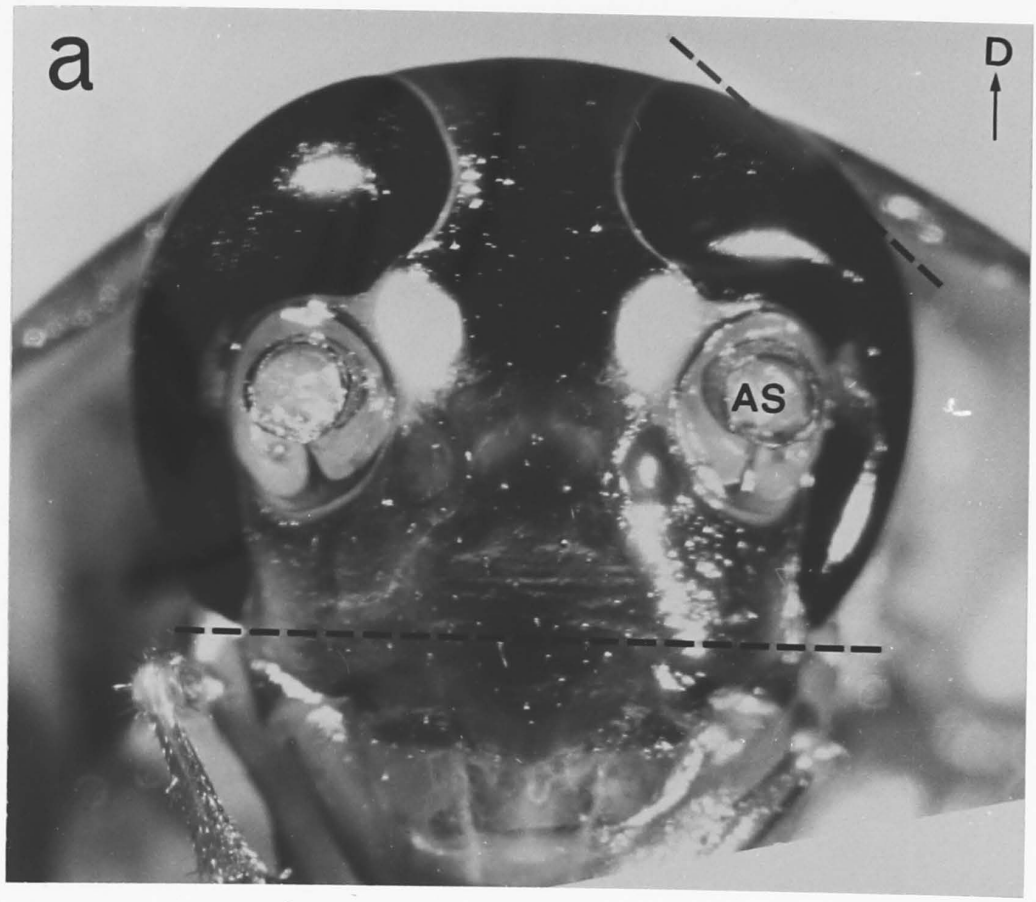
a
D
AS

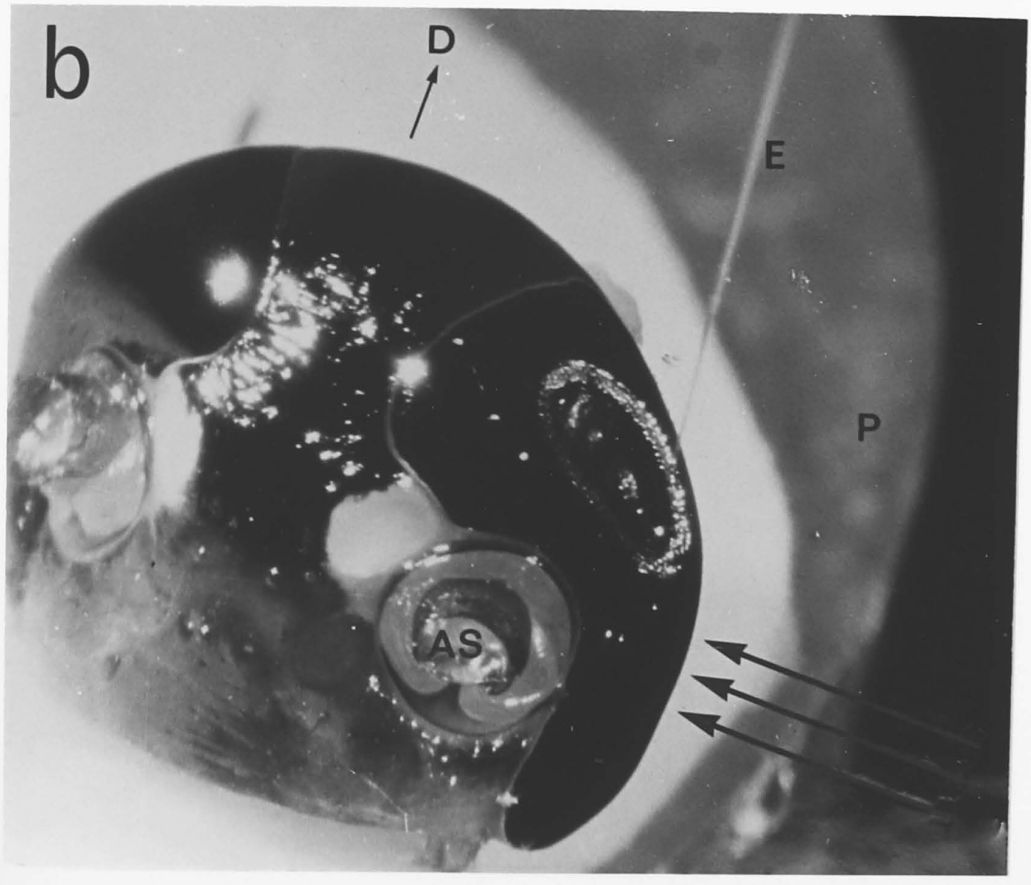
b
D
E
P
AS

Figure 5

Recording and stimulating arrangements.

A is a schematic diagram of the recording and stimulating set up and is described in the text. C camera, CRO cathode ray oscilloscope, PG pulse generator, WG waveform generator, S shutter, L lamp, PA preamplifier, B backing off and 10 mV calibration circuits.

B is the circuit diagram for the high impedance preamplifier used. The 1 KΩ potentiometer (pot.) connected to +V is used to balance the operational amplifier (OA) against small variations in supply voltage (±V). The 10 pF capacitor and 10 KΩ pot. is adjusted to apply capacity compensation. The adjustable pot. (ADJ) is set to produce 10 mV at the contact points which when closed, divided 10 mV between the 100 MΩ resistor and the electrode (in situ resistance check). For a 100 MΩ electrode, 5 mV would appear at the amplifier input (E_i). Resistance values were read from a calibration curve.

continued next page

Figure 5 continued

The two capacitors on the input $\pm V$ lines neutralized any high frequency inductance (looks like high resistance). E_o and E_i are output and input voltages. Gain = E_o/E_i = $(R_0+R_1)/R_1$ = 10.

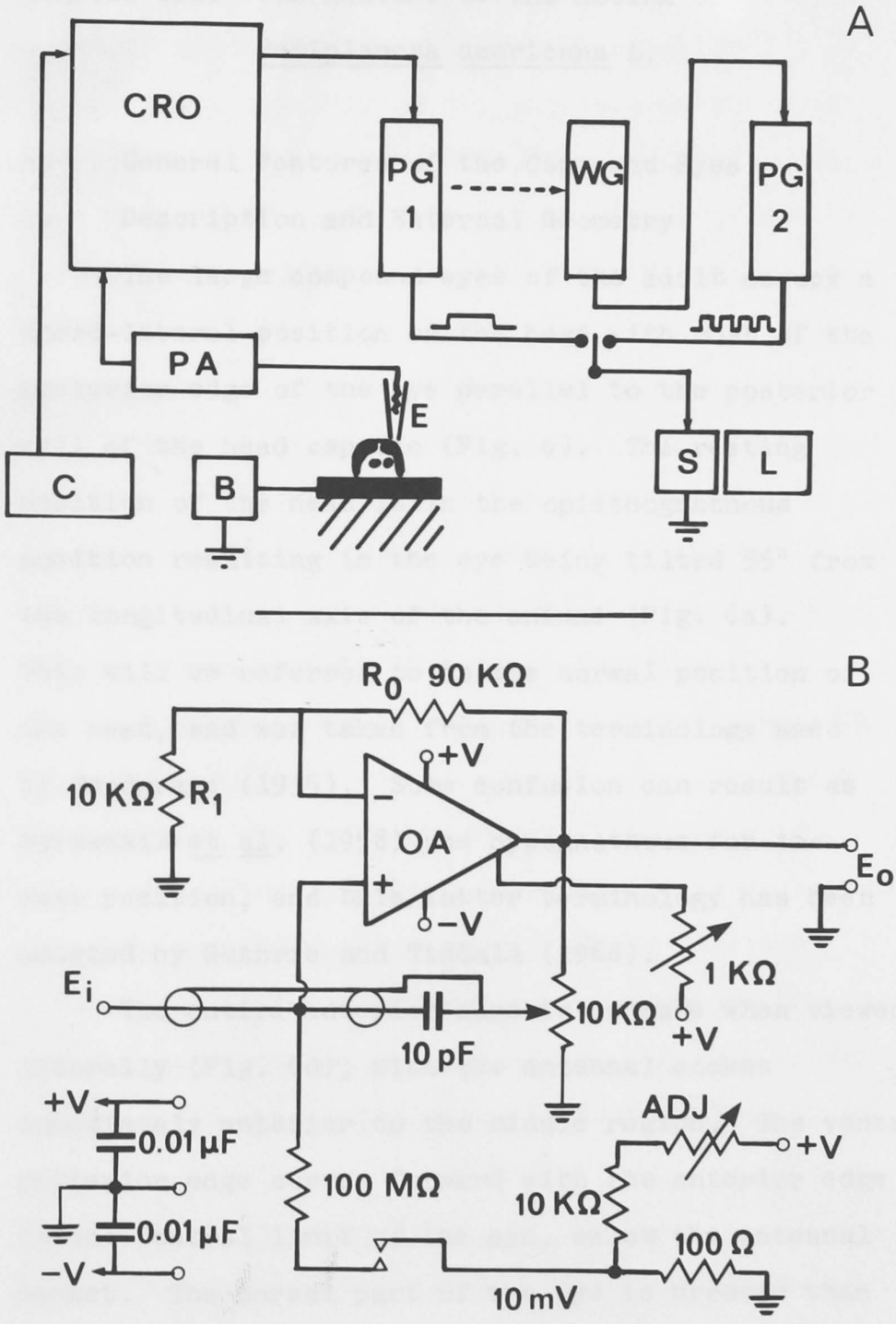
A
CRO
PG 1
WG
PG 2
PA
E
C
B
S
L
B
R_0 90 KΩ
10 KΩ R_1
+V
OA
−V
E_o
1 KΩ
E_i
10 KΩ
+V
10 pF
+V
0.01 µF
0.01 µF
−V
100 MΩ
ADJ
+V
10 KΩ
100 Ω
10 mV

CHAPTER III: THE ANATOMY OF THE RETINA OF *Periplaneta americana* L.

A. General Features of the Compound Eyes

1. Description and External Geometry

The large compound eyes of the adult occupy a dorso-lateral position on the head with most of the posterior edge of the eye parallel to the posterior wall of the head capsule (Fig. 6). The resting position of the head is in the opisthognathous position resulting in the eye being tilted 55° from the longitudinal axis of the animal (Fig. 6a). This will be referred to as the normal position of the head, and was taken from the terminology used by Snodgrass (1935). Some confusion can result as Borradaile *et al.* (1958) use hypognathous for the same position, and this latter terminology has been adopted by Guthrie and Tindall (1968).

The entire anterior edge is concave when viewed laterally (Fig. 6d), with the antennal socket immediately anterior to the middle region. The ventral posterior edge curves forward with the anterior edge to the ventral limit of the eye, below the antennal socket. The dorsal part of the eye is broader than the ventral, with the dorsal edge being straight (Fig. 6c). Lateral separation between the dorsal edges of the two eyes increases posteriorly. When viewed frontally, the lateral edges of the eyes have

the outline of a circular arc (Fig. 6b).

The size of the eyes varies according to the size of the animal, and is in the range of 3-4 mm long. When considering the outlines of the eyes both frontally and coronally, the radii of curvature are always less than that for the head, so the eye tends to 'stand out' from the general outline of the head. This helps to increase the field size encompassed by the ommatidia.

Around the margin of the eye is an internal collar-like ocular ridge which is an apodemal inflection of the cephalic cuticle (Snodgrass, 1935). The ommatidial lenses are slightly convex externally and give the eye its facetted appearance.

The eye of the first instar is different from that of the adult. It is roughly oval in shape and sits behind the antennal socket (Fig. 6a) without the noticeable distinctions between the adult dorsal and ventral regions. The increase in eye size with succeeding instars arises from the addition of ommatidia to the edges of the developing eye, as well as an increase in ommatidial size (Jörschke, 1914).

2. Facet Arrangements

The most distal element of an ommatidium is a specialized region of chitin, the cornea. Above each ommatidium, there is a slight external corneal protuberance with that area called a facet. In Periplaneta, the facet outlines are visible to the

naked eye, but are less than 10 μm high, contrasting with some nocturnal Lepidoptera at 250 μm (Bernhard et al., 1970). As a result of the packing of ommatidia within an eye, the facets are arranged in rows. Bernhard et al. (1970), have concluded that the regularity of these rows is related to protuberance size, irregularity being associated with low amplitudes. The number of facets varies greatly between species and in Periplaneta the number is between 1,800 (Miall and Denny, 1886) and 2,000 (Woken and Gupta, 1961).

Gemperlein (1969) used the very regular array of facets in three Dipterans as a basis of basic coordinates for the exact description of the compound eyes. In eyes of this type, facet rows belong to two systems of concentric circular arcs with dorsal and ventral loci. For this method to work, the entire eye must be covered by these arcs. Variations in facet shape can be described by and attributed to the geometric interference of the systems of circular arcs.

Fig. 7 shows the facet arrangements in Periplaneta. The scanning electron micrographs (SEMs) show the low relief of the facets (Fig. 7a,b). The two systems of concentric circles described above are absent (Fig. 7c) and the facet rows are irregular and appear to originate from several loci. This irregularity is clear in Fig. 7d, where short rows (arrows) abruptly terminate in a disordered array of facets. Where rows occur, the facets are of the usual hexagonal shape, but tend to be irregular in the disordered regions (Fig. 7d). It

has also been noted that two adjacent facet rows can suddenly split apart with a new row originating and occupying a place between them. Such irregularities prevent the use of a coordinate system such as Gemperlein's (1969).

Jörschke (1914) described the presence of small corneal hairs in Stylopyga (Periplaneta) and these were seen in the SEMs (arrow, Fig. 7a). They are short and occur between facets at irregular intervals. Nerves leading from these structures were not found.

3. Apparent Lack of Pseudopupil

The compound eyes of many insects exhibit the optical phenomena of the pseydopupil(s)-usually dark spots against a lighter background. Two basic types exist; one being a single primary pseudopupil and the second a primary pseudopupil surrounded by six accessory pseudopupils. These maintain position with respect to the observer's eye as the compound eye is rotated. Other insects, including Periplaneta americana, lack the apparent pseudopupil(s) and appear a uniform dark colour.

Yagi and Koyama (1963) give an explanation of the origin of pseudopupils (or lack of) and consider positional relationships of screening pigments and crystalline cones as the primary cause with only lip service paid to the physical properties of the dioptric apparatus. Their explanation is not rigorous and is superficial. I will now present an alternative

explanation to account for the phenomenon of pseudopupils, and show that virtually all insects have them, although they may not be visible.

First, consider a conical optical channel of higher refractive index (RI) than the surrounding medium. An optical fibre with diameter variations along its length is analogous to a conical rod. Off-axis light entering the end of a conical rod will be totally internally reflected provided the critical angle (I_c) is less than the angle of incidence at the inner surface of the rod. I_c is defined by : $\sin I_c = n_2/n_1$, where n_1 is the RI of rod, and n_2 the RI of the surrounding medium. This is derived from Snell's law, $n_1 \sin I = n_2 \sin I'$. The critical angle is that angle of incidence which makes $\sin I' = 1.0$.

In a conical channel, each succeeding angle of incidence is less than the preceding one by the apex angle of the cone. There will be an incident angle for which the ray will never reach the exit face but will return to the entrance face. With transparent conical channels, a large part of the light will escape through the walls and only part will return to the entrance face.

The limiting condition for the return of a light ray to the entrance face can be determined by the method shown in Fig. 8a. A conical channel (solid lines) has been successively rotated 180° about alternate edges (dotted lines). All rays (T')

which intersect the polygon formed by the exit faces will be transmitted through the channel (excluding loses through the walls). Rays (R') which do not meet this condition will be lost through the walls or returned to the entrance face. The respective positions for cones of returned (R) and transmitted (T) light are shown (for half the total incidence angles).

Considering data available from RI studies, the crystalline cones of insects can act as such conical channels. Varela and Wiitanen (1970) measured RIs in Apis, assigning RI values of 1.348 to the crystalline cone, 1.311 to distal and 1.351 to the proximal end of primary pigment cells. Seitz (1968, 1969) gave a RI of 1.349 to Phausis cone and 1.344 to the primary pigment cells. The three decimal places given are too optomistic for subjective interference microscopy, and the last two figures quoted in some of the values are so close that they cannot seriously be considered as reflecting the true difference. The Varela and Wiitanen (1970) figures for cone and distal primary pigment cell are spread sufficiently to be believed and reflect the condition required for internal reflections to occur. The Phausis study by Seitz (1969) also applies here, but with less strength, as the figures are close.

The assertion that crystalline cones act as wave guides (Seitz, 1969) is faulty as they do not

meet a basic requirement (1-2 μm uniform diameter). Cones are usually greater than 30 μm at the entrance face.

Fig. 8b shows some crystalline cones in Periplaneta. The rhabdom forms a cup-like structure around the cone and infiltrates the cone in this region (see section C, below). Above this level the cones are relatively smooth - probably enough to reflect light rays. Due to rhabdom investations this level is considered as the exit face of the crystalline cone. Another anatomical feature which will play a role is the primary and accessory pigment cell invagination of the cornea (Fig. 8b).

Fig. 8c shows an adaptation of Fig. 8a to crystalline cones of similar proportions to those in Fig. 8b. The heavier lines protruding above the entrance faces represent the pigment invaginations of the cornea, and are drawn in proportion to the cones. T' represents the limiting transmitted light ray and R' the limiting returned ray for one ommatidium. 'A' represents the cone of incident light absorbed by the screening pigment, while R and T represent cones for returned and transmitted (on axis and reflected) incident light, respectively. Periplaneta has no tapetal reflecting surface at the bottom of the rhabdom and so all light transmitted by the crystalline cone will not return.

The cone of absorbed light, A, will remain

fixed and depends on the degree of corneal invagination by pigment. R could vary depending on the RI of the crystalline cone. If the cones are optically homogeneous and isotropic in all directions (as in Calliphora and Phausis (Seitz, 1968, 1969) and Apis (Varela and Wiitanen, 1970)) then no variation would occur. However, if the cones had a higher RI towards their centre (as in the pseudocone of Phausis (Seitz, 1969) and crystalline cone of Ephestia (Horridge, 1971)), then R would be reduced as R' would bend towards the T' position and some rays would cross it. This bending would similarly affect T', but would not affect the magnitude of T. A similar situation exists for RI gradients in the cornea between the upper limits of pigment cell invagination.

The crystalline cone does not have perfectly smooth walls (see section C, below), and so some of the light will escape into the pigment cells at each reflection. Furthermore, the process of returning light to the entrance face will leak more light out of the cone. These facts, in conjunction with a relatively small R, would make the visibly returned light weak. Dominating this is the complete absorption of incident light due to A and T, resulting in the eye of Periplaneta appearing very dark with no apparent pseudopupil.

It is the relative proportions of A, R and T that create pseudopupils, and as long as some element of

R exists, then a pseudopupil must also exist, although not always visible to the naked eye. Only a very special set of circumstances or a peculiar crystalline cone configuration could remove R, and it is unlikely that these occur in insects. Furthermore, it is the height of screening pigment above the crystalline cone and the position of the rhabdom with respect to the cone that determine the proportions of A, R and T. The lower the height of the screening pigment, the smaller A becomes with a simultaneous increase in R. Also, the sharper the apex of the crystalline cone (i.e. rhabdom terminates near the tip of the cone) the smaller T becomes, simultaneously increasing R. It is when R is a substantial proportion of the total, A + R + T, that a lightish background appears on the eye with T being responsible for the primary (in direct line with observer's eye) and A for the accessory pseudopupils (also in line with observer's eye due to curvature of the compound eye). Beyond the accessory pseudopupils, the lightish background is due to lateral light transmission through the cornea. Primary pseudopupils occur alone when A is very small or non-existent (screening pigment only to top of cones, or lower). Variations in pseudopupil orientation and relations are due to the external geometry of the eye.

A, R and T are cones which diverge and this explains why psueopupils appear to cover several facets when observed from a distance and only one when

viewed with a microscope (Yagi and Koyama, 1963). The result of any reflecting tapetal structures would appear as a small light spot within the primary pseudopupil.

B. General Features of the Retina

1. Ommatidial Mapping

The eye is of the typical eucone, apposition type. Contrary to previous reports (Grenacher, 1879; Hesse, 1901; Jörschke, 1914; Nowikoff, 1932; Wolken and Gupta, 1961), individual ommatidia contain eight retinula cells, each of which extends from the crystalline cone to a region near the basement membrane. All cells contribute to the rhabdom. Four retinula cells have rhabdomeres which extend slightly higher than the rest. These have been numbered 1 to 4 and they lie precisely in the ventral, posterior, dorsal, and anterior planes, respectively, in relation to the normal attitude of the head (Fig. 9; also see Fig. 6a). Cells were numbered according to the order of appearance of rhabdomeres (which is constant) in serial sections. In the left eye, the order of appearance of cells 1 to 4 is counterclockwise. Cells 5 to 8 appear clockwise. This order of appearance in serial sections is a convenient way of identifying the cells. The arrangement in Fig. 9 is absolutely consistent.

An asymmetry occurs in each ommatidium. Cell 8 is apparently out of place for a symmetrical arrangement. In serial sections, cell 5 appeared between 1 and 4, cell 6 appeared between 4 and 3 and cell 7 appeared posterior to 3. Cell 8 did not appear between 2 and 1, but (surprisingly) between 7 and 2.

The distal part of the rhabdom possesses uneven contributions of rhabdomeres from certain cells. Cells 1 to 4 each contribute the major part of the paired contributions for ventral, posterior, dorsal and anterior paired units. Cells 5 to 8 are smaller. In the proximal part of the rhabdom the proportional contributions by cells 1 and 5, 4 and 6, and 3 and 7 to the paired units reverses. However, rhabdomere 8 is always small and rhabdomere 2 always large.

Periplaneta has no dorsal-ventral mirror image of receptor patterns as in the fly (Dietrich, 1909). In fact, the pattern of individual units within each ommatidium remains constant across the retina. However, a mirror image of cell patterns within ommatidia occurs between right and left eyes and hinges about the dorsal-ventral axis (see Fig. 9).

Trujillo-Cenóz and Melamed (1971) have published a paper with a different spatial orientation of the ommatidium. The positions of cells with respect to each other within a single ommatidium concur with my

findings, but their ommatidium is rotated approximately 145° counterclockwise to mine. 35° can be accounted for by the original orientation of the eye. Their work was done "in respect to the main axes of the eye", whereas mine was done in relation to the normal attitude of the head. As has been shown (Fig. 6a) the head and eye are inclined 35° from the vertical. By rotating the drawings a further 35° counterclockwise to orientate the figures with respect to the normal position of the head, their orientation becomes 180° out of phase. This fact implies that either their presentation, or mine, is upside down. I have doubly rechecked my series' of 1 µm thick sections for light microscopy (orientated with notched markers on dorsal and posterior block faces) and am confident that they are properly orientated. The text and detailed drawings of Trujillo-Cenóz and Melamed (1971) suggest that they were traced from electron micrographs. If such were the case, tissue disorientation can result from: 1, how sections were picked up on grids (i.e. from top or underneath); 2, how the grids were inserted into the electron microscope; and 3, image rotations occuring at certain magnification jumps.

2. Interommatidial Angles

Bäumgartner (1928) described regional variations in the interommatidial angles in the vertical plane for worker bee with values of 0.9° at the centre of the eye increasing to 3.6° at the periphery. This was related by Hecht and Wolf (1929) to behavioural studies on visual acuity. Del Portillo (1936) also mentions variations in the horizontal plane. More recently, Seitz (1968) has shown regional variations in interommatidial angles for Calliphora. As with bee, the vertical angles were generally narrower centrally than peripherally (2.6° cf. 3.4°), whereas horizontal angles were narrower anteriorly (2.0°) than in other regions (4.6°).

Variations in interommatidial angles across an eye may be important for central processing of visual information involving the whole eye or large regions of it. Overlapping of the visual fields of ommatidia is greater in regions of small interommatidial angles.

Those who have investigated visual acuity in insects by studying the massed electrical activity of the whole eye (e.g. Burtt and Catton, 1962) or optomotor responses, where the reaction of the whole animal is used (e.g. McCann and MacGinitie, 1965), have been aware of the problem of heterogeneity in interommatidial angles. Invariably, they have used an averaged value from interommatidial angles near

the centre of the eye. Unexpected results, which do not fit directly with independent measures of the same phenomena, have been found. McCann and MacGinitie (1965) predict and emphasize "the dominance of the interommatidial spacing" on experimental results. Perhaps some of the unexpected findings are related to a degree of heterogeneity in interommatidial angles not realised by the investigators.

A map of interommatidial angles over the whole surface of the left eye of Periplaneta was constructed using serial paraffin sections, cut in the horizontal and vertical planes. Interommatidial angles were measured for twelve positions on the eye and Fig. 10 shows these positions as well as representative sections for the five horizontal (A-E) and four vertical (F-I) levels. The ommatidia in both planes are generally set in radial array with those at the edges skewed.

Five series were used (five animals) and measurements of 10 adjacent interommatidial angles around each position from each series were made, for a total of 50 measurements per position. These were averaged for each series and the mean and standard error of the mean ($S.E._m$) determined. Using a Leitz camera lucida, lines were drawn through the optical axes of adjacent dioptric apparatuses and the inclination measured with a protractor. Rhabdom material was not included as a skewed rhabdom

(at the periphery of the eye) seems to be functionally independent of the optical properties of the dioptric apparatus.

Table 1 gives the numerical data, and Fig. 11 shows the graphical results. Two general trends are evident. The horizontal inter-ommatidial angles increase posteriorly and the vertical angles decrease posteriorly. At positions 2, 6 and 9 (along the anterior edge of the eye) there is relatively little separation between horizontal and vertical angles, and posterior to that, they rapidly diverge. Significant separation occurs in the extreme dorsal (1) and ventral (12) regions.

The extremes in the horizontal plane are 1.9° (position 1) and 10.0° (position 11), differing by a factor of 5 times. The vertical plane extremes are 1.0° (position 7) and 4.7° (positions 6 and 9), again differing by approximately 5 times. With no horizontal/vertical differences in the visual fields of single ommatidia (see CHAPTER IV), the greatest degrees of overlapping in the visual fields of adjacent ommatidia occur anteriorly for the horizontal field and posteriorly for the vertical field. This is only relative, as the degree of overlapping along the anterior edge of the eye is about the same in both horizontal and vertical fields.

TABLE 1

The averaged interommatidial angles (degrees) for twelve positions on the eye

Position	Horizontal		Vertical	
	Mean	± SE_m	Mean	± SE_m
1	1.9	0.1	3.0	0.3
2	3.2	0.8	2.5	0.7
3	2.8	0.6	2.0	0.7
4	4.4	0.6	1.4	0.3
5	9.3	2.1	1.1	0.1
6	3.5	1.4	4.7	1.6
7	4.9	1.4	1.0	0.4
8	9.6	0.5	1.1	0.5
9	5.7	0.9	4.7	0.9
10	6.6	2.3	1.2	0.5
11	10.0	0.4	1.8	1.1
12	7.1	1.1	3.1	1.3

3. Composite Field of View

The ommatidia of compound eyes are set in an array so that each one is directed towards a small part of the environment. There is a degree of overlap between adjacent ommatidial fields of view (see CHAPTER IV).

The composite visual field of each compound eye can be mapped from the information available in serial paraffin sections. By projecting the anatomical axis of the dioptric apparatus for the limiting ommatidia, an angular measure of the limits of the composite field of view can be determined for any section through the retina, and this was done for the sections shown in Fig. 10.

The entire field viewed by the eye is a three dimensional space (projecting from the surface, being somewhat similar in shape to the external geometry of the eye). The edges of this space, especially the anterior edge, are not equivalent to that of the eye as the anatomical axes of the dioptric apparatuses are not tangent to the corneal surface of these regions. Fig. 12 shows the maximal extents of the composite fields of view in two dimensions. The arcs joining the straight edges do not imply any limit on the depth of the field of view. The maximal horizontal field

of view is much broader (240°) than the vertical (198°) and is due to the smaller radii of curvature about the long axis of the eye, in conjunction with skewed packing of ommatidia near the edges. This is similar to that found in Calliphora (190° horizontal, 198° vertical) by Seitz (1968). Periplaneta has a dorsal overlap of 40° in the vertical field, and none ventrally. Posterior (56°) and anterior (65°) overlaps occur in the horizontal field with the latter occuring very close to the head.

These maximal extremes occur along row H (vertical) and B (horizontal) in Fig. 10. The dorsal overlap disappears anteriorly by row F, but is still present posteriorly at row I. The anterior and posterior overlaps persist dorsally but disappear ventrally as high as level C.

C. Fine Structure of the Retina

It is unusual that such a common insect as Periplaneta americana has had so little attention paid to the structure and function of its compound eyes. Several authors have described the anatomy of the eye, first at the light microscope level, and more recently with the use of the electron microscope (Grenacher, 1879; Hesse, 1901; Jörschke, 1941; Nowikoff, 1932; Wolken and Gupta, 1961;

Trujillo-Cenóz and Melamed, 1971). Each succeeding investigation improved anatomical correctness, although all are incorrect in one form or another. These will be pointed out at the appropriate places in the following description of the ultrastructure of the retina. Some of the specific detail has been put in the relevant figure texts.

1. Gross Morphology

Each compound eye is composed of up to 2,000 similar ommatidia (Wolken and Gupta, 1961). The gross morphology is represented in Fig. 13 and shown in Fig. 14. Each ommatidium contains eight retinula cells (Fig. 22) and measures approximately 250-350 µm in length. The diameter decreases proximally, from a distal 30-35 µm to a proximal 5-10 µm. Each ommatidium is covered distally by a dioptric apparatus approximately 150 µm in height. Half of this is stratified cornea with a low relief facet (5-10 µm, see Fig. 7) under which lies a crystalline cone.

Surrounding the crystalline cone and retinula cells is an envelope of two primary pigment cells and numerous accessory pigment cells both of which extend about 25 µm into the cornea, above the base of the cone. The former are in contact with cornea and cone cells and extend down as far as the cone tip. The latter extend to the basement membrane.

The rhabdom and much of the retinula cell screening pigment abruptly terminate above the basement membrane. Trujillo-Cenóz and Melamed (1971) claim to have found a fibrous membrane here, but this was lacking in all my material (Fig. 28a). In low power micrographs (Fig. 10) this phenomenon appears as a well defined membrane and is easily mistaken for the true basement membrane. Extensions of the retinula cells, the axons, originate here and travel in discrete bundles through the basement membrane. They then travel for up to 1 mm or more to reach the first optic neuropile, the lamina.

2. Dioptric Apparatus

The dioptric apparatus of the cockroach ommatidium is formed by a stratified cornea and a crystalline cone (Figs. 14-20). A surface view (Fig. 7) shows that each facet is convex and of very low relief, 5-10 µm, often with a hexagonal perimeter (see section A2, above). Trujillo-Cenóz and Melamed (1971) mistakenly picture the facet as being highly convex externally. The facet diameter is 20-40 µm with a radius of curvature of about 300 µm, the diameter variations being due to irregular facets in disorganized regions (Fig. 7). Corneal thickness is directly related to ommatidial length, varying from 50-75 µm. The inner surface of the cornea is highly convex (Figs. 8, 13, 14),

with a radius of curvature of about 25 µm. Grenacher (1879) described the cornea as having two layers, and in a light microscope this is true (Fig. 4a). However, when fresh tissue is examined with an interference microscope (Fig. 14c) three optically different regions can be distinguished. The outer 10-15 µm (layer 1) is layered in alternate optically dense and light bands. Layer 2 (25 µm thick) is much more homogeneous and is of relatively high refractive index (RI). Level 3 (40-45 µm thick) encompasses most of the internal corneal convexity. The RI of this layer increases towards the centre of the convexity, with the upper RI limit about the same as for layer 2.

In the electron microscope, the corneal stroma looks like cuticular chitin (Locke, 1964), composed of alternate dense and light bands. These bands are formed by spiralling filaments (Figs. 15, 18, 19). The band spacing decreases both peripherally (Fig. 15) and proximally (Fig. 18, 19) within each corneal facet. The spiralling becomes evident half-way through layer 2 (Fig. 15). Above this level, only a general limiting outline of the underlying structures can be seen (Fig. 15a).

No evidence was found for innervation of the sparce corneal hairs (Fig. 7; section A2), which is in contrast with honey bee drone (Sanchez, 1920;

Perrelet, 1970).

The inner convex surface of the cornea is separated from the base of the crystalline cone by narrow investations of the two primary pigment cells (Figs.13, 16a). Little, if any, intimate contact is established between cornea and cone (cf. Trujillo-Cenóz and Melamed, 1971).

The crystalline cone is the result of an internal specialization in four cone, or Semper's cells and is of the eucone type. Since Grenacher (1879), the four Semper's cell nuclei in Periplaneta have been known to lie above the base of the cone (Figs. 13, 16, 18). The cone measures approximately 30 µm in diameter at the base and has a base to apex length of about 75 µm. Like the cornea, this latter measure is dependent upon overall ommatidial size.

The cone apex is buried up to one third or more of its length in the rhabdom of the retinula cells. Near the apex of the crystalline cone, the cone cells diverge, giving rise to long extensions which run between pairs of retinula cells, almost to the basement membrane (Figs. 22, 23). The cone cell processes contain microtubules (Fig. 23e), but these were not observed in the cones themselves (Fig. 17).

The walls of the cones are relatively smooth

but do possess certain variabilities (Fig. 17). These are more evident in sections longitudinal to the ommatidial axis (Fig. 18). On the average, these variations are less than 1 μm deep and tend to be over emphasized in (slightly) oblique sections.

The crystalline cones lack organelles and in electron micrographs appear filled with electron dense particles. These were not considered in detail in Periplaneta, but other studies have indicated that they are β-glycogen (Fig. 25a, cf. Perrelet, 1970), with the conclusion that cone glycogen is non-metabolic with only an optical function, contributing to the RI.

3. Pigment Cells

Closely associated with the dioptric apparatus and retinula cells are two types of pigment cells; the primary and accessory pigment cells. The pigments in both these cell types, which chemically, are pterins and ommochromes, only have a screening function (Patat, 1965; Langer and Hoffman, 1966; Langer, 1967; Mote and Goldsmith, 1970). The pigment itself is thought to act as an electron trap (Shearer, 1969). They appear as large, dense spheroid particles in electron micrographs (Fig. 30). The retinula cells also contain substantial amounts of screening pigment.

The pigment particles of the primary pigment cells are larger (1 - 1.5 μm diameter) than those of

the accessory pigment cells or retinula cells (0.5 - 1.0 µm diameter; see Fig. 30). The last two types appear very similar, with the latter being slightly smaller. Primary pigment particles appear very dense (Fig. 30d) and often with surface deformations. Very thin sections of retinula cell pigment (Fig. 30c) reveal a granular, particulate substructure.

There are two primary pigment cells which surround the crystalline cone. These were not seen by Grenacher (1879) or Hesse (1901), and were first described in Periplaneta by Jörschke (1914). These cells extend distally, well above the crystalline cone base (25 µm), as a corneal invagination (Figs. 13, 18, 19) and proximally to a position level with the cone apex. They are in intimate contact with the cornea and about one-half to two-thirds of the cone cell (Fig. 13), as well as the most distal portions of the retinula cells. Microtubules are evident in close proximity to the cornea (Fig. 19c). The cytoplasm is rich in other organelles (Fig. 30a) as well as pigment particles. The nuclei are large and lie at the level of the Semper's cell nuclei (Fig. 16).

The accessory pigment cells envelope the entire ommatidium from cornea to basement membrane and are often shared by adjacent ommatidia. Whether

individual cells traverse the entire retinal depth or not remains unknown. It was impossible to determine the exact number of them due to irregular cellular arborization. Nevertheless, they were numerous, exceeding the 6 or 12 number given by Bullock and Horridge (1965), and seemed to approach (a guess only) the 27 to 31 limit (for each ommatidium) given by Perrelet (1970) for honey bee drone. Their numbers are greatest around the primary pigment cells and decrease proximally.

Pigment distribution within accessory pigment cells is random. Some regions are dense with pigment (Fig. 16d) whereas others are relatively or completely devoid (Fig. 22). This latter case can be mistaken for glia (as in the case of Nowikoff's (1932) "accompanying" cells). Their nuclei are relatively large and occur randomly in the cells.

It was difficult to ascertain whether the most proximal of the pigment cells (Fig. 28a) were accessory cells or a third type, the basal pigment cells, described generally by Bullock and Horridge (1965). Nowikoff (1932) described 'basal' cell nuclei in this region in Periplaneta. I was unable to resolve this point completely, although the appearance of these cells favours them being basal pigment cells (Fig. 28a, cf. Varela and Porter

(1969) and Perrelet (1970)).

Tracheoles were never seen above the basement membrane, although Nowikoff (1932) reports their occurrence between the 'true' basement membrane and 'false' basement membrane (lower limit of the rhabdom and retinula cell pigment).

Faint cellular outlines could sometimes be seen around axon bundles above the basement membrane. Varela and Porter (1969) saw these in worker bee and attributed them to processes of glial cells from beneath the basement membrane.

4. Retinula Cells

The ommatidium of Periplaneta contains eight retinula cells of unequal size, all of which contribute to the rhabdom. The exact number of such contributing units has been a contention since Grenacher (1879), who saw 4. Hesse (1901) increased this to 7 (4 proximal and 3 distal nuclei). Jörschke (1914) and Nowikoff (1932) both report 8 retinula cells, with the latter reporting 8 axons emerging from one ommatidium. It is surprising then to find Wolken and Gupta (1961), who did the first electron microscope study on Periplaneta, reporting only 7 retinula cells. This has been re-established at 8 by this study and independently by Trujillo-Cenóz and Melamed (1971). Aspects of

the ultra-structure of Periplaneta retinula cells is detailed in Figs. 20-25.

All retinula cells extend over the entire depth of the retina with their distal ends engulfing the apex of the crystalline cone (Figs. 13, 20, 21). Four cells extend more distally than the rest and all appear (in sections cut transverse to the longitudinal axis) in predictable sequence (see section B1, above). Distally, they are 6-7 μm in diameter. In cross section, they appear somewhat irregular in outline (Figs. 22, 23) this being determined by the packing space available. At all levels, the retinula cells contain a variety of organelles and inclusions (Fig. 31), the most conspicuous of which are the screening pigment particles. These are very similar to the accessory pigment cell particles, although slightly smaller.

The retinula cells are joined along apposing membranes by eight desmosones near the region where the rhabdom arises (Fig. 23). The rest of the membranes of adjacent retinula cells are not held together by junctional specializations. Even in low power micrographs (Fig. 22) gaps can be seen between the retinula cells, favouring the hypothesis that retinula cell membranes bathe in extracellular fluid through open channels between cells (Perrelet, 1970). It should be noted that penetration of

ferritin and lanthanum into the extracellular space within the rhabdom has been found (Perrelet and Baumann, 1969), contrasting with Fahrenbach's (1969) view that demosomes seal the rhabdom against extracellular space. The oval nuclei generally lie at different levels (4 distally, 4 proximally). This is not a rigid arrangement (as in Hesse (1901)) but merely a generalization (Fig. 13).

The inner border of each retinula cell is a highly specialized region known as a rhabdomere and all eight rhabdomeres together form the rhabdom (Figs. 24, 25). The depth distribution of the rhabdomeres is considered in CHAPTER V. Early workers discerned a rod-like striation in the rhabdom (Grenacher, 1879) and assumed a nervous function. Nowikoff (1931, 1932) rejected that interpretation, favouring a dioptric function of the rhabdom as a way of distributing light over the whole length of the retinula cell. The ultrastructure of rhabdomeres (at the electron microscope level) has been known since first described by Fernández-Morán (1956). The rhabdom(eres) of Periplaneta has the usual lamellar structure associated with this organelle (Fig. 20-25). The rhabdom varies in shape and size according to depth in the retina.

The lower one-half to one-third of the crystalline cone is in intimate contact with the rhabdom (Figs. 13, 20, 21, 25), the longitudinal axes of the lamellar

substructure being orthogonal to the cone (Figs. 21, 25a). In this region, the rhabdom infiltrates the cone to a great extent (Figs. 20, 21).

The cylinders created by the lamellae are of variable length, but have a consistent diameter of approximately 600-650Å (Fig. 24c). They contain an irregular dense core and are limited by what appears to be a beaded unit membrane 100 Å thick. The beaded characteristic appears in both vertebrate and invertebrate photoreceptor membranes and has been interpreted as a possible site for visual pigment (Fahrenbach, 1969). The cylinders are tightly packed, form tight junctions, and all are orthogonal to the longitudinal axis of the ommatidium.

As mentioned before, the rhabdom and much of the retinular cell pigment particles abruptly stop above the basement membrane (Jörschke (1914) recognized this "false basement membrane"). Above this level, one or two retinula cells leave the rhabdom and take on an axon-like appearance (Fig. 23; Trujillo-Cenóz and Melamed, 1971) and below the level, the remaining retinula cells become axons. The axons travel in discrete bundles to the basement membrane, where they constrict, pass through and expand again, but not to the same previous degree (Fig. 28).

The basement membrane is 2-4 μm thick, and composed of diffusely fibrous material (Fig. 28), probably collagen filaments (Harper et al., 1967). Its sole function is in mechanical support for the retina (Fahrenbach, 1969).

5. Changes Upon Light/Dark Adaptation

The retinula cells contain both granular (rough) and agranular (smooth) endoplasmic reticulum, and during dark adaptation, cisternae develop in the reticulum giving rise to the palisade (Horridge and Barnard, 1965).

This appears in light and electron micrographs as a clear zone (Fig. 26) which has been referred to by several names (Schaltzone, subrhabdomeric cisternae, lacunae, palisade, etc.). The palisade is generally limited by the amount of adjacent rhabdomere (see CHAPTER V) and is the only visible structural change occurring when an eye of Periplaneta is dark adapted. In the light-adapted state, pigment particles lie close to the rhabdom (Figs. 22, 23), and either migrate or are displaced as the palisade develops (see CHAPTER V). The development and nature of the palisade is shown in Fig. 27.

The fully developed palisade never comes into direct contact with the rhabdom. A thin layer of cytoplasm over the rhabdom extends as cytoplasmic

bridges to the rest of the retinula cell separating the palisade from rhabdom (Fig. 27a).

6. Axons

The eight axons are extensions of the eight retinula cells in each ommatidium and arise in the proximal retina (see above). Below the basement membrane, the axon bundles fuse and vermiculate in great tracts (1^{+} mm long) towards the lamina (Fig. 29a). Their diameter slowly decreases from 3 µm to less than 1 µm just above the lamina. At this latter position, the track subdivides and appears in sections as arches, accommodating lamina cell bodies (Fig. 29b).

The axons are packed with microtubules along their entire length and near the retina, contain considerable quantities of retinula cell pigment particles. Trachea are closely associated with the axon tracts.

7. First Instar

Periplaneta americana L. is a heterometabolous insect. The compound eyes of newly hatched first instar larvae (Fig. 6) were examined to see if any significant structural differences from the adult existed.

Some differences are evident in the gross morphology (Fig. 14d). The ommatidia are predictably fewer and smaller (50 μm long) than the adult and have an interommatidial angle of 15-20° in the horizontal plane. The Semper's cell nuclei are relatively larger in the first instar than adult, covering the top of the cones. The proportion of crystalline cone and rhabdom to the rest of the ommatidium is very large, and changes with development. The cornea has a more prominent convexity externally with a radius of curvature of about 40 μm. It is relatively thinner than the adult with the internal convexity being less prominent (radius of curvature about 25 μm). The dual layering found in light micrographs of the adult (Fig. 14a) is evident in the first instar (Fig. 14d).

At the ultrastructural level, all the basic features of the adult ommatidia are present (Figs. 32, 33). This is a contrast to the situation the holometabolous Coleopteran, Attagenus, where extensive post emergence changes in eye morphology can occur as the adult eye matures (Butler et al., 1970).

D. Discussion

The peculiar ommatidial arrangements, as manifest by the facet patterns are intriguing as far as the lamina and medulla neuronal projections are concerned. Several complete series of 1 µm thick sections from epoxy embedded tissue were cut from the cornea through to the medulla, with the idea of tracing the retinula cell axons through these projections. All these series were incredibly difficult to follow for several reasons (contortions of the axon tracts, dense pigmentation, decreasing axon diameters) and were finally abandoned. However, from the studies of Horridge and Meinertzhagen (1970 a, b) it can be predicted what will probably occur. As Periplaneta has a fused rhabdom, two of the retinula cell axons probably go through the lamina to the medulla. The other six axons probably terminate in a lamina cartridge which would have exactly the same spatial relationships with neighbouring cartridges as does the parent ommatidium with neighbouring ommatidia, and so the peculiarities of retinal spatial geometry ought to be mirrored exactly in the lamina. The medulla ought to bear a mirror image of the laminar arrangements due to chiasmal inversions.

The precision with which intra-ommatidial geometry is repeated across the retina implies a great degree of rigidity and specificity in the control of development and growth of ommatidia. Meinertzhagen (1971) has shown that for fused rhabdom eyes, the long axons (through to medulla) arise from the same pair of retinula cells in each ommatidium. If this applies to Periplaneta and the two long axons correspond to cell 1 or 5 or 7, then an anatomical basis for colour vision may be implied (see Fig. 9 and CHAPTER V).

A large degree of variation was found in vertical and horizontal interommatidial angles across the eye. The relevance this has for vision will be discussed in CHAPTER IV in conjunction with the physiological results.

The large overlapping of the composite fields of view, in both vertical and horizontal planes, raises the possibility of binocular vision for specific regions. The simple fact that the visual fields of each eye overlap shows that ommatidia in each eye can, anatomically, look at the same point. Assuming normal function in each ommatidia, then there will be a dual input to higher CNS centres. There is no information as to what, if any, is the nature of the neural integration of the two inputs. A series of papers dealing with prey catching in

mantids has been interpreted as evidence for functional binocular vision in this insect (Maldonado, Levin and Barrós Pita, 1967; Maldonado and Levin, 1967; Maldonado and Barrós Pita, 1970; Barrós Pita and Maldonado, 1970; Levin and Maldonado, 1970; Maldonado, Benko and Isern, 1970). The overall conclusions of this series was the precise estimation of both long and short distances is accomplished in mantids by a binocular method, based on some triangulation mechanism, and that there exists a region of the compound eye necessary and sufficient for such fine estimations which is equivalent to a 'fovea'. The two morphological peculiarities described by the authors as distinctive features of the 'fovea' region, small radii of curvature and a large number of ommatidia per unit area, were not included in my anatomical evaluation of the eye of Periplaneta and so no direct comparisons can be made with the mantis eye. However, the photographs and sections of the eye (Figs. 6, 10) show that the radii of curvature is large in the regions where overlap occurs, but the interommatidial angle data indicate that inclination between adjacent optical axes are nearly equivalent for horizontal and vertical planes and narrow in the regions where binocular vision might occur (Fig. 11, positions 1 and 2).

The general plan of individual ommatidia did not vary across the eye, except for ommatidial length, which tended to be longer in central than peripheral regions, due to the general curvature of the eye as a whole. The fact that four retinula cells extend further distally than the others, plus the fact that the nucleii are stratified, provides a temptation to postulate that Periplaneta possesses a retina intermediate in form between the tiered Lepidopterans and columnar Orthopterans, that Nowikoff (1932) could not resist. It is very difficult to decide whether this is true. The Lepidopterans are relatively advanced over the more primitive Blattidae. Whether or not the tiered retina of Lepidoptera has remained relatively unchanged or has evolved from a columnar type is unknown. The Blattid retina could be intermediate to either or could itself be close to the original plan. It is also possible that the two types may not have evolved from a similar ancestor. Blattids are more closely related to the very primitive Apterygotes, which have a tiered retina. Again, the same arguments hold.

Lasansky (1967) classified all non-neural elements of the Limulus ommatidium as glia. Fahrenbach (1969) rejected this generalization on functional grounds, which also apply to Periplaneta.

The primary pigment cells appear to function as an iris, while the accessory pigment cells fill the spaces between ommatidia. In Smith's (1968) illustrative book, large 'extracellular spaces' and 'tracheoles' appear between ommatidia, but these were never seen in my material. Large extracellular spaces were evident, however, after killing in boiling water (CHAPTER V).

The nature of the crystalline cone and its parent cells, being of stable composition and noticeably lacking in organelles, would relegate it to a passive optical function. The retinula cells, on the other hand, are rich in organelles and are highly metabolic. The endoplasmic reticulum is extensive in retinula cells and develops an array of cisternae under the rhabdomeres upon dark adaptation. This is usually concomitant with a near-by aggregation of mitochondria, and are the only visible changes occurring with dark adaptation. This palisade vanishes upon light adaptation either by disappearance or displacement and is replaced by retinula cell screening pigment. Ruck (1964) and Lasansky (1967) have suggested that the palisade participates in photochemical transduction, but is more likely that it functions in a more passive role, such as changing the refractive index of the medium surrounding the rhabdom (Horridge and Barnard,

1965). Varela and Porter (1969) have reviewed the evidence against the argument that the cisternae are fixation artifacts.

The old microscopists (Granacher, 1879; Hesse, 1901) saw striations in the rhabdom and postulated a rod-like substructure with neural functions. Nowikoff (1931, 1932) concurred with the reported structure but re-interpreted rhabdom function dioptrically. The use of the electron microscope has revealed the ultrastructure of the rhabdom(ere) in great detail and was initially described in terms of a laminated structure (Fernández-Morán, 1956). It was Miller (1957) who first interpreted the structure of rhabdomeres as being "microvilli of the retinula cell's border". This was based on material cut longitudinally to the lamellar structures of the rhabdomere which were "often observed to be open and continuous with the cytoplasm of the retinula cell". The term "microvilli" has been retained to describe the nature of the rhabdomere despite Fernández-Morán's (1958) seeming hesitation, where he only admitted that the microvillus interpretation could be applied. Considering the impressive micrographs of these structures which show apparent unit membranes (e.g., Perrelet, 1970) little reason has appeared to doubt the interpretation.

Some of the micrographs that I have obtained show features of the rhabdom which cannot be explained by the microvillus theory (Fig. 24d). In this micrograph, the rhabdom is disrupted, probably due to poor fixation in this region. The presence of long membraneous strands is quite evident in the region where the normal structure has been disturbed. If the units of the rhabdomeres were true microvilli, with true unit membranes, then those properly fixed would appear intact and the rest swollen, lysed or collapsed, without any special relationships to one another. In the micrograph, the membraneous strands are continuous with the undisturbed rhabdomere. In these regions, where the strands leave the organized units, "half microvilli" are evident. In other areas, the intervening membrane between two "microvilli" is disrupted, leaving a "double microvillus". The nature of this disruption suggests that rhabdomeric substructure is not based on the microvillus hypothesis, but that it is a lamellar organization of membrane organized to hold photopigment molecules in specific orientations. Random or very local membrane disruptions would disrupt only short lengths of membrane adhesions (the tight junctions), resulting in the "double microvillus". Massive disturbances (as in poor fixation) would "unzip" long lengths of

adhering membranes, resulting in long membraneous strands. Goldsmith and Philpott (1957) suggested the rhabdomere was such a single structural unit, and this interpretation was favoured by Fernández-Morán (1958). The hexagonal honeycombed appearance (Fig. 24c) of the rhabdomere would be a result of regularly spaced membrane adhesions in a lamellar organization. The distal ends of the laminar channels are closed (Fig. 25a) and Fernández-Morán (1958) has implied that the nature of these end 'caps' are different from the membraneous 'walls'.

The proximal ends are open and continuous with retinula cell cytoplasm (Figs. 24a, 25b) and these micrographs could easily be interpreted by the microvillus theory. The evidence is not clear cut either way.

Several approaches have indicated that the rhabdom is the primary site of photoreception. The rhabdom has many morphological features in common with the photoreceptor discs of vertebrate rods and cones (briefly reviewed by Fahrenbach, 1969). Langer and Thorell (1966) have shown microspectrophotometrically that peak absorption in Calliphora rhabdomeres occurs at wavelengths identical to those absorbed by rhodopsin in vitro, and these were related to Burkhardt's (1962) physiological data. Invertebrates contain a retinal-protein complex, presumed to originate in the rhabdomeres, which is part of the rhodopsin

regeneration cycle (Goldsmith, 1964; Wald, 1968). Frog rods (Bownds and Gaide-Huguenin, 1970) and cones (Dewey et al., 1969) have been shown to contain rhodopsin (see also: Kirschfeld, 1969). Physiological evidence has come from Mote and Goldsmith (1970) who recorded normal intracellular potentials from retinula cells in white-eyed mutants of Periplaneta. Shaw (1968a; 1969a, b) recorded polarized light sensitivity in the retinula cells of several arthropods and the phase of maximum sensitivity correlated with the orientation of the laminations in the rhabdomeres.

Figure 6

The general features and external geometry of the compound eyes.

a. The resting position of the head. The region enclosed by the black dotted line is part of the compound eye but does not show well in the photograph. The region enclosed by the white dotted line approximately represents the relative size and position of a first instar compound eye. Note the inclination of the head (35° from the perpendicular).

b. Frontal view of the head and compound eyes. Antennae removed.

c. Dorsal (coronal) view. Antennæ removed.

d. Lateral view. Antennae removed.

Scales. a-d, 1 mm

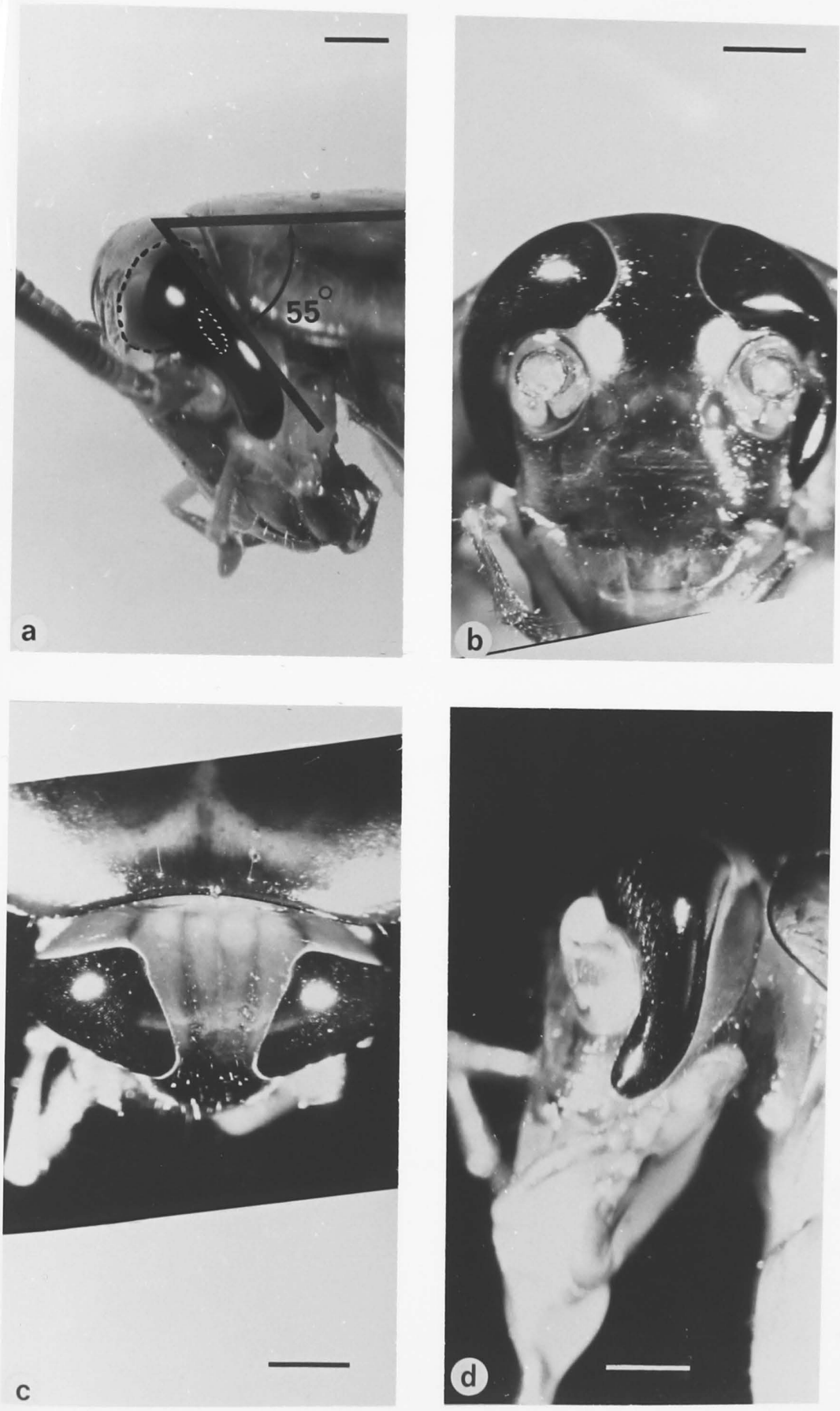
55°
a
b
c
d

Figure 7

Facet arrangements.

a and b. Scanning electron micrographs of the corneal surface. The facets have a low relief and are not aligned in well defined rows. Small corneal hairs (arrow, 7a) occur randomly between facets.

To obtain the SEM, whole heads were fixed as for electron microscopy, dried and fixed to stubs with a rapid setting epoxy glue. They were coated in an evaporator with Au-Pb and examined in a JOELCO JSM-U3 scanning electron microscope (courtesy of CSIRO, Division of Entomology, Canberra).

c and d. Light micrographs showing facet rows. In (d) the arrows indicate small rows of hexagonally shaped facets which terminate at a disorganized region of irregular facets.

Scales. a and c, 0.25 mm; b and d, 100 µm

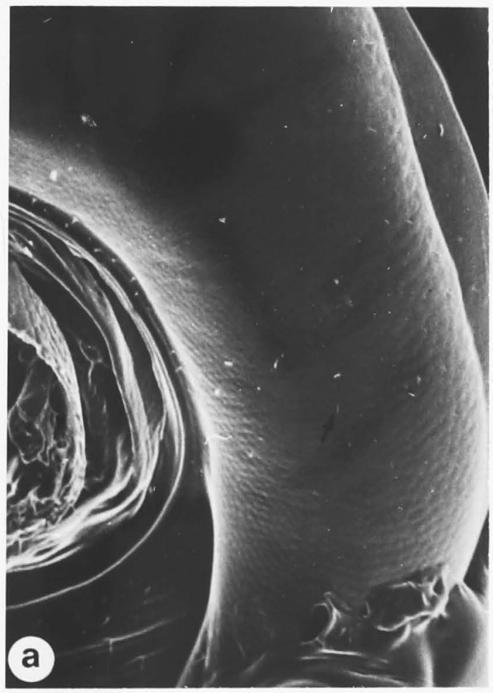
a

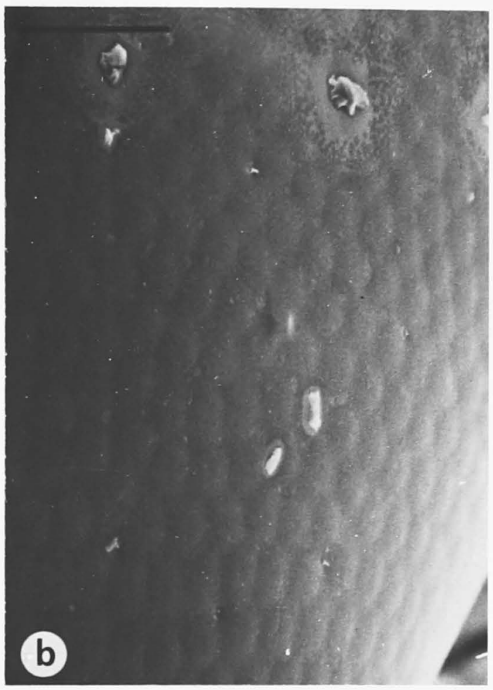
b

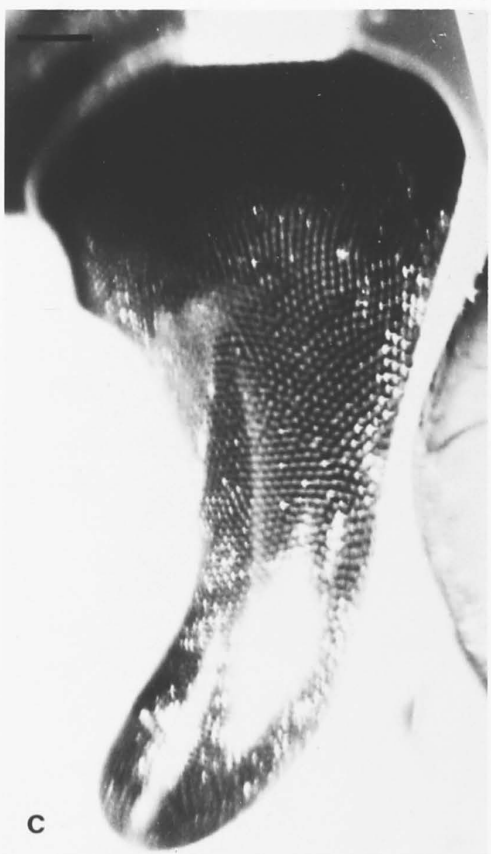
c

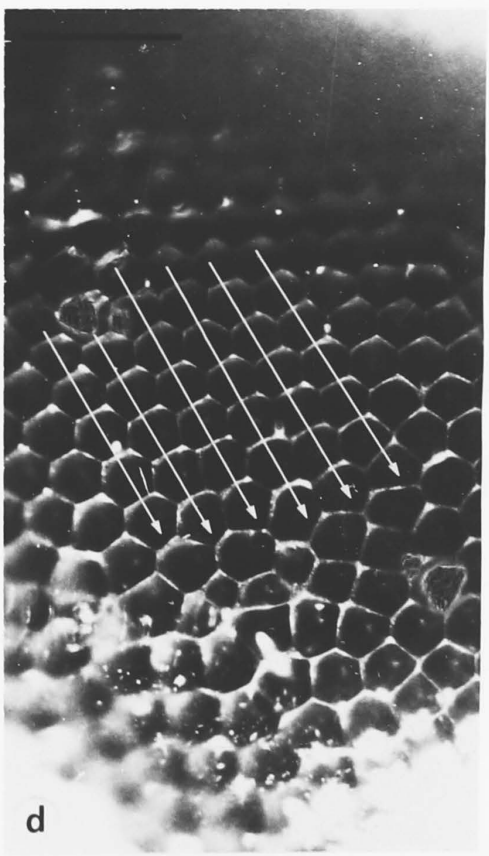
d

Figure 8

An explanation of the origin of pseudopupils.

a. Limiting conditions for returned and transmitted light in a conical channel (adapted from Brown, 1965).

b. Light micrograph of the crystalline cones of Periplaneta americana. The arrow indicates the invagination of the screening pigment into the cornea.

c. An adaptation of (a) to fit the cone shapes of Periplaneta. The heavy lines represent corneal invaginations of screening pigment. Lengths are proportional.

a and c. R', path of a light ray which will return to the entrance face; T', path of a light ray transmitted by the conical channel. A, cone of incident light which will be absorbed by screening pigment; R, cone of incident light which will be returned to the entrance face; T, cone of incident light which will be transmitted by the conical channel.

b. C, cornea; CC, crystalline cone; R, rhabdom.

Scale. b, 25 µm

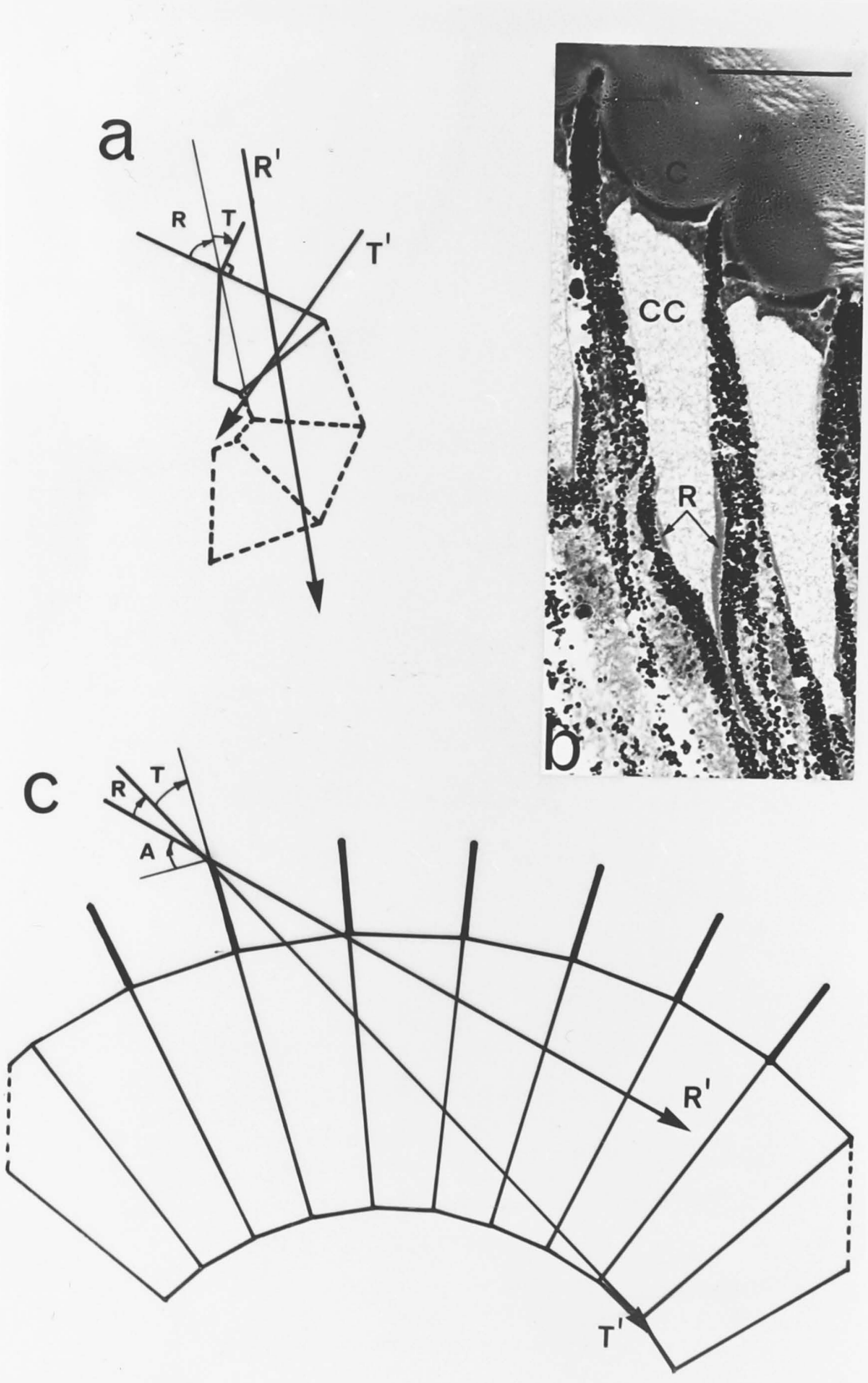
a
R'
R
T
T'
C
CC
R
b
c
T
R
A
R'
T'

Figure 9

Intra- and inter-ommatidial geometry.

Cells are numbered 1 to 8. Units outlined in heavy lines are UV receptors, the remainder are green (see CHAPTER V). Stippled central area in the schematic ommatidia represents the rhabdomeres. The light micrographs (Zeiss Planapochromat X 100/1.3, oil immersion objective) correspond to their neighbouring schematic diagram. Four ommatidia are shown with their areas of origin on the retina.

Eyes were dropped into boiling water before histological preparation. This instantaneously stopped pigment migration and usually destroyed most of the inter-ommatidial accessory pigment cells. Destruction of extraneous cellular material facilitated ommatidial reconstructions from a series of sections cut transverse to the ommatidia, and had no apparent effect on the ommatidial structure at the level of the light microscope.

D, dorsal; A, anterior; M, medial; R, rhabdom(eres)

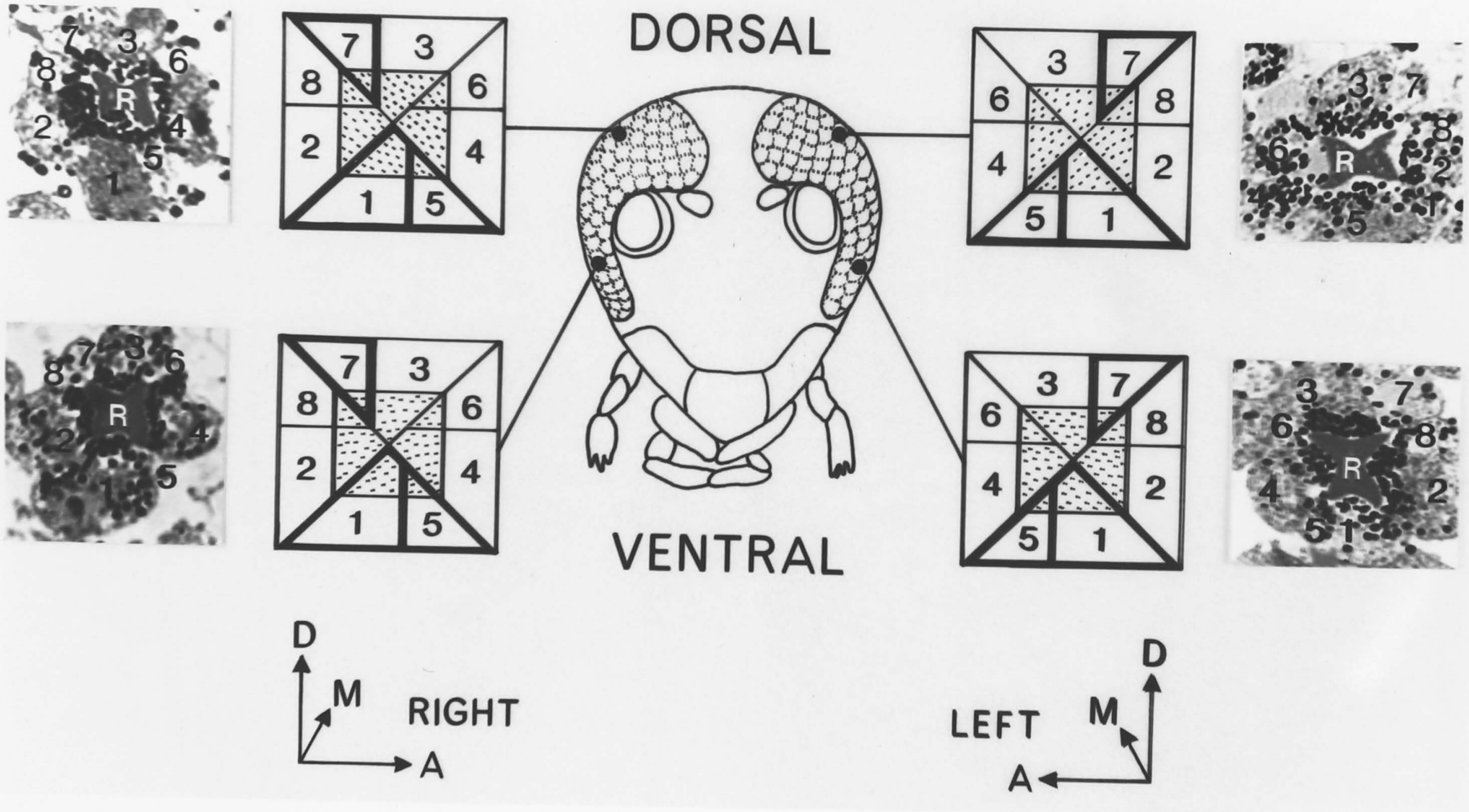
DORSAL
VENTRAL
D
M
RIGHT
A
LEFT
D
M
A

Figure 10

Interommatidial angles.

The photograph of the eye shows the twelve positions for which interommatidial angles were measured. Sample horizontal sections (levels A-E) and vertical sections (levels F-I) are shown with respective positions indicated. Interommatidial angles were measured between the optical axes of adjacent diptric apparatuses. The ommatidia are generally radially arranged but skewed towards the periphery of the eye.

A, anterior; M, medial; D, dorsal

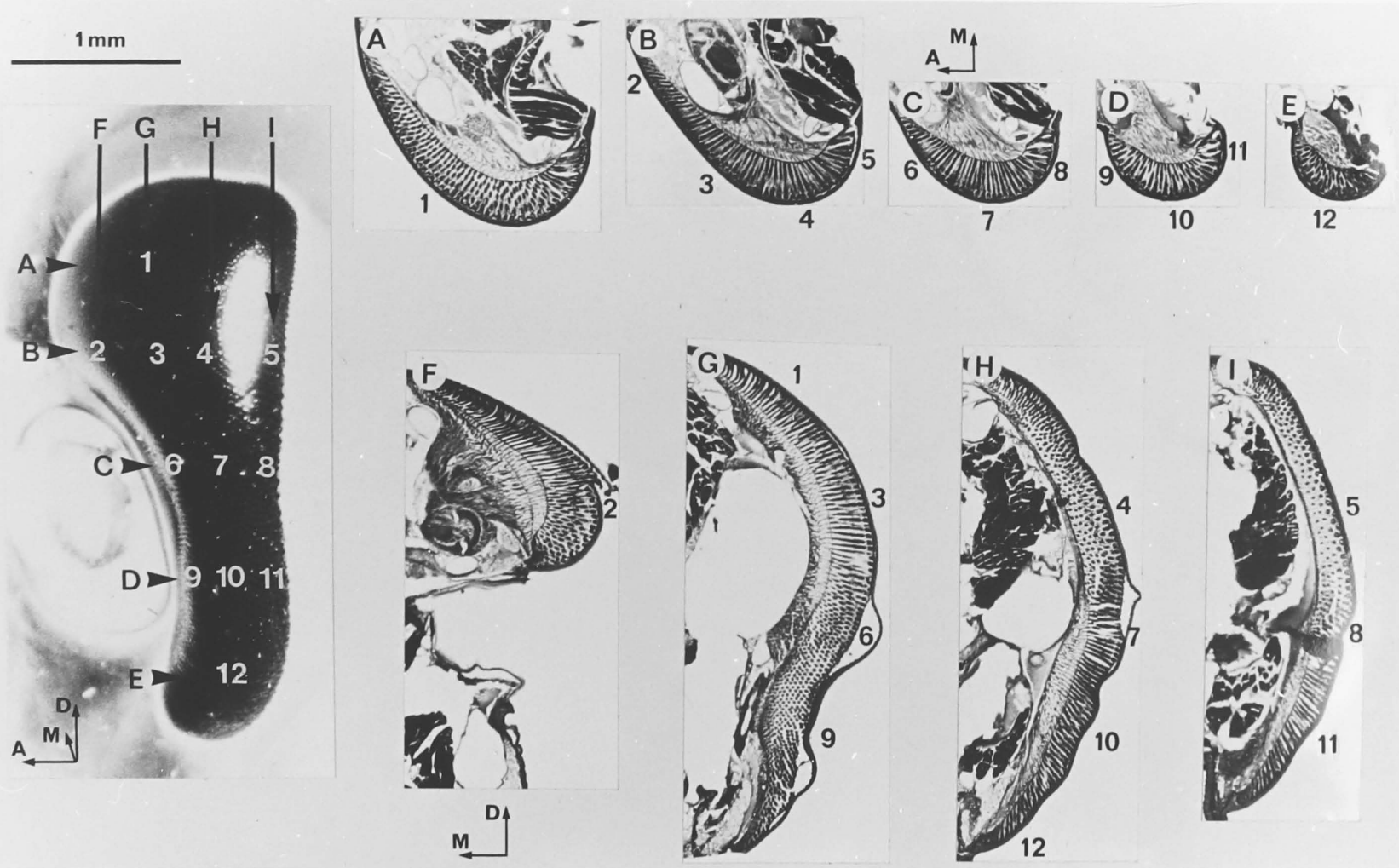
1mm
F G H I
A
B
C
D
E
1
2 3 4 5
6 7 8
9 10 11
12
D
M
A
A
1
B
2
3
4
5
M
A
C
6
7
8
D
9
10
11
E
12
F
2
D
M
G
1
3
6
9
H
4
7
10
12
I
5
8
11

Figure 11

Interommatidial angles.

A plot of averaged interommatidial angles (degrees) against position on the retina (as in Fig. 10). The horizontal angles increase while the vertical angles decrease, posteriorly, both by a factor of about five times.

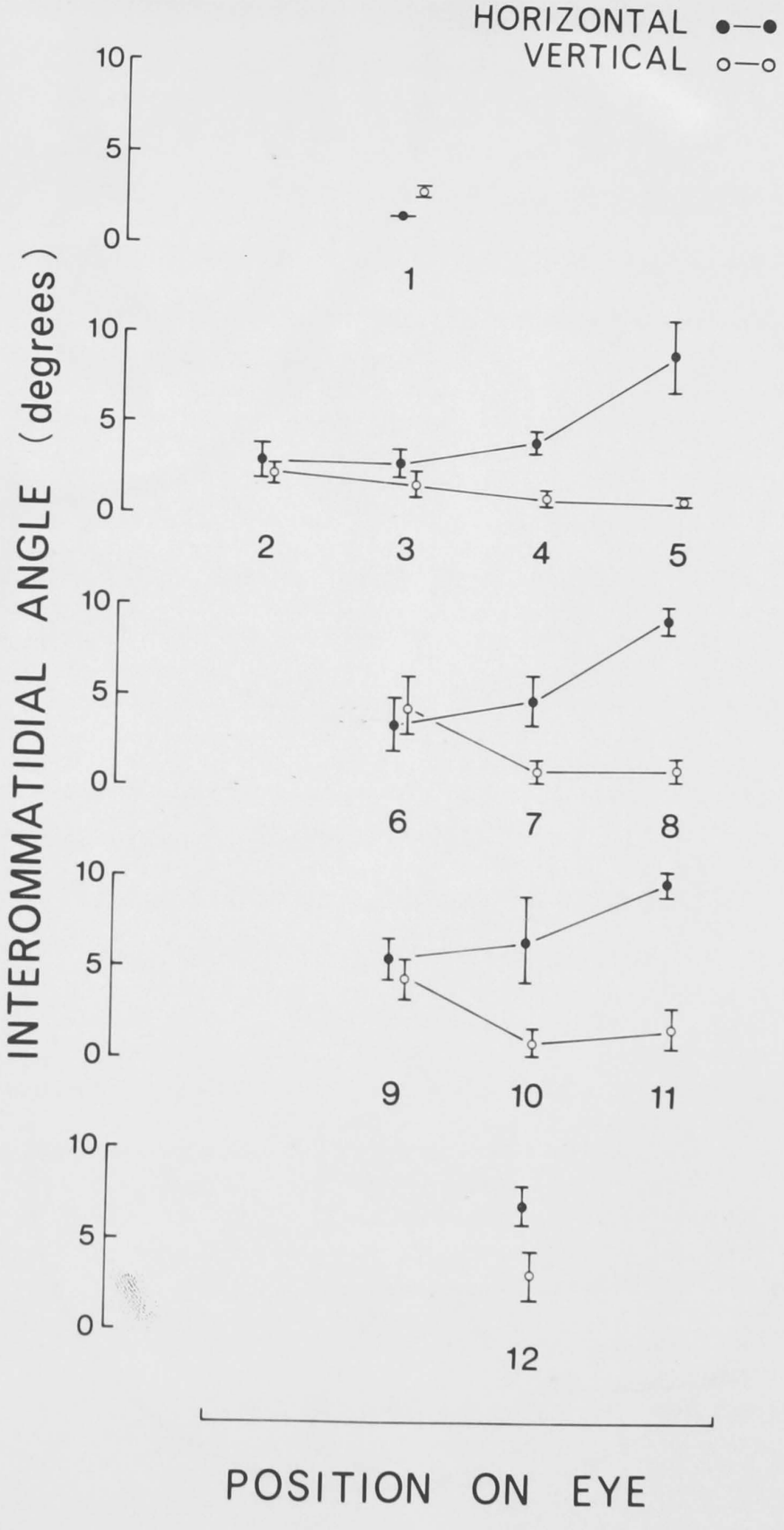
HORIZONTAL
VERTICAL
INTEROMMATIDIAL ANGLE (degrees)
10
5
0
1
2
3
4
5
6
7
8
9
10
11
12
POSITION ON EYE

Figure 12

Extent of the composite field of view, showing regions of overlap.

a. The composite field of view for each compound eye in the vertical plane is 198° with a dorsal overlap of 40°.

b. The composite field of view for each eye in the horizontal plane is 240° with posterior and anterior overlaps of 56° and 65°, respectively.

Note that the anterior overlap occurs much closer to the head than the dorsal or posterior overlap, and is the largest of the three.

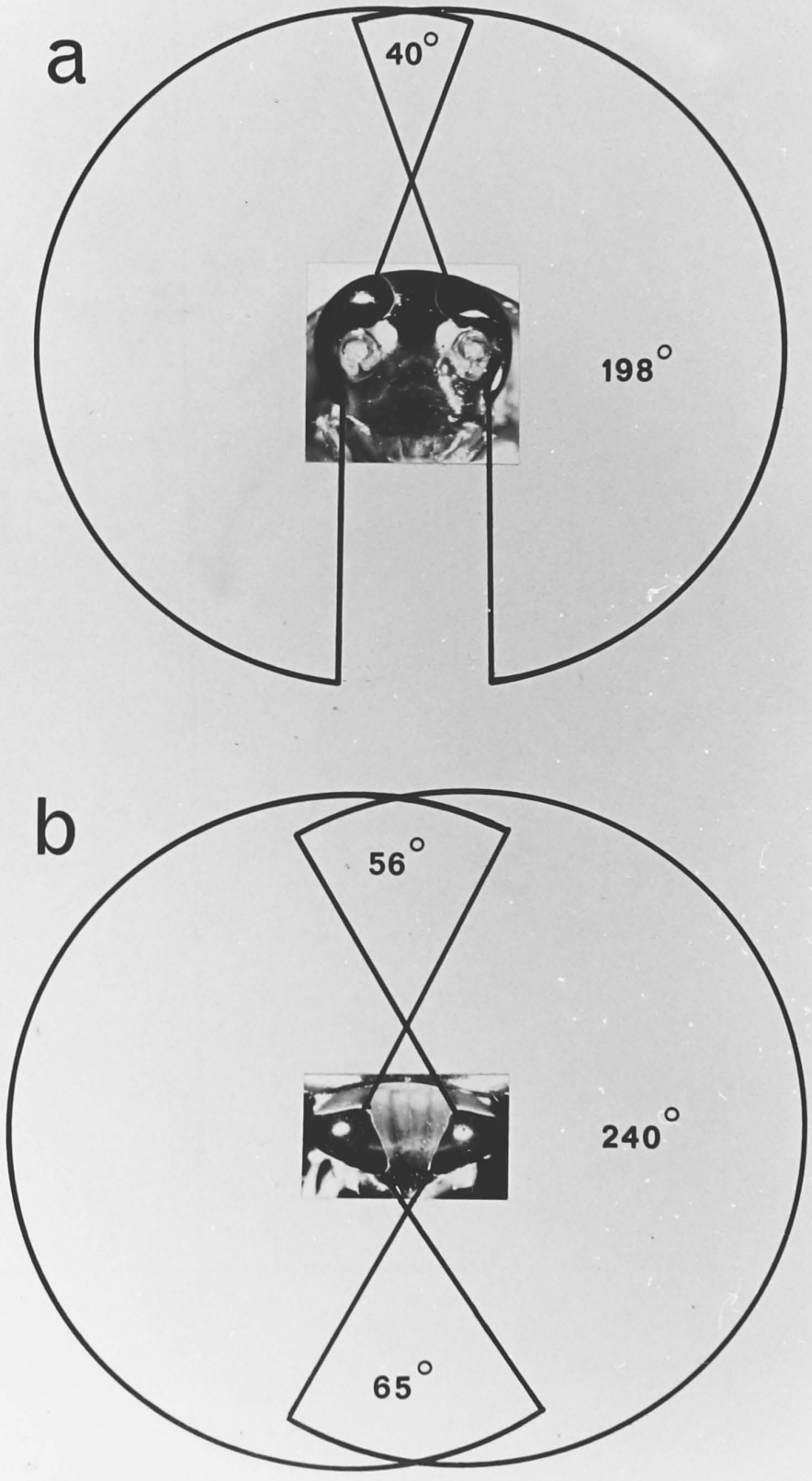
a
40°
198°
b
56°
240°
65°

Figure 13

Diagrammatic representation of one ommatidium in Periplaneta americana.

The major features are shown and labelled. The two sections in the centre, cut transverse to the longitudinal axis, show the anatomical changes which occur on light/dark adaptation. In the dark-adapted (DA) state, pigment is separated from the rhabdom by a palisade. This disappears with light adaptation (LA).

Trachea were not observed above the basement membrane.

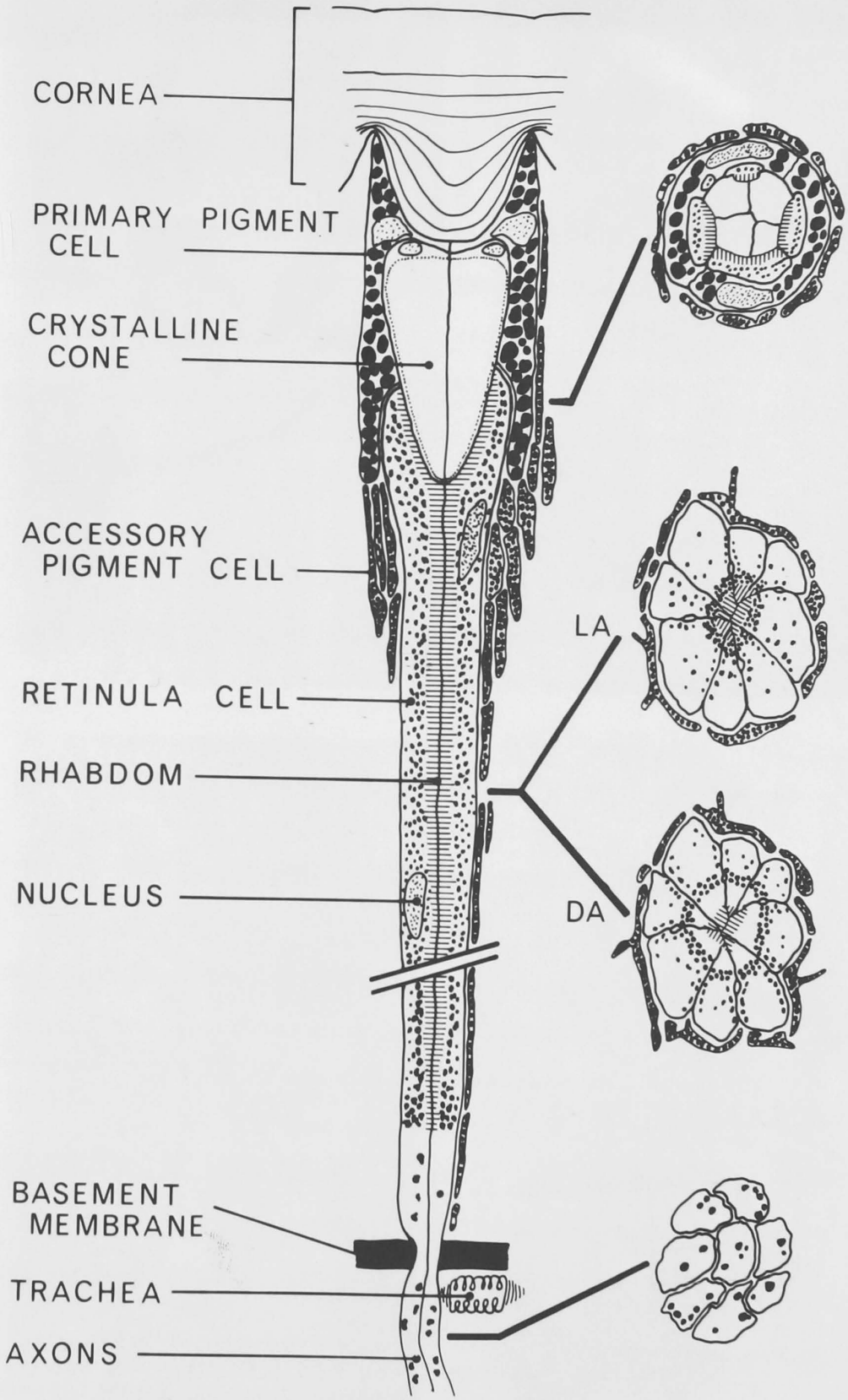
CORNEA
PRIMARY PIGMENT CELL
CRYSTALLINE CONE
ACCESSORY PIGMENT CELL
RETINULA CELL
RHABDOM
NUCLEUS
BASEMENT MEMBRANE
TRACHEA
AXONS
LA
DA

Figure 14

Gross morphology of the retina.

a. Longitudinal section to ommatidial axis, showing the thick, stratified cornea and the crystalline cones with rhabdom engulfing the apex. Inset. Similar section, emphasizing the rhabdom-cone relationship.

b. Transverse section to ommatidial axis, simultaneously showing crystalline cones at three different levels. The contributions made by the four cone, or Semper's, cells are clearly evident at the distal end (right side).

c. Interference micrograph of the cornea, showing the three strata referred to in the text. The micrograph was taken on a Zeiss interference microscope, of fresh tissue cut at 15 µm with a Leitz freezing sledge microtome. As the Eringhaus rotary compensator is turned, the points where the fringe turns black last have the highest refractive index.

d. Longitudinal section through the retina of a newly hatched first instar larva (in the horizontal plane). Inter-ommatidial angles and the proportions of cone and rhabdom to ommatidial size are greater than in the adult.

C, cornea; CC, crystalline cone; R, rhabdom

Scales. a-d, 25 µm


C
CC
R
a

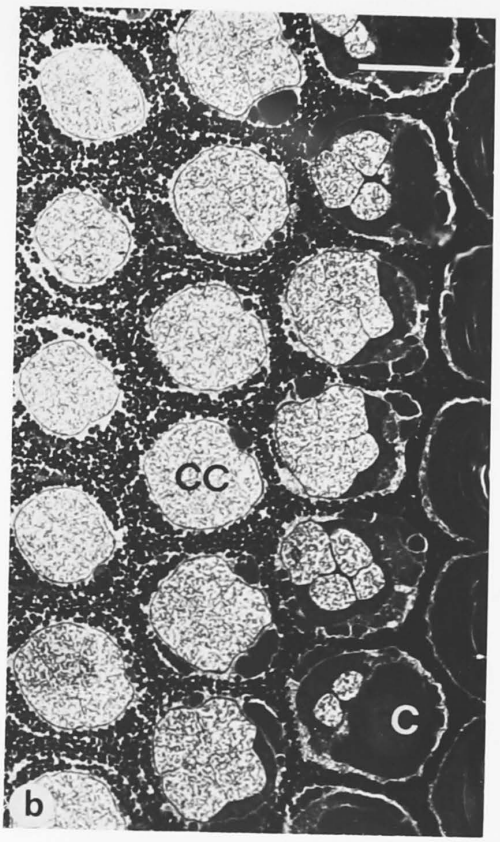
CC
C
b

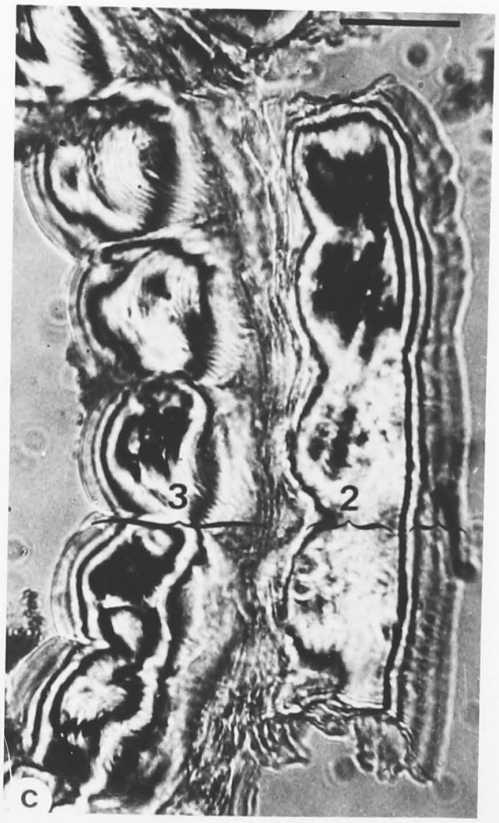
3
2
c

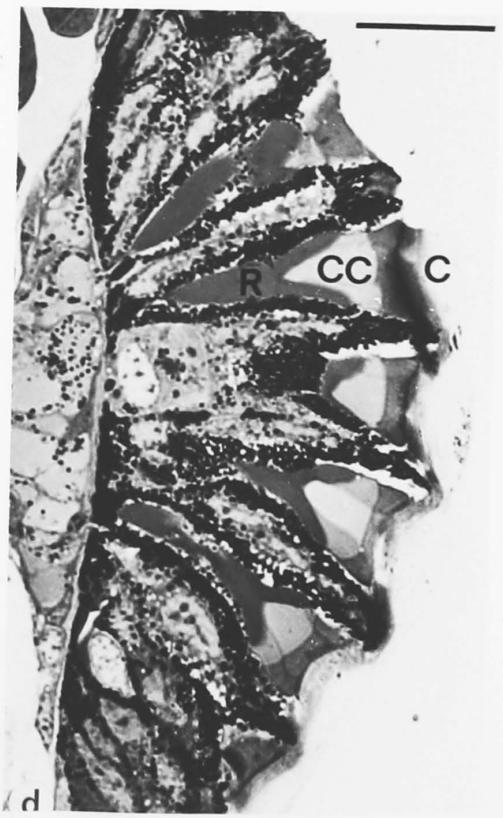
R
CC
C
d

Figure 15

Ultrastructure of the cornea.

a. In the first (distal) corneal stratum, the limiting outline of the underlying corneal convexity is evident in transverse section. There is just a hint (arrow) that this is at the uppermost level of the spiralling filaments.

b. The spiralling filaments are quite evident at the top of level 3. They appear to originate in the centre, and are more closely packed at the periphery.

c. About half way down level 3, the primary and accessory pigment cells can be seen between the internal corneal convexities.

d. Near the bottom of the cornea, two primary pigment cells surround the convexity, and these, in turn, are surrounded by accessory pigment cells.

C, cornea; PPC, primary pigment cell; APC, accessory pigment cell

Scales. a-d, 5 µm

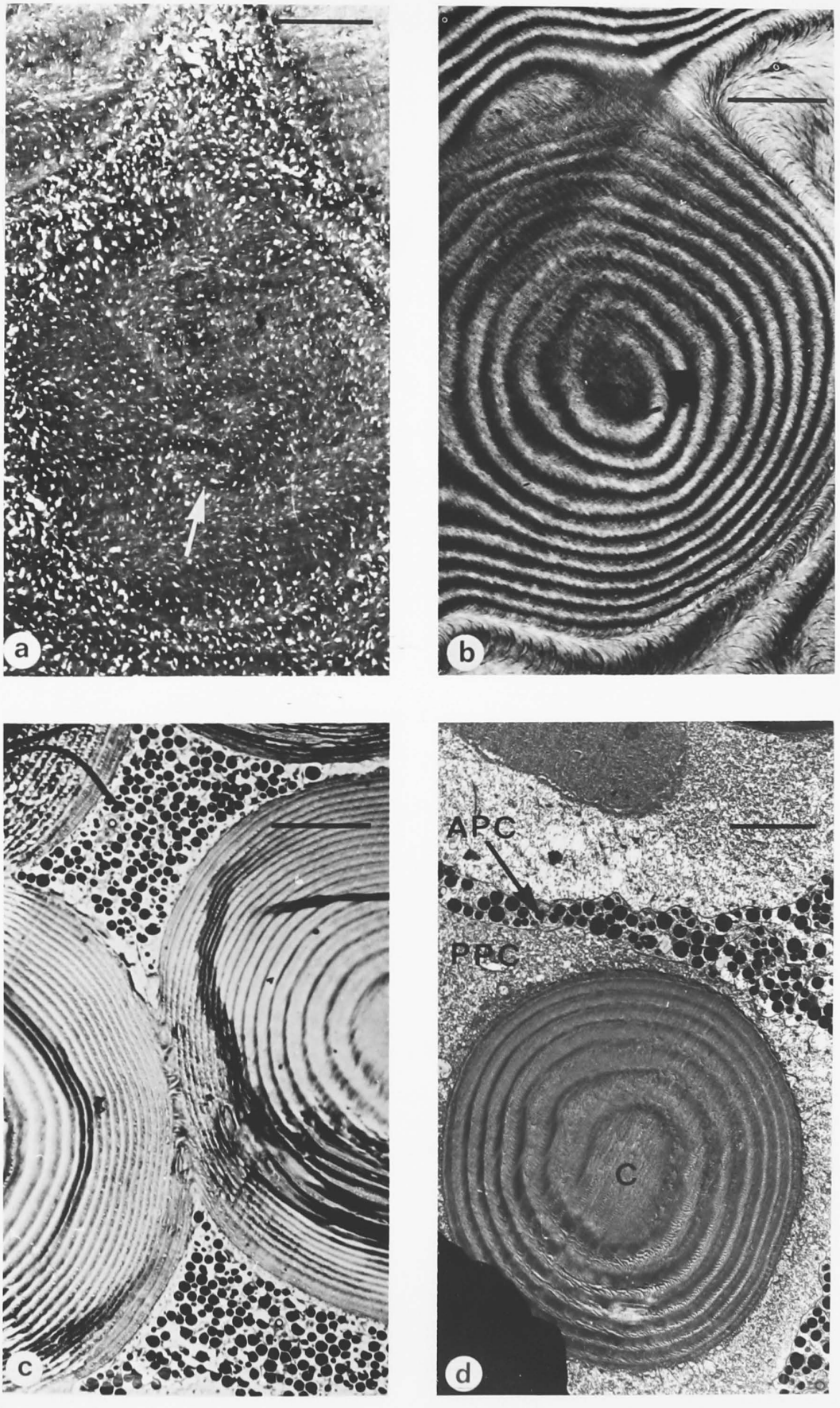
a
b
c
APC
PPC
C
d

Figure 16

Ultrastructure of the dioptric apparatus.

a. Most of the cornea and crystalline cone (and perhaps all) are separated by thin processes of the primary pigment cells.

b. Slightly oblique section near the top of the crystalline cone.

c. The primary pigment cell nuclei and the cone, or Semper's, cell nuclei lie at the same level and are morphologically different.

d. The primary and accessory pigment cells are usually in intimate association. Accessory pigment cells can be distinguished by regions of densely packed pigment particles and nuclei which are morphologically different from the primary pigment cell nuclei.

C, cornea; CC, crystalline cone; PPC, primary pigment cell; SCN, Semper's cell nucleus; APC, accessory pigment cell

Scales. a-d, 5 µm

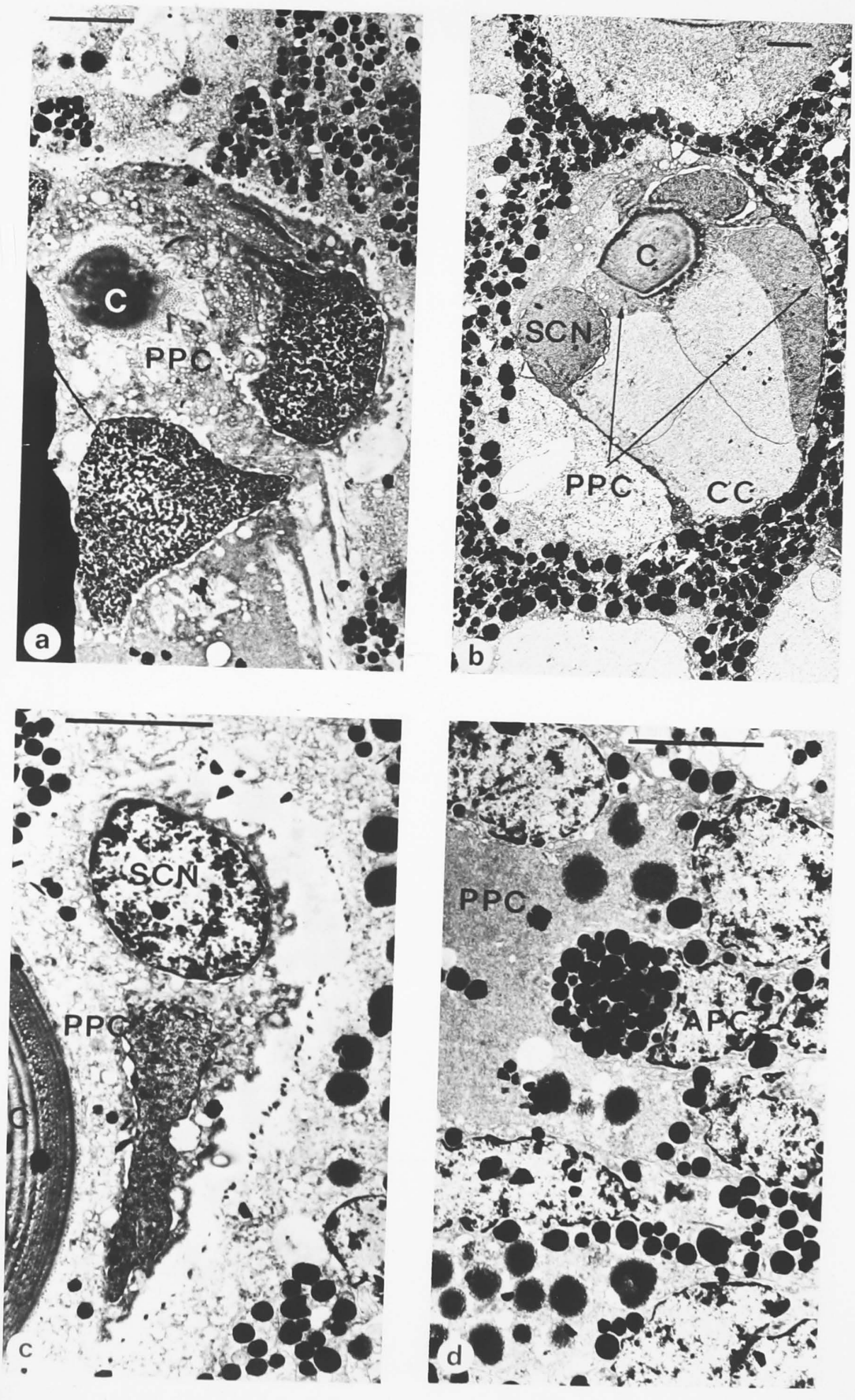
C
PPC
a
C
SCN
PPC
CC
b
SCN
PPC
C
c
PPC
APC
d

Figure 17

Ultrastructure of the dioptric apparatus.

a. The four elements which form the cyrstalline cone are easily seen in this section, cut transverse to the ommatidial axis. The symmetry of these elements was characteristic of all crystalline cones. The cones are immediately surrounded by two primary pigment cells whose adjoining borders are indicated by arrows. Outside these lie accessory pigment cells. The most distal part of one retinula cell is seen between one primary pigment cell and the cone. The cones were usually oriented so that the first four retinula cells to appear did so at the junctions of the Semper's cells.

b. Crystalline cone - primary pigment cell boundaries often exhibited irregularities, as shown in the micrograph.

CC, crystalline cone; PPC, primary pigment cell; APC, accessory pigment cell; RC, retinula cell

Scales. a and b, 5 µm

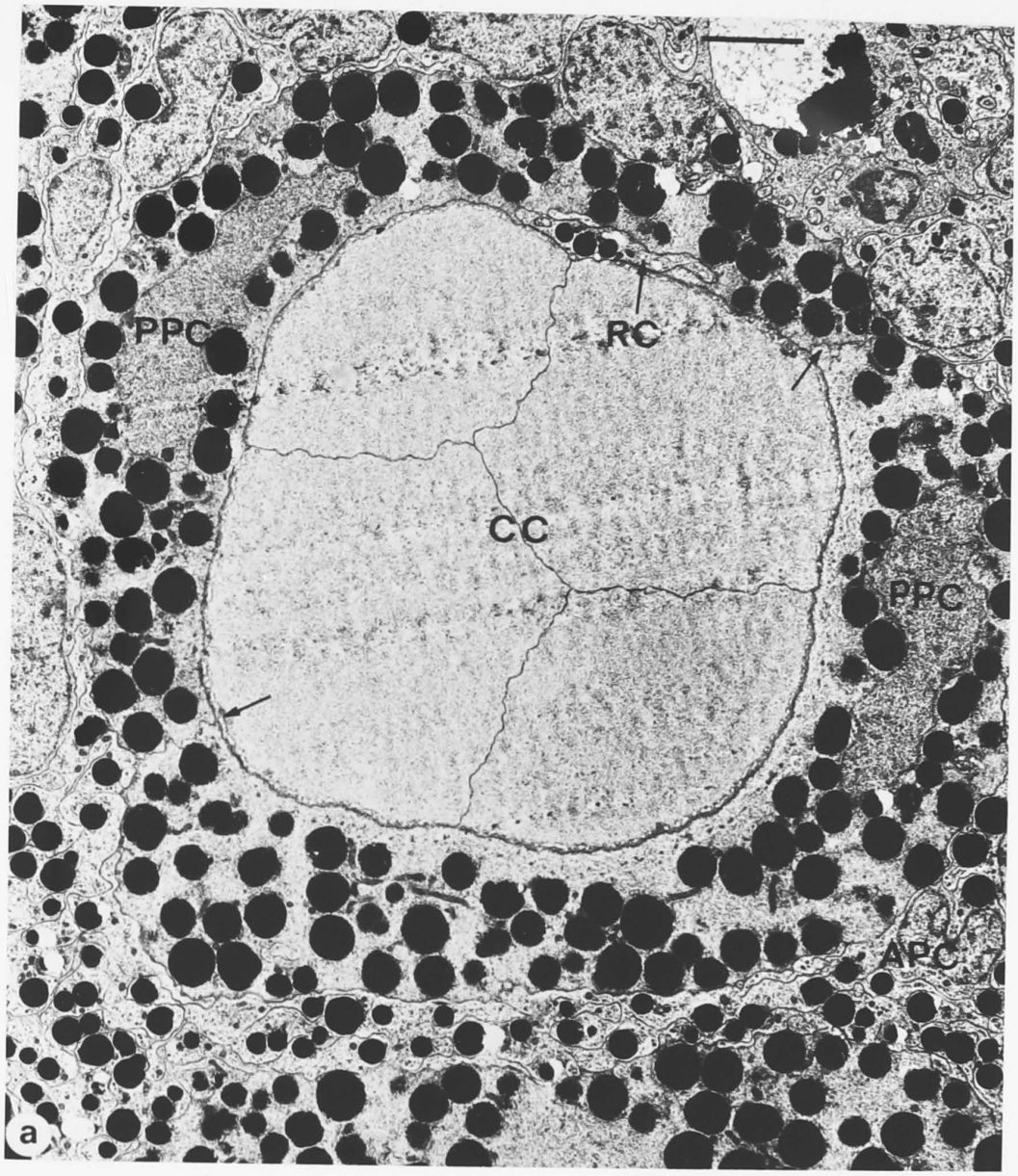
PPC
RC
CC
PPC
APC
a

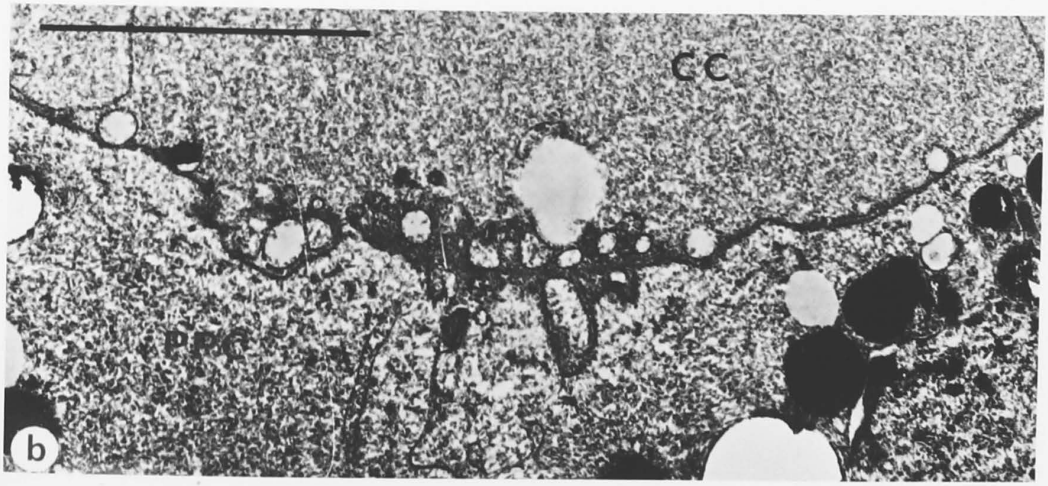
CC
PPC
b

Figure 18

Ultrastructure of the dioptric apparatus.

a. A section cut longitudinal to the ommatidial axis showing the relationship between cornea, primary pigment cells and crystalline cone. In this case, the base of the crystalline cone complex is flat.

b. A section similar to (a), but showing how the base of the cone complex can conform to the convexity of the cornea.

C, cuticle; CC, crystalline cone; PPC, primary pigment cell; SCN, Semper's cell nucleus.

Scales. a and b, 5 μm

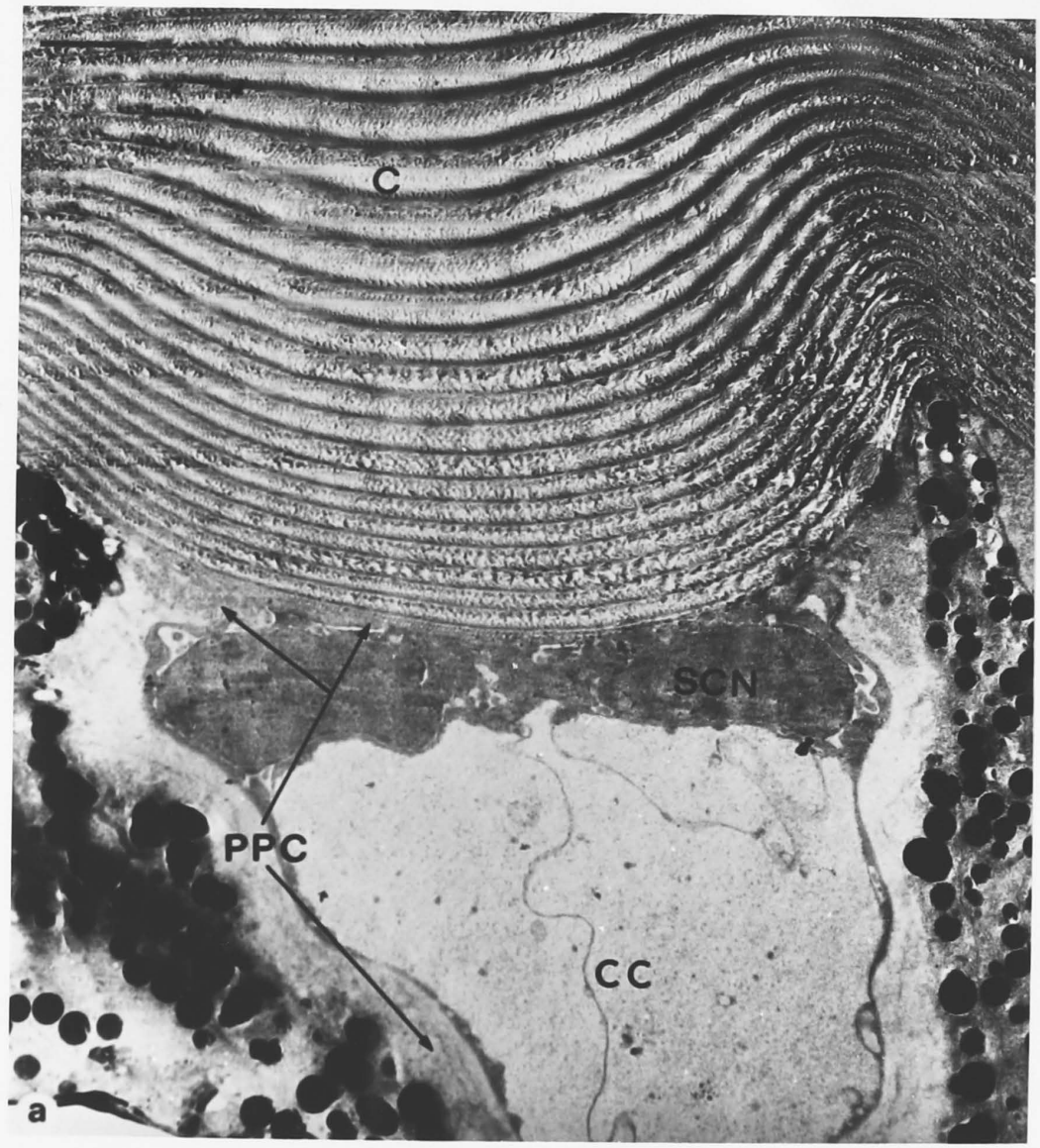
C
SCN
PPC
CC
a

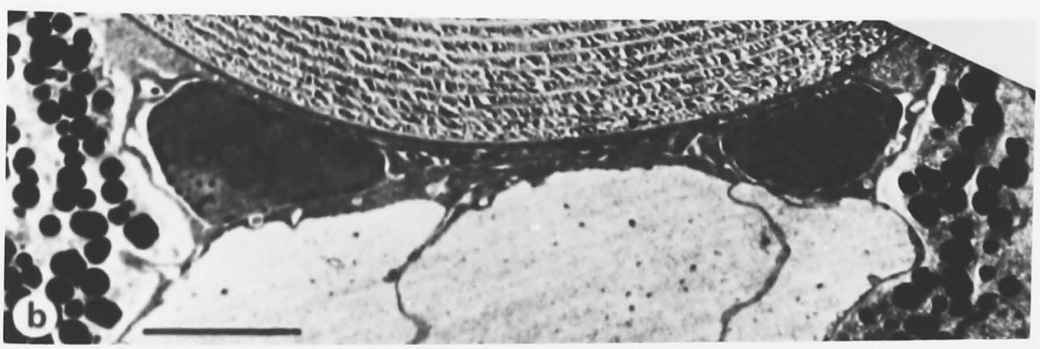
b

Figure 19

Ultrastructure of the dioptric apparatus.

a. This micrograph was included to show just how narrow the banding becomes as the spiralling corneal filaments approach their proximal limit.

b. The primary and accessory pigment cells extend distal to the cone base and form intimate contacts with the cornea.

c. Microtubules are evident in the pigment cells (shown in (b)) and appear to be associated with cell adhesion to the cornea.

C, cornea; PPC, primary pigment cell; APC, accessory pigment cell; MT, microtubules

Scales. a and b, 5 μm; c, 2.5 μm


a

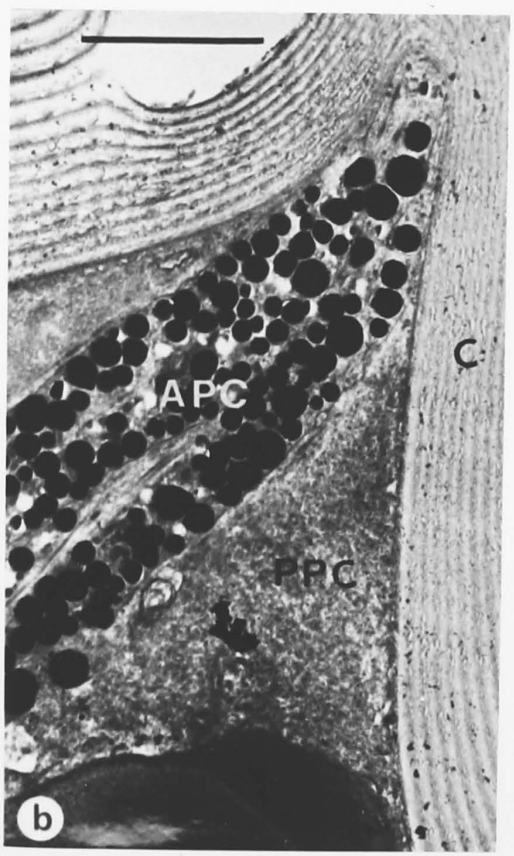
APC
C
PPC
b

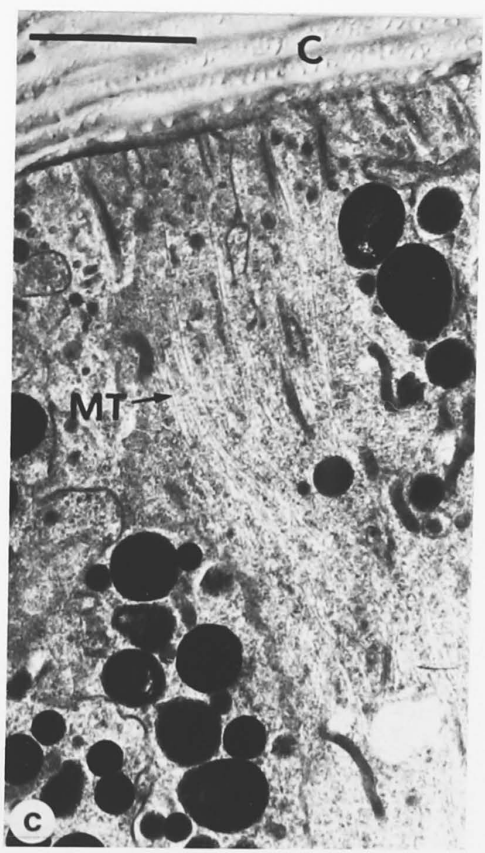
C
MT
c

Figure 20

Ultrastructure of the retinula cells.

a. Rhabdomeres extend distally nearly as far as the retinula cells themselves, and infiltrate deeply into the cone, as shown in these transverse sections. The retinula cell can be identified between the primary pigment cell and cone by the smaller size of the retinula cell pigment particles.

b. One rhabdomere (LHS) is penetrating deeply into the cone, while the other appears to have penetrated the cone either above or below the section, and is infiltrating the cone vertically.

c. Near its apex, the cone loses its symmetry and the rhabdomeres have nearly completed fusion.

d. The extent to which the cone can be infiltrated by rhabdom is evident by its vermiculations in this micrograph.

CC, crystalline cone; PPC, primary pigment cell; R, rhabdom(ere)

Scales. a and b, 5 µm; c, 2.5 µm; d, 1 µm

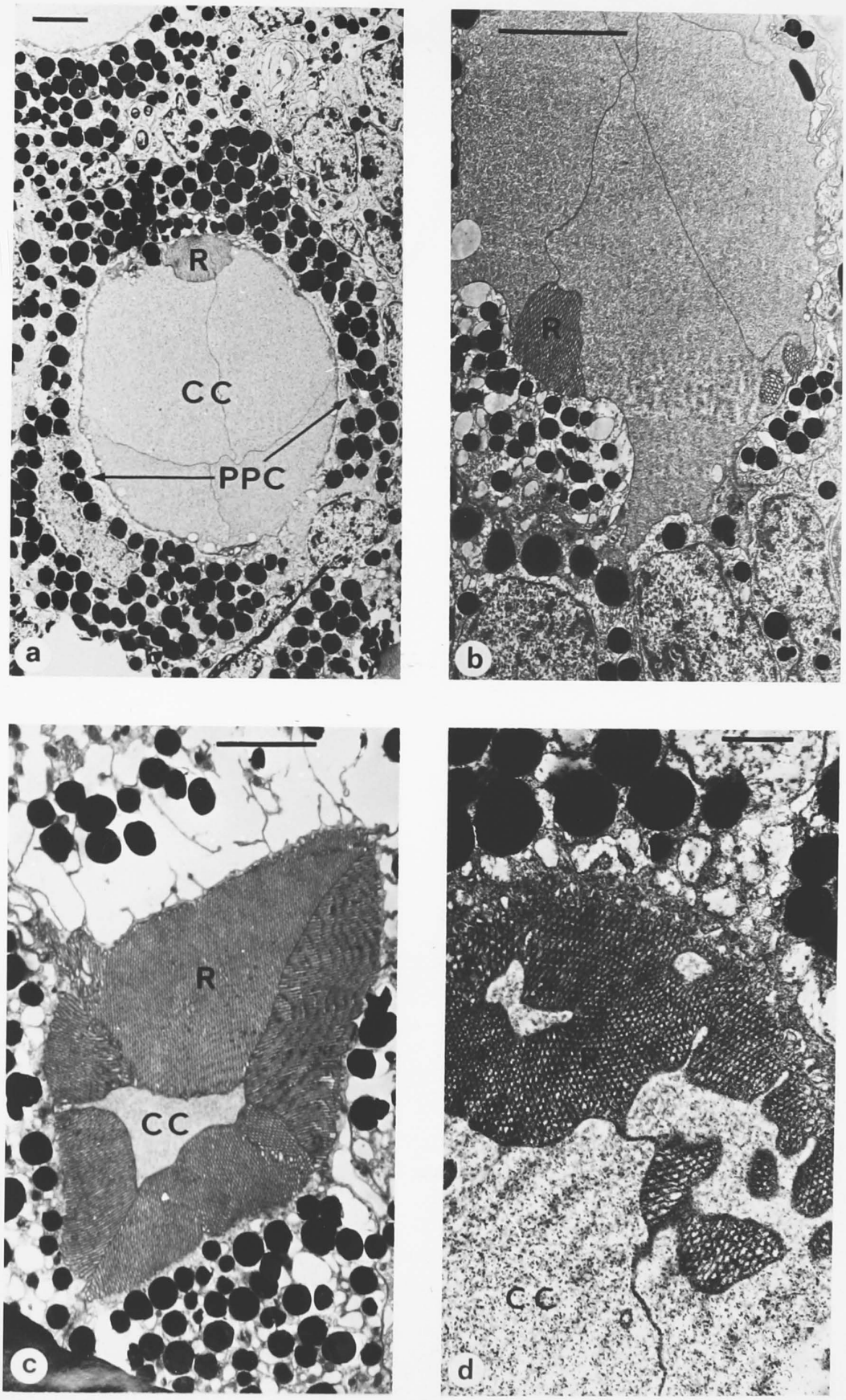
R
CC
PPC
a
R
b
R
CC
c
CC
d

Figure 21

Ultrastructure of the retinula cells.

a. This longitudinal section shows the rhabdom engulfing the apex of the crystalline cone. Note how irregular the cone walls have become at this level. The top of the retinula cell on the left hand side of the cone is indicated by the arrowheads.

b and c. Further illustrations, in longitudinal sections, of rhabdomere infiltration of the crystalline cone.

CC, crystalline cone; R, rhabdom(ere).

Scales. a-c, 2.5 µm

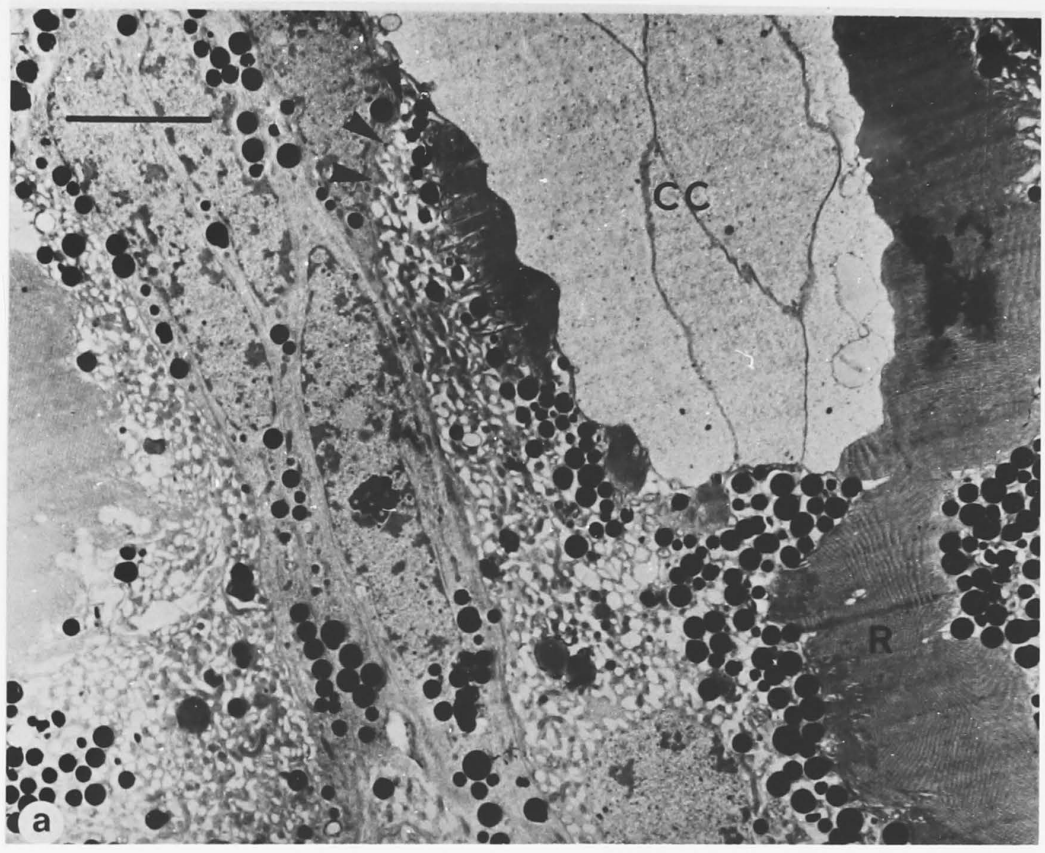
CC
R
a


CC
R
b

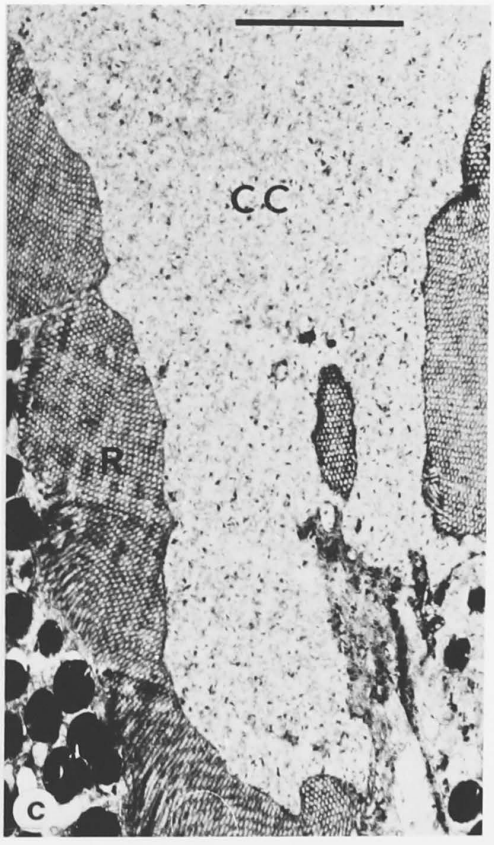
CC
R
c

Figure 22

Ultrastructure of the retinula cells. The light-adapted state.

Each ommatidium is composed of eight retinula cells, each of which contributes to the rhabdom. These are numbered 1 to 8, but DO NOT necessarily correspond to the numbering sequence of this chapter, section B1, and CHAPTER V. There is no evidence of extracellular space (cf. Smith, 1968). Accessory pigment cells fill the spaces between adjacent ommatidia. This ommatidium is light adapted and the retinula cell screening pigment particles lie adjacent to the rhabdom. Four cone cell processes run proximally through the retina between pairs of retinula cells and are indicated by the arrows.

APC, accessory pigment cell; R, rhabdom

Scale. 5 µm

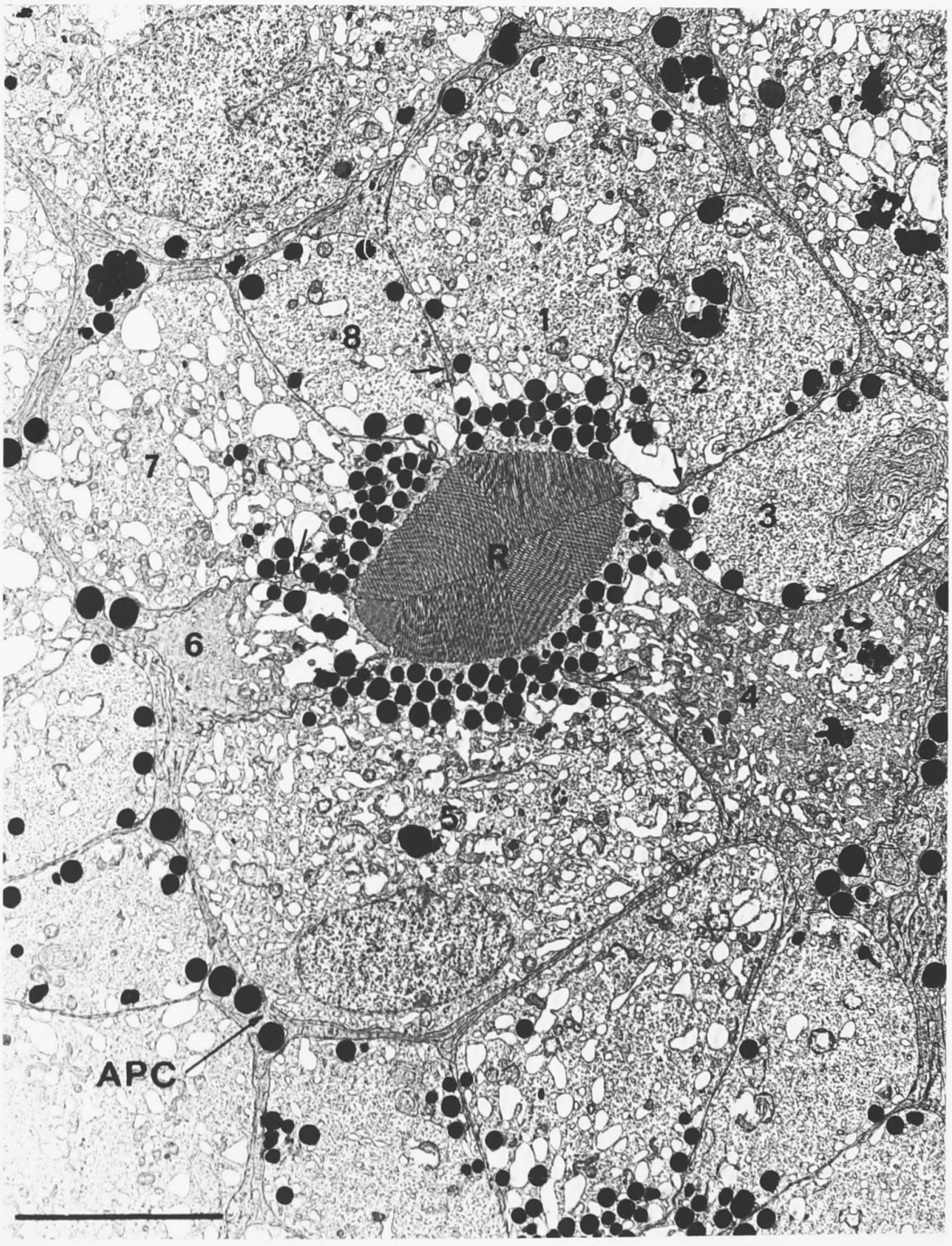
1
2
3
4
5
6
7
8
R
APC

Figure 23

Ultrastructure of the retinula cells.

The light-adapted state.

a, b and c. These transverse sections show ommatidial profiles similar to that in Fig. 22, but at increasing depths in the retina from the corneal surface. In each case, eight retinula cells are present and again these DO NOT necessarily correspond to those described in section B1 and CHAPTER V. The rhabdom and retinula cells generally decrease in diameter with increasing retinal depth. In (c), cell 1 has left the rhabdom and cells 3, 4 and 6 seem to be ready to do the same. Cell 1 corresponds to cell number three of Trujillo-Cenóz and Melamed, (1971).

d. In the light adapted state, the retinula cell screening pigment assumes a position adjacent to the rhabdom. Pigment particles rarely touch the rhabdom with a narrow band of cytoplasm usually remaining between the most proximal particles and rhabdom.

e. The cone cell extensions have the same general appearance as the cone. The example shown here contains microtubules. Desmosomes, which hold the retinula cells together, are also clearly visible.

CC, cone cell extension; R, rhabdom; D, desmosome

Scales. a-c, 5 µm; d, 0.5 µm; e, 1.0 µm

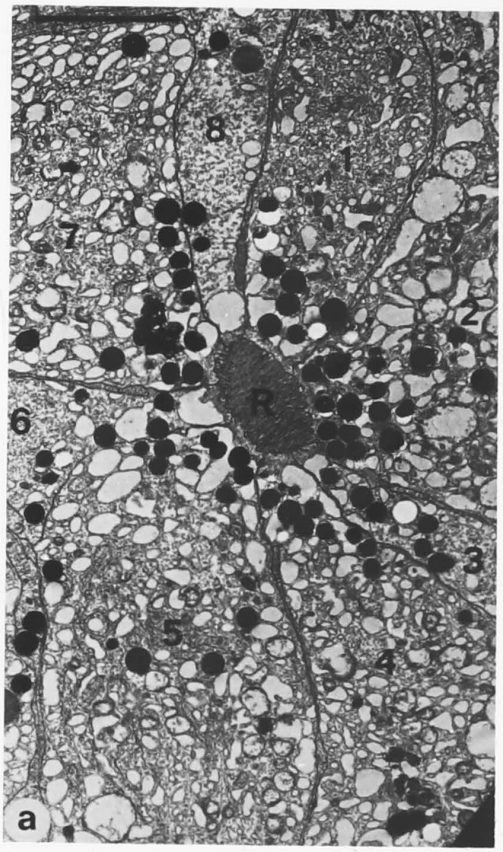
8
1
7
2
R
6
3
5
4
a

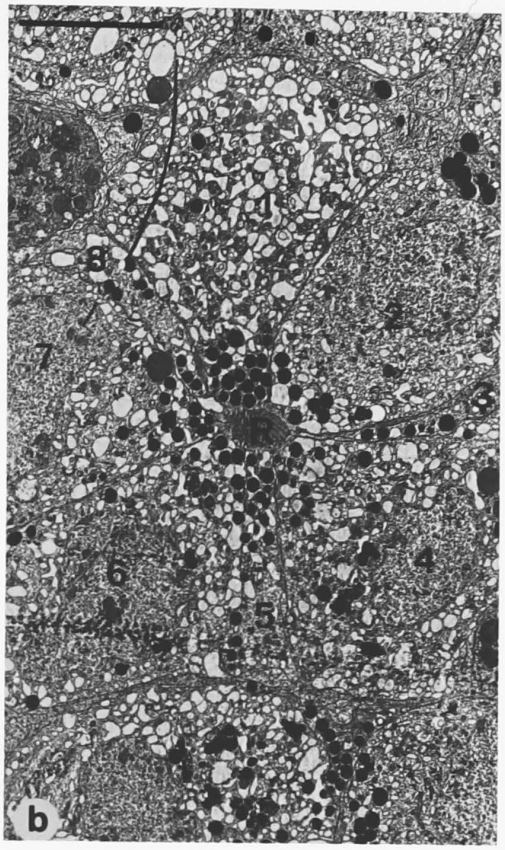
1
8
7
3
R
6
4
5
b

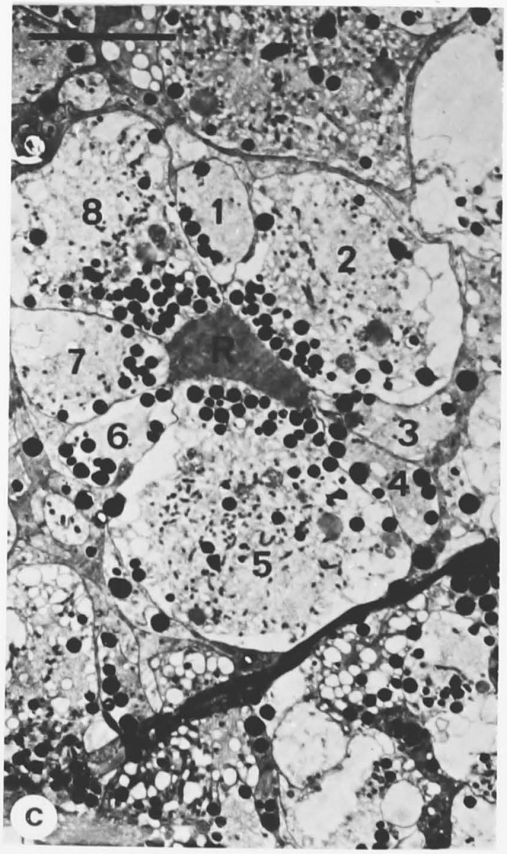
8
1
2
7
R
6
3
4
5
c

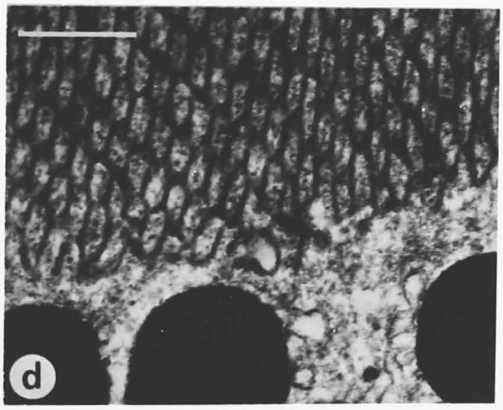
d

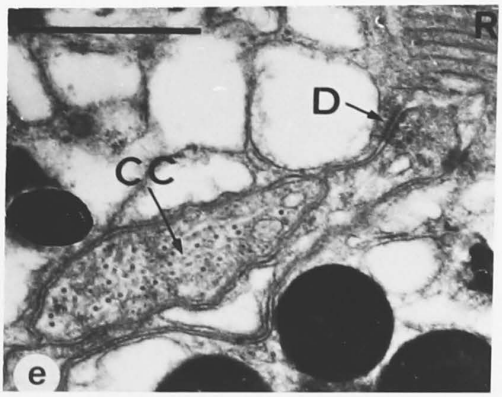
R
D
CC
e

Figure 24

Ultrastructure of the rhabdom.

a. The contributions to the rhabdom of three retinula cells are shown. In this case, they appear to be retinula cell microvilli. The material is rather poorly fixed, but is used as an example to show how rhabdomeres with parallel lamellae fuse together to form one cohesive structure.

b. This micrograph shows proof that the rhabdom is not a single unit structure but composed of the fused rhabdomeres of individual retinula cells. The rhabdomeres on the left hand side appear intact and are easily distinguished from the disordered rhabdomere on the right.

c. Substructure of the rhabdomere. The tubules of the honey-comb array contain a dense core. Some of the walls appear to be joined by tight junctions (arrows).

d. Disrupted rhabdomere which does not fit the microvillus theory (see text). Examples of a "double microvilli" are indicated by arrowheads and "half microvilli" by arrows.

R, rhabdom(ere); D, desmosome

Scales. a and d, 0.5 µm; b, 1 µm; c, 0.25 µm

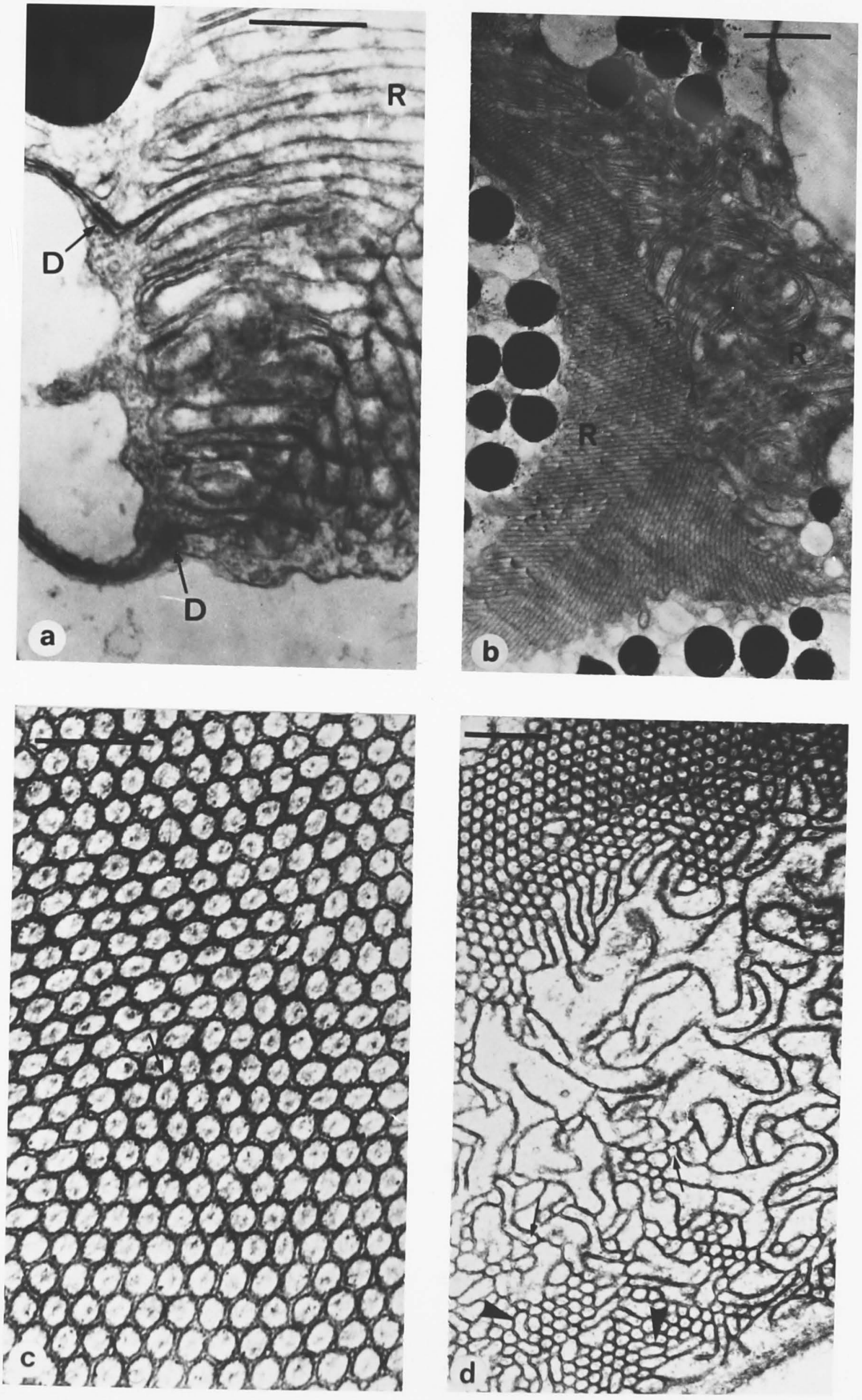
R
D
D
a
R
R
b
c
d

Figure 25

Ultrastructure of the rhabdom.

a. The lamellae of the rhabdomeres all tend to be orthogonal to the longitudinal axis of the ommatidium, and the cone as well, as is shown in (a).

b, c and d. These are different longitudinal sections through the rhabdom showing that the walls of the rhabdomere lamellae in adjacent retinula cells lie exactly opposite each other, appearing as if they were continuous across the whole rhabdom.

Note : The crystalline cone in (a), contains particulate organelles which have been identified in other insects as β-glycogen (Perreleta, 1970).

CC, crystalline cone; R, rhabdom(ere)

Scales. a, 0.25 µm; b, 0.5 µm; c and d, 2.5 µm

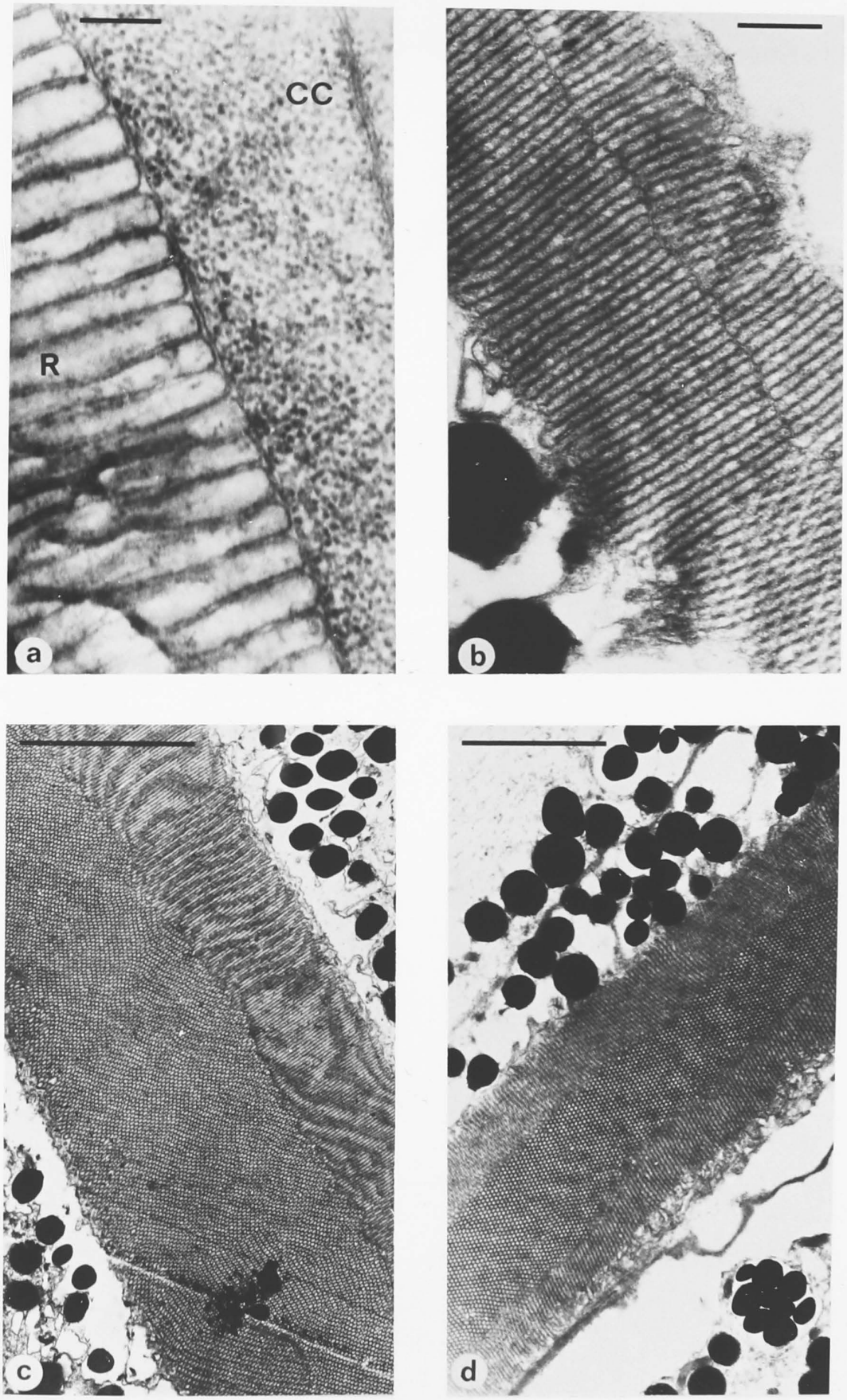
CC
R
a
b
c
d

Figure 26

Ultrastructure of the retinula cells.
The dark-adapted state.

When an ommatidium is dark-adapted, the endoplasmic reticulum develops cisternae which collect beside the rhabdom, forming a palisade. Unusually high concentrations of mitochondria were often seen behind the palisade. Eight cells are evident within the ommatidium but are not numbered. The narrow channels between retinula cells seem to be filled with long extensions of accessory pigment cells. Cone cell extensions are indicated by arrows.

R, rhabdom; P, palisade; M, mitochondria

Scale. 2.5 µm

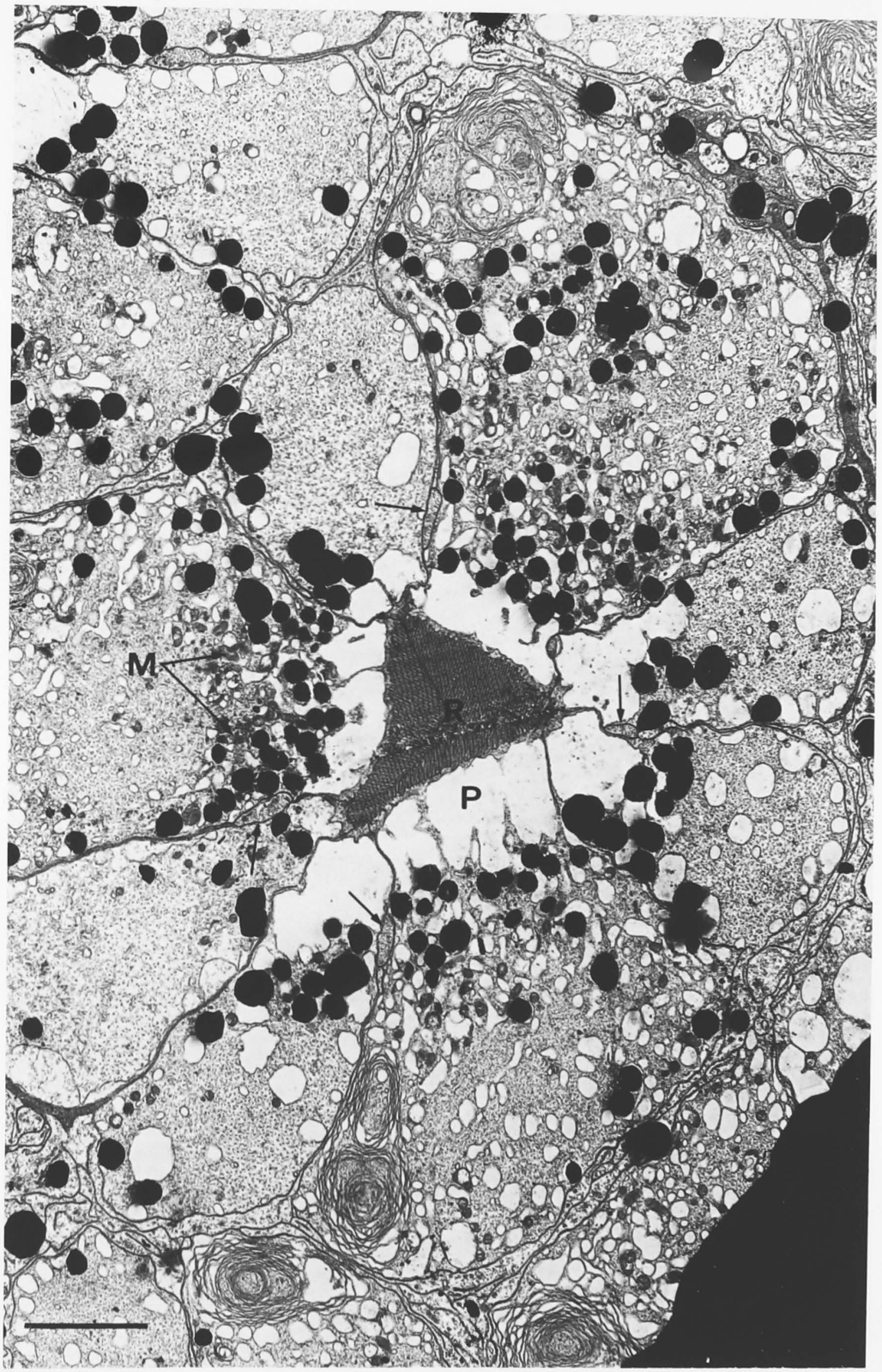
M
R
P

Figure 27

Development of the palisade.

a. Cisternae of the endoplasmic reticulum are collecting (or developing) beside the rhabdom. A thin layer of cytoplasm separates the palisade from rhabdom and forms bridges with the rest of the retinula cell cytoplasm. Longitudinal section.

b. Similar to (a), but in transverse section.

c. Early development of the palisade, showing developing cisternae.

d and e. Cisternae developing within the endoplasmic reticulum.

R, rhabdom(ere); P, palisade; D, desmosome; M, mitochondria; CIS cisternae; ER, endoplasmic reticulum

Scales. a, 2.5 µm; b, 0.5 µm; c-e, 0.25 µm

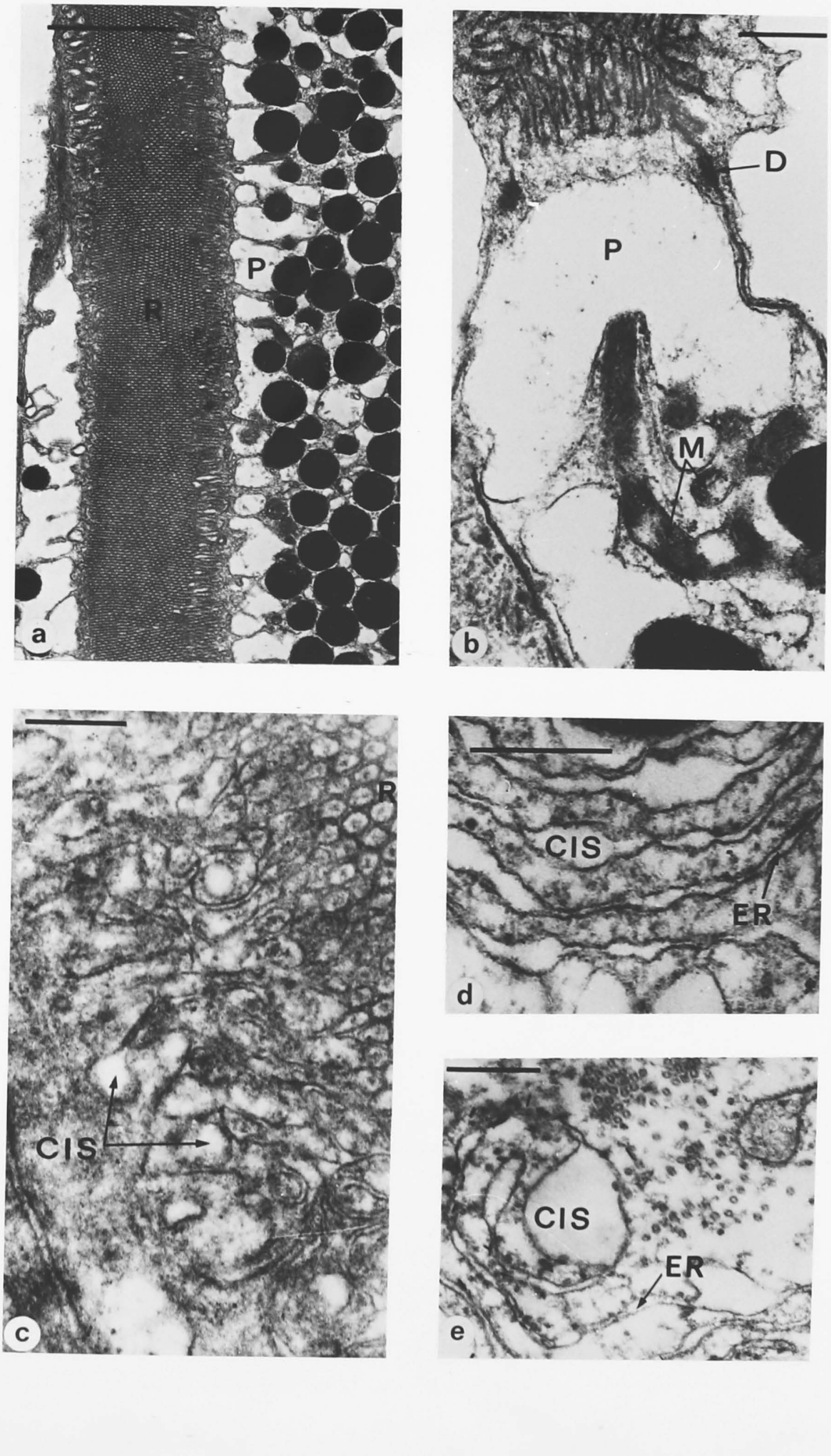
R
P
a
D
P
M
b
R
CIS
c
CIS
ER
d
CIS
ER
e

Figure 28

Ultrastructure of the proximal retina and axons.

a. The rhabdom ends abruptly some distance above the basement membrane. From this point, the retinula cells become axons, travelling in discrete bundles of eight. Longitudinal section.

b. The axon bundles constrict as they pass through the basement membrane, then expand again. Trachea are evident below the basement membrane only. Oblique section.

c. Transverse section through axon bundles. The upper right hand corner bundle is above the basement membrane, the upper left bundle is passing through and the lower left bundle is beneath the basement membrane. Axons in the latter bundle are numbered 1 to 8, and DO NOT necessarily correspond to the retinula cells as numbered in section B1 (this chapter) or CHAPTER V. Glial cells are evident beneath the fibrous basement membrane. Axons contain retinula cell screening pigment particles.

R, rhabdom; AX, axons; PC, pigment cell (whether basal or accessory is unknown); P, palisade; BM, basement membrane; T, trachea; G, glia

Scales. a and b, 2.5 µm; c, 5 µm

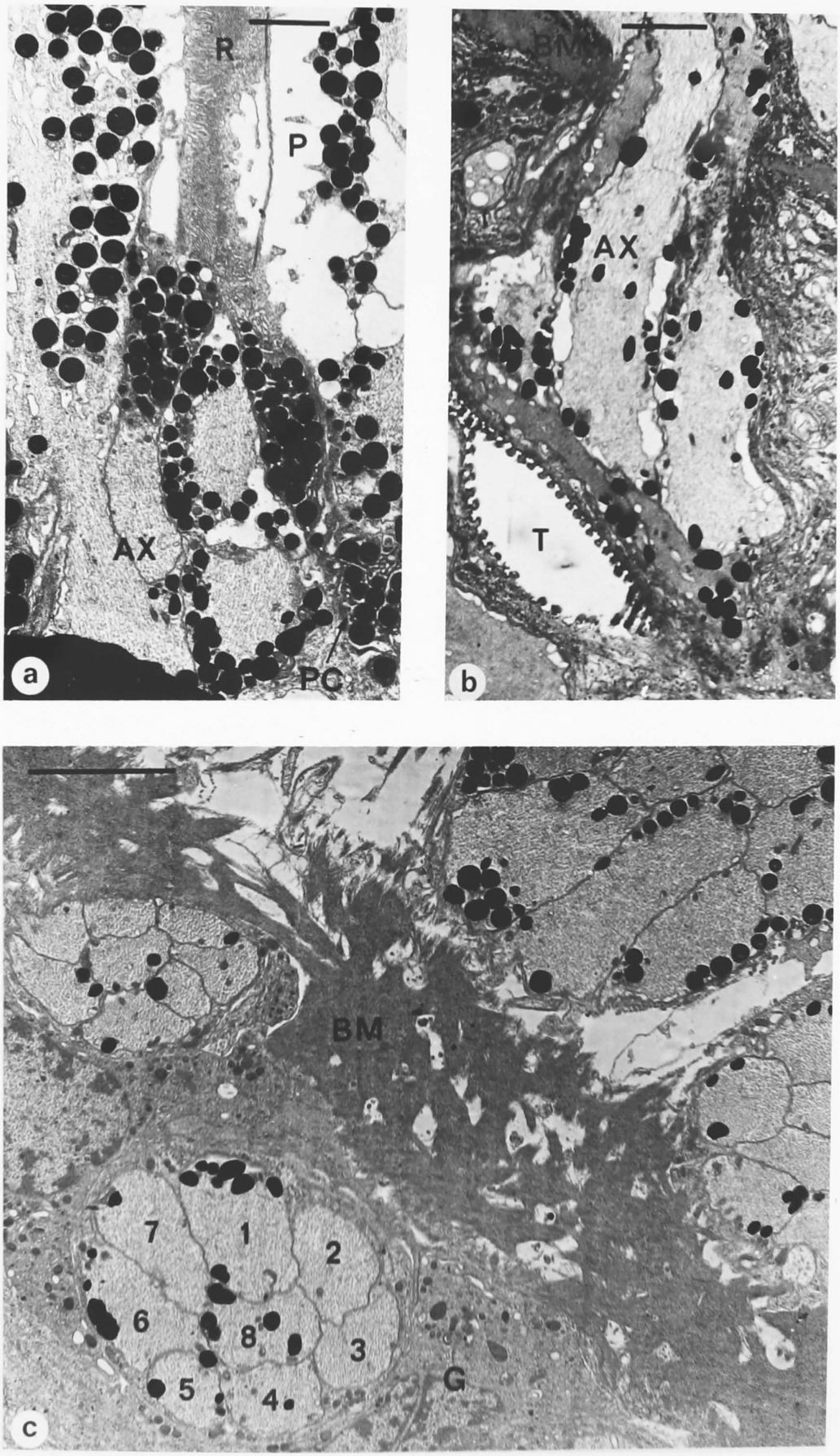
R
P
AX
PC
a
BM
AX
T
b
BM
7
1
2
6
8
3
5
4
G
c

Figure 29

Ultrastructure of the optic tract.

a. Beneath the basement membrane, the axon bundles blend together in the optic tract. Here they vermiculate within the tract as they proceed towards the lamina. Microtubules are evident in all axons. Elements of glial cells usually isolate axons from one another.

b. Lamina cell bodies occur distal to the lamina. The optic tract splits into arch-like configurations, passing between ordered stacks of somas.

G, glia; LCB, lamina cell body

Scales. a and b, 5 μm

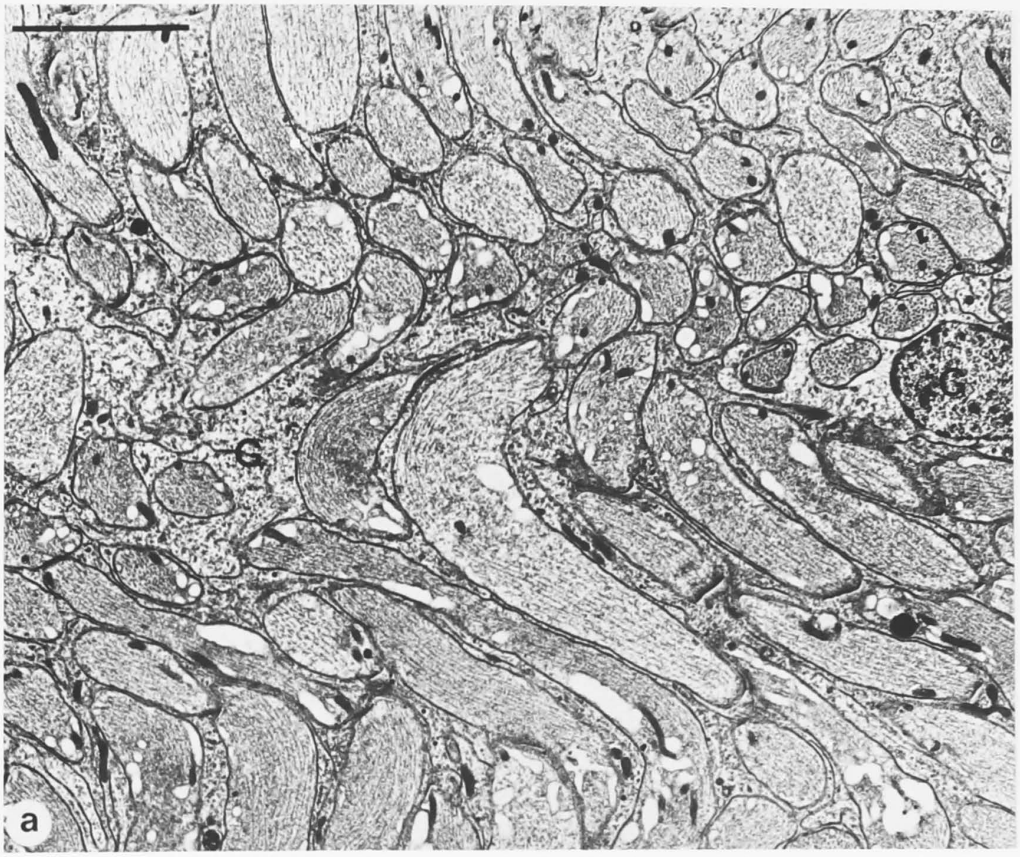
G
G
a

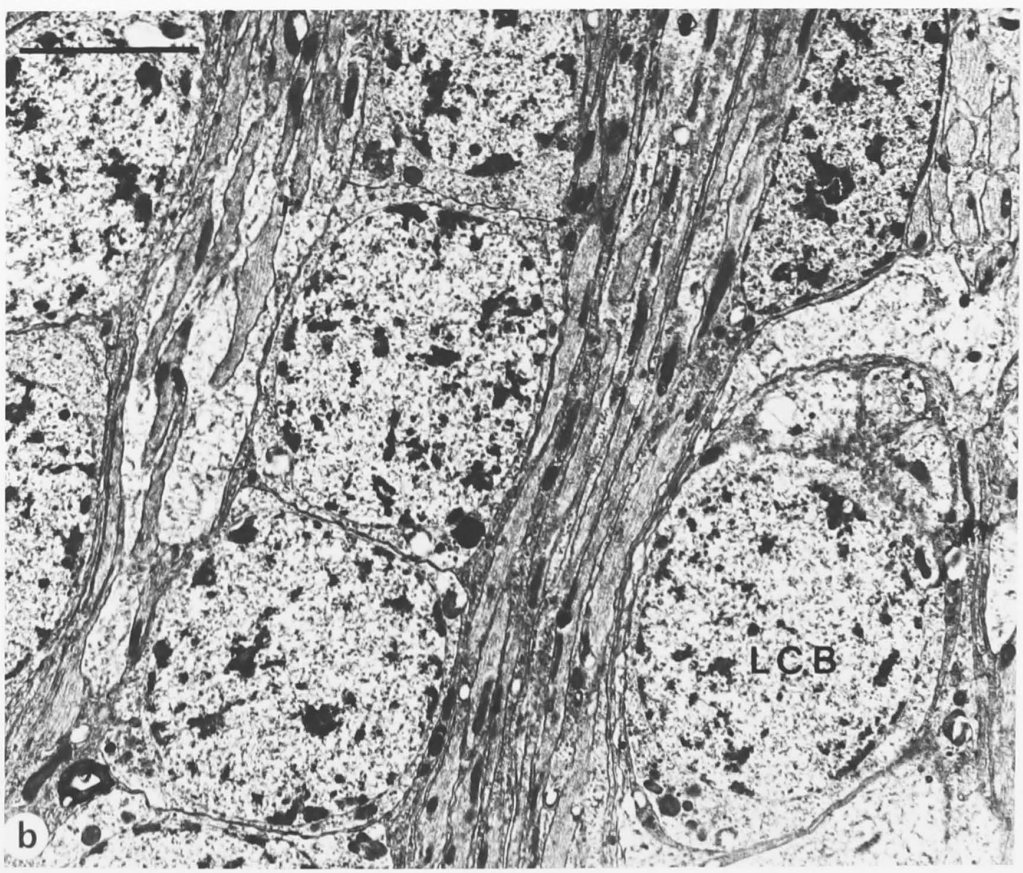
LCB
G
b

Figure 30

Inclusions

a. Primary pigment cell inclusions. The usual array of microtubules, endoplasmic reticulum, pigment particles, and vesicles is evident.

b. The differences between primary pigment cell and retinular cell pigment particles can be seen, the latter being smaller in diameter, with less diffuse edges.

c. Very thin sections of retinula cell pigment particles reveal a particulate substructure.

d. Primary pigment cell particles appear very dense, with no apparent substructure. The surface morphology is very variable.

PPC, primary pigment cell; R, rhabdomere, V, vesicle; ER, endoplasmic reticulum; MT, microtubules

Scales. a and d, 1 µm; b, 2 µm; c, 0.5 µm

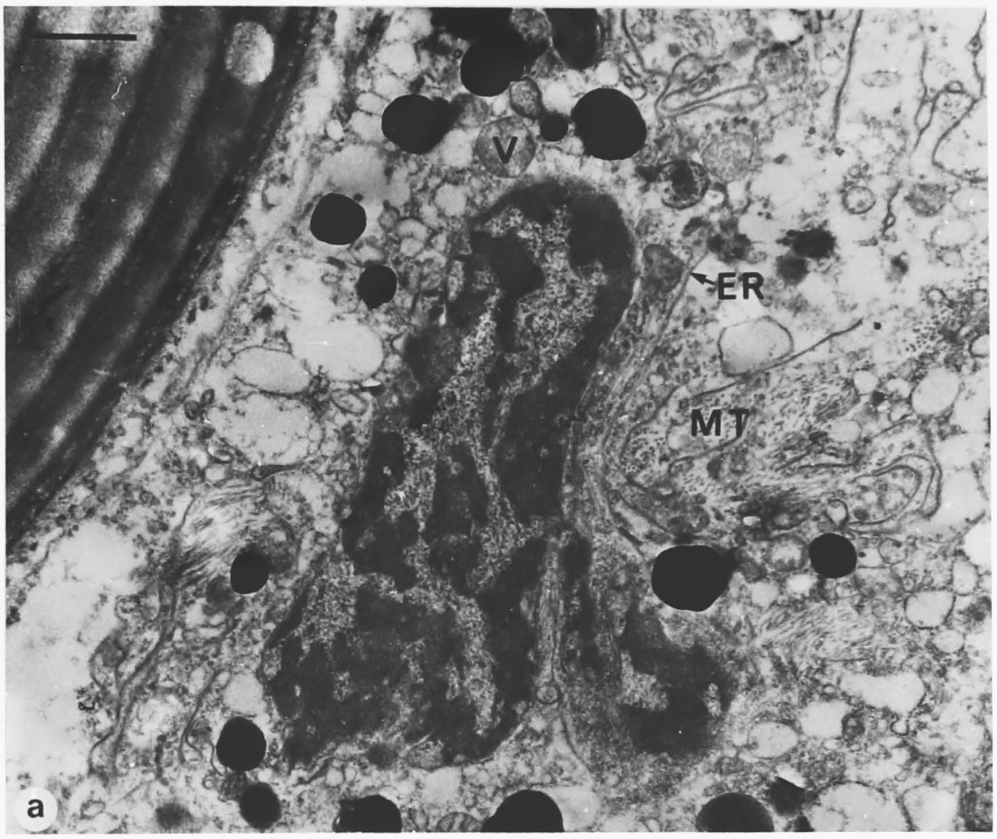
V
ER
MT
a

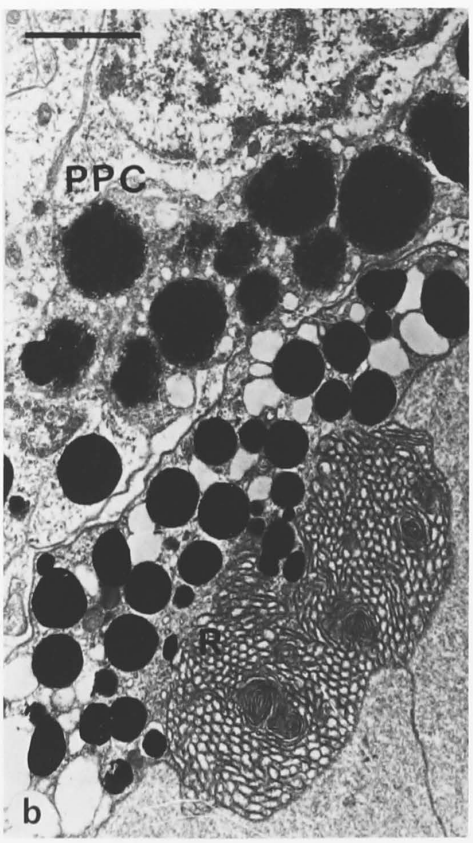
PPC
P
b

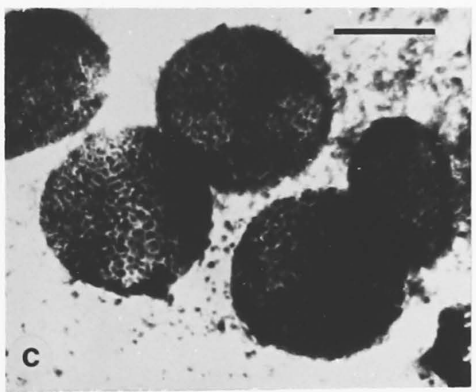
c

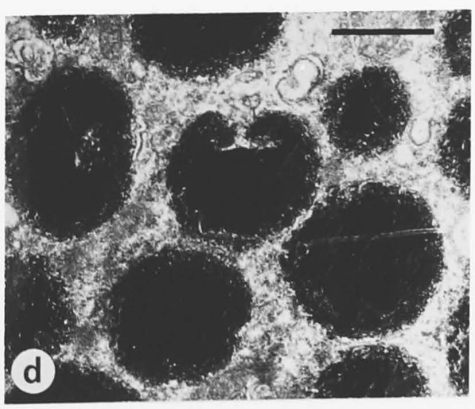
d

Figure 31

Some retinula cell inclusions

a. Microtubules.

b. Mitochondria.

c. Granular (rough) and agranular (smooth) endoplasmic reticulum.

d. Pigment particles enclosed in what Perrelet (1970) describes as a lyosome-like structure. He reports finding these in basal pigment cells.

e. Multivesicular bodies. Although these structureshave been related to lysosomal activities (Gordon et al., 1965), Fahrenbach (1969) suggests that their predominance in arthropod photoreceptors might be somehow related to vesicular storage of photopigment components.

f. A small intact (lower) multivesicular body and another (upper) which appears to be either coalescing or dispersing.

Scales. a-d, and f, 0.25 µm; e, 0.5 µm

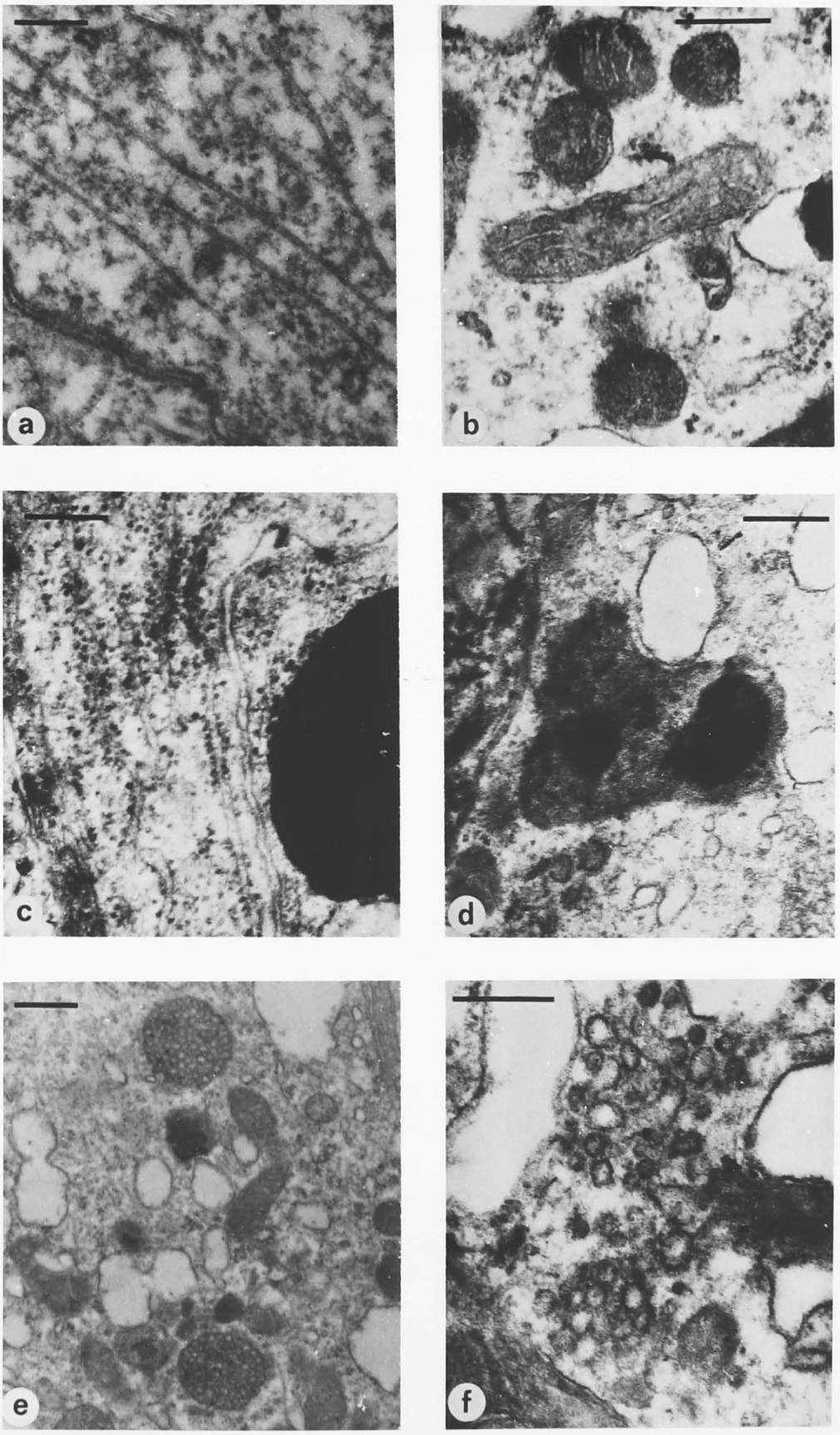
a
b
c
d
e
f

Figure 32

Ultrastructure of the first instar dioptric apparatus

The ultrastructure is very similar to that of the adult.

a. Longitudinal section of corneal laminations produced by spiralling filaments.

b. Oblique section through the crystalline cone and rhabdom.

c. Transverse section through the cone and rhabdom. The two primary pigment cells are evident and the rhabdomeres are infiltrating the cone, as in the adult. However, one rhabdomere (arrow) appears to have its tubular substructure parallel to the longitudinal axis of the ommatidium, instead of orthogonal.

C, cornea; CC, crystalline cone; SCN, Semper's cell nucleus; PPC, primary pigment cell; R, rhabdom(ere)

Scales. a-c, 2.5 µm

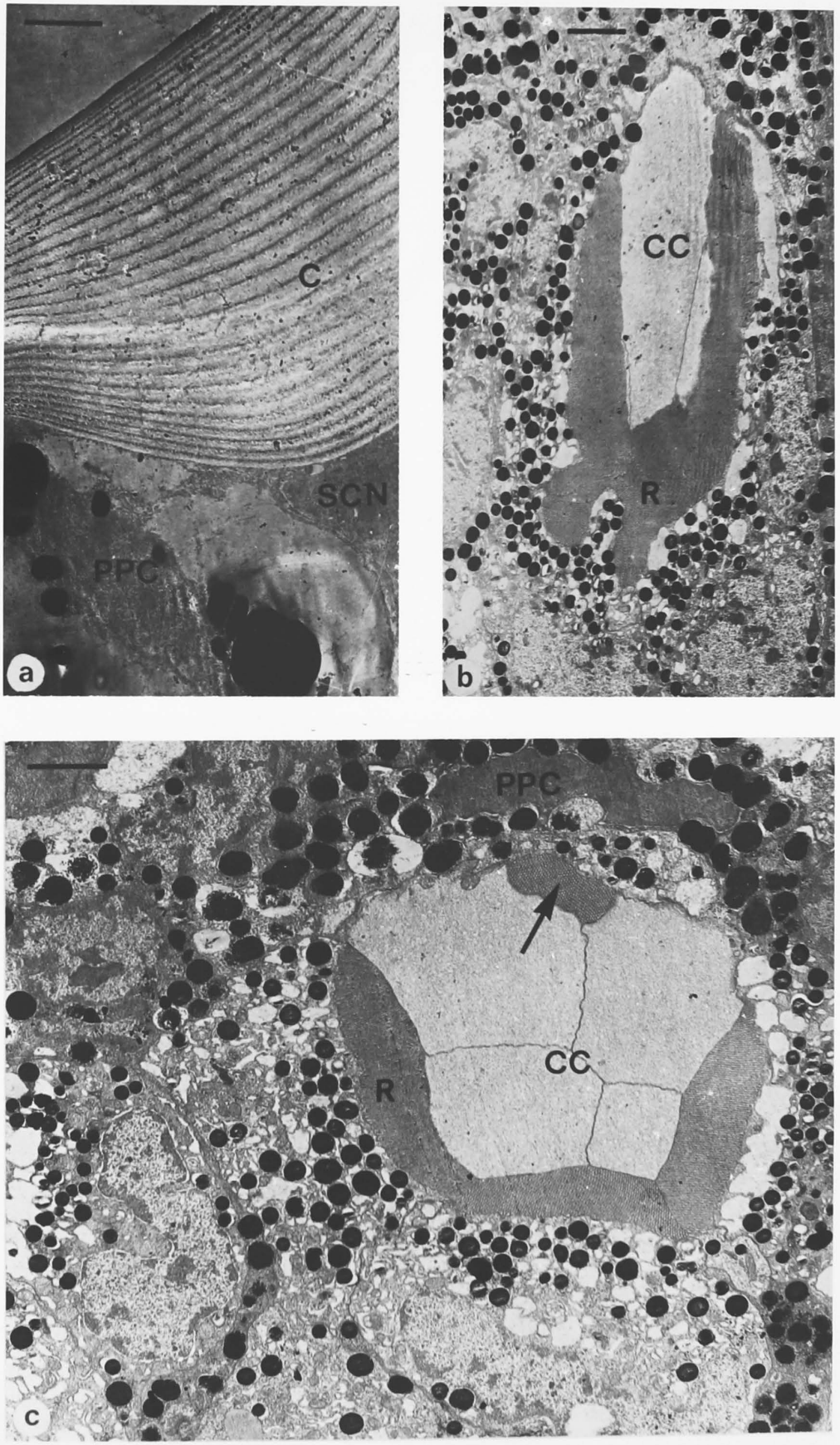
C
SCN
PPC
a
CC
R
b
PPC
CC
R
c

Figure 33

Ultrastructure of the first instar ommatidium

a. The morphology of the ommatidium is generally similar to the adult. Eight cells, are present and are numbered 1 to 8 (no reference is implied to section B1 or CHAPTER V). Cells 1, 2 and 3 seem to have their rhabdomere tubular substructure parallel to the ommatidial longitudinal axis, instead of perpendicular to it. Associations with pigment cells are, again, the same as the adult.

b. This is an aberrant ommatidia with only seven retinula cells present. This was noticed on two or three occasions in first instars, but never in the adult. Arrows indicate the presence of cone cell processes.

APC, accessory pigment cell; R, rhabdom

Scales. a and b, 2.5 µm

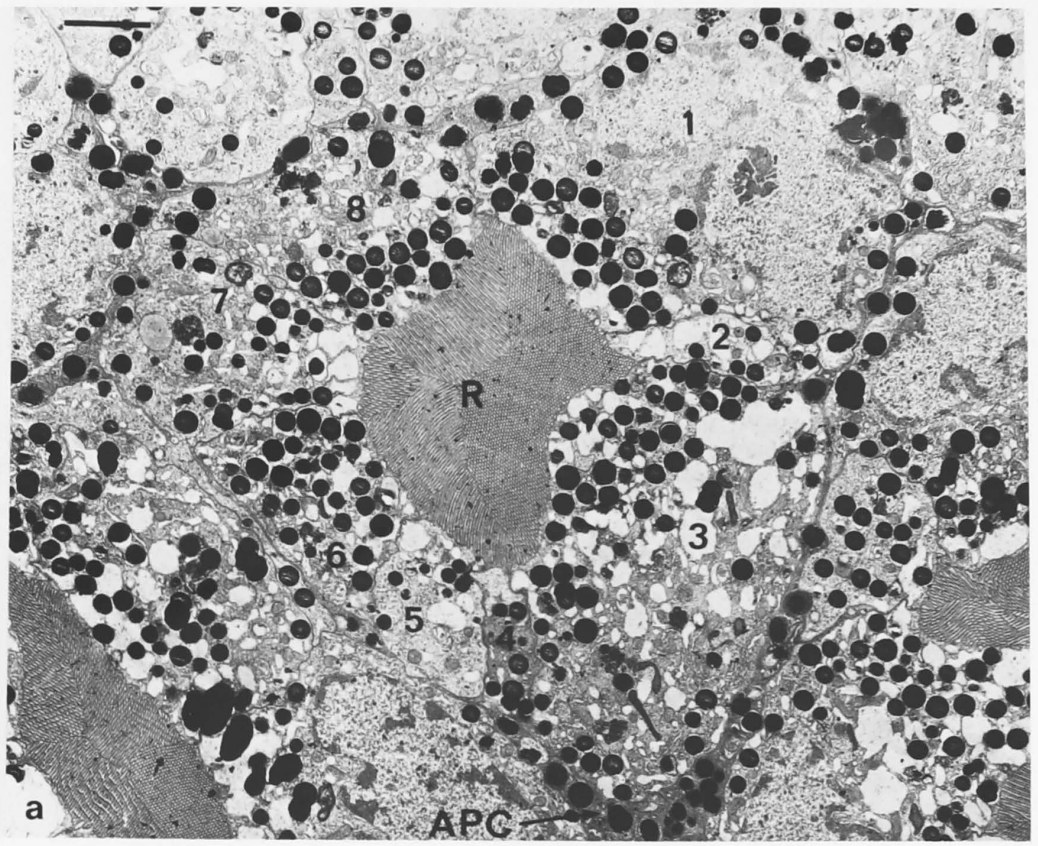
1
8
7
2
R
3
6
5
4
a
APC

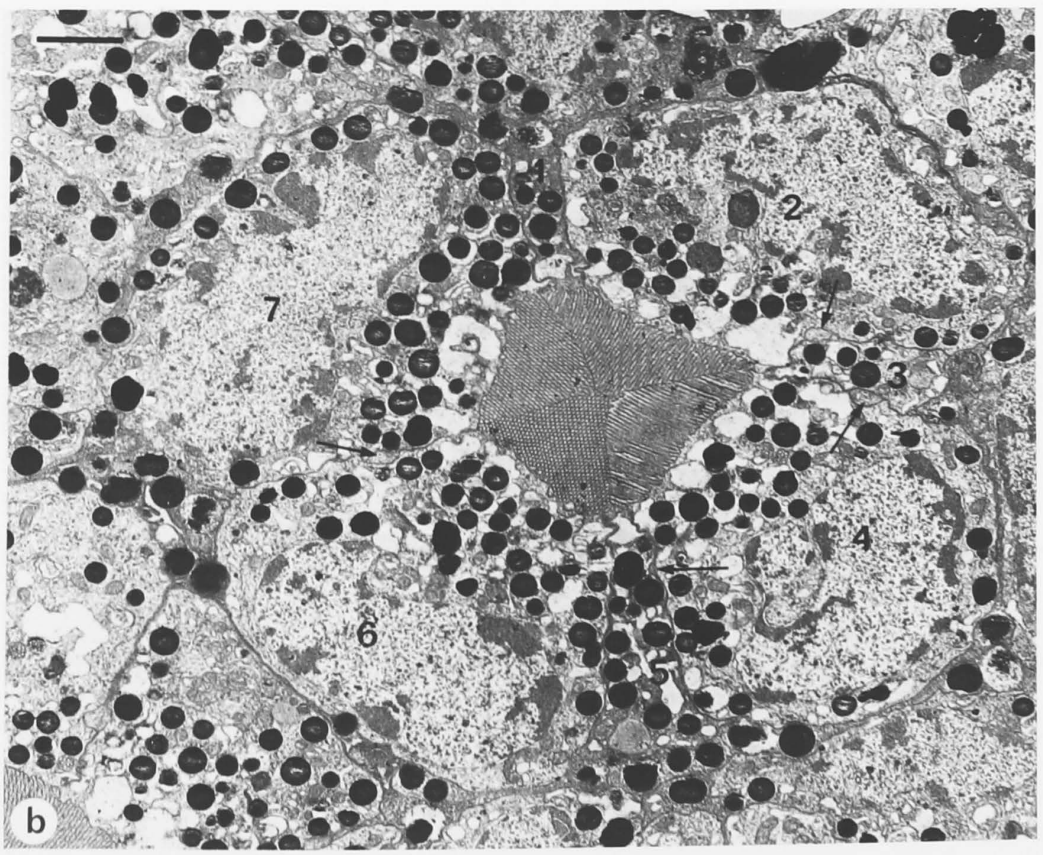
2
7
3
4
6
5
b

CHAPTER IV: THE ELECTROPHYSIOLOGY OF THE RETINA OF *Periplaneta americana* L.

All electrophysiological results were obtained by intracellular recordings from retinula cells using glass microelectrodes. Stable penetrations were extremely difficult to achieve and generally lasted no longer than 5 min. This may have been due to the regional anatomy of the retinula cells, for successful penetrations only occurred when the electrode was in the middle of the retina between the two strata of nucleii. At this level, retinula cell diameters are 3 - 5 μm.

The high tip potentials encountered (up to 100 mV) were neutralized with a backing-off voltage between the preparation and ground (see CHAPTER II, section D3).[1]

---

[1] A standing tippotential of 100 mV and a preamplifier input resistance of 10^{11} Ω would drive only 10^{-12} amp. through a cell, for a membrane potential change of less than 1 mV (Shaw, 1968a). When neutralized, the effect would be negligible. Several authors have investigated the possible effects of tip potentials on impaled cells and have warned against inaccuracies in the readings, especially the underestimation of true membrane potentials (Adrian, 1956; Martin and Pilar, 1964; Kostyuk, 1965). The results presented here are confined to measurements of changes in membrane potential which are unlikely to be grossly affected by any tip potential.

A limiting factor in these studies was the stimulating lamp. Fig. 3c (CHAPTER II) shows that the lamp's output in the UV was negligible. Taking into account the results of CHAPTER V plus Mote and Goldsmith's (1970) findings of two spectral receptor types, it must be assumed that the electrophysiological results are most likely restricted to the green sensitive cells.

A. Intracellular Depolarizing Responses

Standing negative potentials of up to -40 to -50 mV were encountered as the microelectrode was advanced through the retina. These did not necessarily indicate the successful impalement of a retinula cell, as high negativity was often recorded extracellularly. Responses to light flashes of graded intensity, recorded in presumed extracellular regions, often took the form of small amplitude (5 - 10 mV) negative going slow potentials, graded with respect to stimulus intensity. This was the electroretinogram (ERG), and responded to the point source over very wide fields (often up to 90°).

Impalement of a retinula cell is usually accompanied by a precipitous potential drop, but this alone is not sufficient evidence for assuming intracellular recording. The resting potentials

ranged from -15 to -50 mV, with maximal depolarizing amplitudes increasing in proportion to the magnitude of the resting potential as in other insects (Naka, 1961). There are criteria for showing that the depolarizations are from intracellular recordings. The anatomy of the region where impalements occur shows that the retinula cells are the only type large enough to be penetrated. The nature of the depolarizing response is very similar to those of other studies where large changes in membrane input resistance during depolarization were recorded (eg. Fuortes, 1959; Shaw, 1968a, 1969a; Ioannides, 1971). This resistance change was a decrease, and according to an electrical analogue of arthropod photoreceptor membranes (see below), should result in a depolarization, of the type recorded experimentally. Marking cells with Procion dyes has substantiated the above physiological finding (Ioannides, 1971; Mote and Goldsmith, 1971).

Intracellular recordings from retinula cells in Periplaneta americana are shown in Fig. 34. The responses to graded light intensities (on - axis) are similar to those found in other arthropods and consist of graded depolarizations (receptor potentials). The best responses reached maximum amplitudes of 35-40mV. Four components of the response can be seen in the light-adapted cells at high stimulus intensities. At the onset of the stimulus, (1) a rapid rising depolarizing transient is followed by (2) a slower

transient which partially repolarizes the cell. This partial repolarization terminates in (3) the steady state plateau depolarization which remains for the duration of the stimulus. After stimulation, (4) the cell repolarizes almost completely, but at high stimulus intensities, a noticeable after-polarization (initially about 5 mV) exists for up to 8 s after a 0.5 s flash. After-polarization refers to the long decay of the response after the stimulus is off.

In the dark-adapted state, the same four components are present but with some noticeable differences. The plateau phase has a much greater magnitude in dark-adapted cells, producing a higher plateau/peak ratio.

It should be noted that light-adapted eyes were maintained in that state by adequate but low level background illumination (not measured). This was confirmed by histological checks. Experiments on dark-adapted eyes were done in a blacked-out room. Light-adapted cells were easier to hold and record from than dark-adapted cells. Although this is opposite to the general findings of others, it bears marked similarities to the recording properties of barnacle ocellus (Stratten and Ogden, 1971).

In both light and dark-adapted cells, the transient phase is more sensitive to intensity variations than the plateau phase. Response height

(in mV) versus intensity (log I) plots are sigmoidal for both transients and plateaus, with the former having a steeper slope.

At non-saturating stimulus intensities, "bumps" can be seen riding on the static phases of the responses (Fig. 34). Scholes (1964, 1965a, b) showed statistically that these bumps were not summation effects and inferred that each bump corresponds to a single quantum capture at the rate of 1 in every 10^3 photons striking the cornea. This was revised by Shaw (1968a) to 1 in 12. If they are quantum bumps, it is surprising to find them at the higher light intensities (LA, Fig. 34), as bump frequency is linear with light intensity until frequency determination become unreliable (Scholes, 1965b).[2]

Adaptation phenomena were evident from the beginning of the study, with two types being recognized. Anatomical adaptation takes about three minutes to complete (either way) and is associated morphologically with the palisade. Physiological

---

[2] The possibility of the bumps being action potentials must be considered. With the exception of drone bee, spike discharges are not known to occur in insect retinula cells, although small spikes of less than 2 mV have been observed occasionally in locust (Scholes, 1965a, b; Shaw, 1968a, b). These spikes are evident with the cell at its resting potential and are inhibited by light-induced depolarizations (a paradox exists here, as current depolarizations increase frequency (Shaw, 1968a, b)). None of these events were found in Periplaneta, and it is assumed that the irregularities are quantum bumps.

adaptation (biochemical) which occurs in both light- and dark-adapted cells is associated with each stimulation, is rapid and may involve the rate of regeneration of photopigment and/or ionic effects. Each type of adaptation produces a reduction in response amplitude, and anatomical adaptation will be considered in the next section. The effect of physiological adaptation on results can be removed by adjusting appropriately the timing and intensity of stimulation.

Fig. 35a - d shows some aspects of rapid physiological adaptation. If one stimulation is followed too quickly by a second identical light flash, the second response will be smaller than the first. However, if sufficient time elapses between flashes then the responses will be identical (Fig. 35a cf. Fig. 35b). In Periplaneta americana, a stimulus duration of 50 ms with an interval of 10 s was sufficient to prevent this type of adaptation in both the light- and dark-adapted states. Fig. 35c shows that this adaptation is localized in the transient phases. The traces are from a series of intensity related responses run on one light-adapted cell. Interval times were 10 s between log I = -1.0, -0.6 and the first 0 (3rd trace). Two seconds after the first stimulation with log I = 0, a second record was superimposed on the first, showing the adaptation. In this record, the lower of the two

resting potential levels belongs with the higher peak, the difference in resting potentials being attributed to the after-potential of the first response. Four seconds later, the final record was made, showing partial recovery in the transient phase .

Early microelectrode work on Limulus resulted in an electrical analogue model of the photoreceptor membrane, based on a light-dependent conductance channel with its associated equilibrium potential (Na^+ battery) in parallel with a resistance equivalent to the portions of the membrane producing the resting potential with its associated equilibrium potential (K^+ battery) (Fuortes, 1959; Rushton, 1959; Benolken, 1961). This model has been extended to vertebrate cones (Baylor and Fuortes, 1970) and to insect retinula cells (Shaw, 1968a; Ioannides and Walcott, 1971), The following relationship between response amplitude and stimulus intensity has been derived from the model: $V/V_{max} = I/(I+k)$, where V is the magnitude of the response (mV) to stimulus intensity I, V_{max} is the response (mV) at saturating intensities and k is a constant for each cell equal to I for the particular case of $V = V_{max}/2$. The constants, k, were determined empirically for the transient peaks and plateaus of 5 light-adapted retinula cells and for the transient peaks of 4 dark-adapted cells. They were averaged for each case and used to plot the function $I/(I+k)$ versus

log I, against which the experimentally measured ratio (V/V_{max}) could be compared.

Fig. 36 shows how the retinula cells fit the theoretical model. The solid curves are the functions $I/(I+k)$ for experimentally determined k's for (a) light-adapted transients, (b) light-adapted plateaus and (c) dark-adapted transients. The points represent the averaged ratio values (V/V_{max}) for (a) light-adapted transients (5 cells), (b) light-adapted plateaus (5 cells) and (c) dark-adapted transients (4 cells).

The measured response-intensity relation fits the model only reasonably well. The fit is not as good as in Lethocerus (Ioannides and Walcott, 1971). The experimental determination of k is only possible when V_{max} is saturating (light-dependent conductance approaches an infinite value). This condition is approached in drone bee and locust (Shaw, 1969a) and a good approximation occurs in Lethocerus (Ioannides and Walcott, 1961; Walcott, 1971b). For Periplaneta, the solid curves suggest that responses in question may not have been completely saturated at the highest stimulus intensity, although most sensitivity curves do indicate saturation (Fig. 43A). Unsaturated maximum responses would account for a poor fit of the points to the curve.

The plateau is probably more complex than the transient (for which the analogue applies) as more

than one ion species would be participating. However, the points to curve fit is similar to that for the transients.

B. Angles of Acceptance

Acuity is commonly defined by the ability to distinguish two points at a minimum angle of separation (Horridge, 1968). The acuity of a whole eye can be measured by relating the optomotor responses of an animal to the stripe width (angular stripe repeat period) of a pattern of contrasting stripes passed in front of the eye. However, the response is made by the whole animal and the effect of integrative and auxillary mechanisms between stimulus and output is unknown.

Acuity of the whole eye is directly related to the acuity of individual receptors (Horridge, 1968) and direct measurements of the angle of acceptance on retinula cells by intracellular recordings can provide a good index of a single receptor's acuity (Götz, 1964, 1965; Horridge, 1966; Tunstall and Horridge, 1967). The rationale for using these is discussed in section E. In compound eyes, such as Periplaneta's (apposition, fused rhabdomeres) the amount of light reaching the rhabdom from a constant intensity source varies with the angle of incidence at the corneal surface. Therefore, photo-induced excitations in the retinula

cells are graded accordingly, with the maximum response occuring on axis. With an electrode inside a cell and the light source moved stepwise around the eye, the recorded responses (appearing as vertical deflections on a trace when recorded with very slow time base) outline a curve. This curve can be converted to per cent sensitivity (see below) and the angular width of the curve at 50 per cent sensitivity is defined as the angle of acceptance (as first used by Washizu et al. (1964)).

Angles of acceptance were obtained in the following way. The retina was probed with a microelectrode until a retinula cell was successfully impaled and a steady resting potential observed. The stimulating lamp (point source, without focusing lens) was then moved around until the visual axis (assumed to be the optical axis in apposition, fused rhabdomere eyes) of the cell was found, here defined as that position which elicits maximal response. This does not imply coincidence with the anatomical axis of the ommatidium. The lamp was then swung off axis (8° - 12°) and moved in either 1° or 2° steps (during the 10 s interval between 50 ms flashes) through visual axis to an equivalent position on the other side.

It was most important to have the experimental runs made through the visual axis as it was the reference point to which all angular measurements were made in each cell. Sometimes the axis would shift

(up to 2°) during an experiment and its position was rechecked after each run. Results were used only for those units whose axes did not vary during an experiment.

The horizontal and vertical angles of acceptance were determined in Periplaneta for both the light- and dark-adapted states.[3] Results for the light-adapted state are presented in Fig. 37 (horizontal plane) and Fig. 38 (vertical plane). In each, A is a typical record of responses for a lamp moved in 1° steps through the visual axis, and B is the ND series for the cell in A. C is the per cent sensitivity curve[4]

---

[3] Most cells could be held only long enough for either a horizontal or vertical run, although both were obtained from a few cells. The latter cases provided an additional check on the visual axis. An appropriate neutral density filter was inserted to keep the responses in the best dynamic range and to prevent adaptation effects.

[4] Different retinula cells do not have the same absolute sensitivity. In order to adjust the responses so that different units can be compared, each cell was calibrated with respect to its own sensitivity by first bringing the lamp back onto visual axis after a run and then recording responses (in mV) for different stimulus intensities (Neutral density (ND) series in units of log I) and plotting a V - log I sensitivity curve for that cell. The response sizes of the angular sensitivity curve can then be converted to equivalent log intensities plotted against inclination of the stimulus to the visual axis. In this way, the curves are comparable and most useful as variations in sensitivity are still present. A further transformation to per cent sensitivity ties all curves to a common point (peak at 100 per cent) so that the normalized data can be handled statistically for acuity studies. This is accomplished by arbitrarily setting the maximum peak at an equivalent log I = 2.0, and scaling the other equivalent log intensities appropriately. By taking antilogs, per cent sensitivity values for degrees of inclination can be calculated. A drop in sensitivity of 0.3 of a log unit is equivalent approximately to a 50 per cent sensitivity drop on a linear plot.

for the unit in A and D is the V - log I sensitivity curve of B. E shows the averaged curve with the mean and 1 SD for N units, and F shows the distribution of units.

Angles of acceptance ($\Delta\rho$) in the light-adapted state are 2.4° ± 0.9° for the horizontal plane and 2.3° ± 0.6° for the vertical plane. Considering the estimated precision with which the lamp was positioned (0.25°) and the degree of spread of the standard deviations, the horizontal and vertical angles of acceptance must be considered as the same. Furthermore, the averaged curves (E, Figs. 37 and 38) indicate that the general trend is towards symmetry about the visual axis contrasting with the elliptical fields found in Calliphora (Washizu et al., 1964), Musca (Vowles, 1966) and Locusta (Tunstall and Horridge, 1967). However, this is an averaged trend and as can be seen in Fig. 42 individual curves vary considerably. When a strong background illumination was used, the curves were normal, but with very small responses (Fig. 35d).

The angles of acceptance for dark-adapted cells are about three times wider than for light-adapted units. The results for the dark-adapted state are presented in Fig. 39 (horizontal plane) and Fig. 40 (vertical plane). For each, A and B are again, the actual records and C and D are the curves for that particular cell. E is the averaged curve (mean ± 1 SD) for N cells and F is the distribution. Acceptance

angles are 6.7° ± 1.8° in the horizontal plane and 6.9° ± 1.3° in the vertical plane. As above, the means are too close and the standard deviations too wide to reflect any difference. Again, as in the light-adapted state, the general trend is towards symmetry about the visual axis, as is the case in Libellula (Horridge, 1969), Apis workers (Laughlin and Horridge, 1971) and Lethocerus (Ioannides and Walcott, 1971; Walcott, 1971b), but with individual variations.

The recordings probably represent the physiology of the five green sensitive cells (see CHAPTER V) as a consequence of random sampling in the retina. There is justification for the amalgamation of results, as Shaw (1967) has shown that pairs of cells in the same ommatidium of Locusta (which has an apposition, fused rhabdomere eye, similar in structure to Periplaneta) have identical angular sensitivities and, hence, a common visual axis.

The results given above are for cells known to be either light- or dark-adapted (by histological tests of the method). The angles from partially adapted cells fell between the values given, and if any doubt existed about the state of adaptation, the results were not used.

On several occasions, records were obtained from units with double peaks (Fig. 35e). Generally, these were not included in results but one was used in the

sensitivity studies (Fig. 42; LA group).

A map of the interommatidial angles in horizontal and vertical planes was given in CHAPTER III, section B2 (Fig. 11), with extremes of 1° (position 7, vertical plane) and 10° (position 1, horizontal plane). A graphical picture of the extent of overlap of the visual fields in adjacent ommatidia (with these extreme interommatidial angles) for both the light- and dark-adapted states is presented in Fig. 41. The curves representing the acceptance angles are Gaussian functions, arbitrarily chosen to fit the experimental data by setting the band-width at the 50 per cent level equal to the angle of acceptance ($\Delta\rho$), and plotting the rest of the curve from appropriate tables (Alder and Roessler, 1964). The experimentally determined curves closely approximate Gaussians, but tend to be slightly more pointed at the apex.

Interommatidial angles of 1° result in extensive overlapping in both the light- and dark-adapted state. Considering the 50 per cent sensitivity level as a reference, the acceptance angles of every second light-adapted ommatidium intersect at about this point. However, in the dark-adapted state, similar crossovers occur between every seventh ommatidium. There is a continuous transition of the degree of overlapping between this condition and the other extreme where interommatidial angles are 10°. In this latter condition, light-adapted angles do not overlap at all,

with gaps of up to 4° existing between the lower angular sensitivity limits of two adjacent ommatidia. In the dark-adapted state, slight overlapping between adjacent ommatidia occurs but only at the 20 per cent sensitivity level. The significance that this may have for motion perception is considered in section E.

C. Sensitivity

As angular sensitivity increases upon dark-adaptation, there is a simultaneous increase in receptor sensitivity to light. The best method to illustrate sensitivity changes as related to state of adaptation is to have angular sensitivity records from single cells at various stages of adaptation, as has been done for Locusta (Tunstall and Horridge, 1967). These results however, are suspect as the adaptation times between curves (as short as 5 s) could not have allowed an ND series for each curve to be made and so correct sensitivity curves could not have been plotted. This would be an insurmountable problem with any preparation, even if cells could be held for the long periods required. The best alternative method would be to measure acceptance angles and relative sensitivities in a single cell in the two extreme states of adaptation, and compare results. This was not feasible in Periplaneta as cells could not be held for long periods (5 min maximum)

and the only alternative left was to compare sensitivities of different cells. This was further complicated by the fact that sensitivities of two cells in the same state of adaptation can be different (also noted in Libellula and Anax by Horridge (1969)). The problem was resolved by selecting records from cells which were similar in one physiological respect.

The V - log I sensitivity curves of cells are sigmoidal with a fairly straight middle region (the dynamic region) with tails flattening off. Angles of acceptance were made with an appropriate ND filter in the stimulus beam to prevent the maximal responses from saturating. The curves used for sensitivity comparisons were selected from those cells whose maximum response fell about half-way ($V_{max}/2$) up their own intensity-response curve. In that way, the cells are similar as peak responses occur in the middle of each cell's dynamic range.

Ten light- and ten dark-adapted cells were chosen and their angles of acceptance plotted on a logarithmic scale of relative sensitivity against position (Fig. 42). As there was no difference between horizontal and vertical acceptance angles both are included for each state. It is quite evident that cells in different states of adaptation fall into two groups with the dark-adapted group being more sensitive (ie. DA cells give larger responses

than LA cells for the same stimulus intensity). The spread within each group is about one log unit, but even so they do fall into distinct groups on the log scale, roughly one log unit apart.

Plots of the V - log I sensitivity curves mentioned above were made for all the cells shown in Fig. 42 and are presented in Fig. 43A. Again dark-adapted (solid lines) and light-adapted cells (broken lines) fall into two groups, but they are less distinct as in Fig. 42. In most cases, the responses are saturated at the top of the curves.

For many arthropods, the V - log I sensitivity curves for cells in different states of adaptation are the same shape (sigmoidal) and coincide when slid laterally, with the amount of lateral shift (in log units) being a measure of the difference in sensitivity (Naka and Kishida, 1966). The same authors also suggest an additional vertical shift to compensate for the slightly depolarized membrane potential resulting from background illumination in the light-adapted state.

The curves in Fig. 43A cannot be directly compared as response heights vary, generally, with the state of adaptation. Dark- and light-adapted curves (from Fig. 43A) were normalized to compensate for this by plotting V/V_{max} against log I, and appear in Fig. 43B and Fig. 43C, respectively.

The spread within each (saturated) group is slightly more than half a log unit. The dark-adapted curves saturate generally about one log unit down from the light-adapted curves (ie. DA more sensitive) and reflect the same sensitivity difference as seen in Fig. 42.

D. Polarized Light Sensitivity

When a polaroid, inserted into an on-axis stimulus beam, is rotated, the intracellularly recorded responses from a retinula cell show response variations (Fig. 44a, b). The polaroid was rotated in 20 steps, starting with the e-vector 40° from the vertical plane, and all experiments were done on dark-adapted cells, to benefit from their greater sensitivity. Although on-axis stimulation gives maximal responses, it is not essential as Shaw (1968a) has shown that PL response is independent of the position of the stimulus within the visual field of the cell.

Complete runs (including an ND series) were made successfully on only nine cells. Four of these cells were maximally sensitive where the e-vector was in the vertical plane relative to the normal attitude of the head (Fig. 44a, and solid line in c), and their minima were 90° from the maxima. The other five cells constituted a second group whose maxima

were 90° out of phase with the first group (Fig. 44b, and broken line in c). Curves whose maxima were within 10° - 15° of what appeared as general trend maxima (ie. at 90° and 180°) were translated laterally for coincidence, and the error was assumed to have originated with improperly tilted preparations.

A few experiments showed that some cells had maxima inbetween the ones shown in Fig. 44, but unfortunately these were incomplete experiments and could not be used in the final analysis. Irregular cases have been reported for other arthropods as well (eg. Shaw, 1968b; Horridge, 1969).

In order to make comparisons, each polarized light (PL) response curve was converted to a per cent sensitivity curve by using its V - log I sensitivity curve. The curves for each group were averaged and appear with standard deviations in Fig. 44c. For both groups the maximum : minimum sensitivity ratio is 5 : 1. PL sensitivity in Periplaneta is not as good as that measured in Crustaceans by the same techniques,with ratios of 7.7:1 for Carcinus and 6.2:1 for Astacus (Shaw, 1966, 1969b). It is better than that measured for some insects with ratios of : 2.6:1 for Calliphora as predicted by Shaw (1969b) and coinciding with measurements by Burkhardt and Wendler (1960) and Autrum and von Zwehl (1962a); 2.35:1 for Locusta and 1.26:1 for Apis drones (Shaw, 1968a, 1969a);

and 3:1 for Lethocerus (Walcott, 1971b). These are only rough comparisons as PL absorption depends on rhabdom length and diameter, whether the rhabdom is fused or open, and on photopigment concentration probably similar in all cases) (Shaw, 1969b). Scholes (1969) showed slightly different sensitivity ratios for different cells in the open-rhabdomere eye of Musca.

The basic structure of Periplaneta's rhabdom is two sets of orthogonal lamellae, with the anterior and posterior pairs in an ommatidium comprising one set with horizontal tubules and the dorsal and ventral pairs comprising the other set with vertical tubules. This anatomical arrangement accounts for the 90° phase difference in receptor sensitivity to polarized light (Shaw, 1968a, 1969a, b), as the orthogonal lamellae lie in precisely the same planes as the e-vector orientation for peak responses.

In an elegant series of experiments, Shaw (1968a, 1969a, b) measured electrical coupling between pairs of retinula cells and found it to be relatively strong in drone bee, but relatively weak in locust. He suggests that inter-receptor coupling may reduce apparent PL sensitivity by an inverse relationship, which would account for some of the higher sensitivity ratio in locust than drone bee. In the absence of coupling, he calculates that the basic PL sensitivities in locust and drone retinula cells may be as high as

9:1, a ratio which approaches that measured for crabs. If such a relationship between coupling and PL sensitivity holds in Periplaneta, then the measured 5:1 ratio may imply weak coupling. This same conclusion is implied in CHAPTER V, by an independent means.

E. Discussion

The responses described probably originate in the green sensitive cells and are much like responses found in other insects except drone bee, where spiking phenomena are found (Naka and Eguchi, 1962). The notch between the transient and plateau, seen at high light intensities in many arthropod photoreceptor cells (eg. Baumann, 1968; Millecchia and Mauro, 1969a; Scholes, 1969; Brown et al., 1970) was absent, even in saturated responses. A persistent after-potential was seen, especially at the higher stimulus intensities. Shaw (1968b) considered the effects of the receptor after potential on second order neurons in the lamina in Locusta, but found none.

Mote and Goldsmith (1970) show the UV-sensitive cells in Periplaneta americana with both transient and plateau phases, but claim the green cells have only the transient phase. My records indicate that the green cells possess both transient

and plateau phases in the response. There is no evidence to suggest that responses from the two cell types should be, or are, different.

The absence of spikes from intracellular recordings of retinula cells (except drone) is common to all arthropods which have been examined. Ioannides and Walcott (1971) have extended this to show that retinula cell axons in Lethocerus lack action potentials as well. They have noted Kennedy's (1964) suggestion that tissue damage was the prime reason for the lack of spikes but the weight of evidence against it, as well as their own experiments indicate the validity of their results, (Burtt and Catton, 1956, 1959; Naka and Eguchi, 1962; Autrum and von Zwehl, 1962b, 1964; Baumann, 1968; Shaw, 1968b, 1969a; Scholes, 1969). The current hypothesis is that electrotonic spread of slow potentials is the mode of information transmission in the primary photoreceptors (and their axons) of insects (and perhaps arthropods in general). This is not an isolated phenomenon as non-spiking transmission also occurs in crab muscle receptors (Ripley et al., 1968; Bush and Roberts, 1968).

One of the most interesting problems to be investigated is the synaptic mechanism involved with non-spiking retinula cell axons, where the synapse can be as far as 1 - 2 mm away from the

receptor potential generating site. In Musca, 1 mV quantum bumps in the primary photoreceptors not only produce responses in the lamina 50 μm away, but also elicit behavioural responses (Scholes and Reichardt, 1969).

The electrical analogue of the photoreceptor membrane has already been mentioned (section A, above) and it was shown that the retinula cells of Periplaneta fit the model reasonably well (Fig. 36). The validity of the analogue[5] rests on the assumption that at V_{max} the response is saturated with the light-dependent conductance

[5] The analogue was originally postulated for Limulus, and since Fuortes (1959) and Rushton (1959), it has been known that light increases conductances in the photoreceptor cells of this animal. Similar observations have been made on dragonfly (Fuortes, 1963), Calliphora (Washizu, 1964), and Shaw (1969a) gives an indication of a large conductance change in drone bee retinula cell spikes (from about 12 M Ω to 200 K Ω). Recent voltage-clamp experiments on barnacle photoreceptor cells (Brown et al., 1969) and on Limulus ventral photoreceptor cells (Millecchia and Mauro, 1969b) have also shown a large increase in conductance upon illumination. This latter work on Limulus showed that the input resistance of these cells changed from about 10 M Ω to 50 K Ω during the transient (300 nA current driven by 15 mV). The authors also showed that the physiological response (light-dependent conductance) was composed of a voltage-time dependent dark conductance and a light-voltage-time dependent light conductance. All this evidence suggests that the analogue is conceptually correct, and probably universal, as it also applies to vertebrate rods and cones.

value approaching infinity (ie. membrane is short-circuited). The responses with which I was working were believed to be saturated (from looking at the V - log I curve), and closely approximated these conditions.

Much of the physiological proof that the rhabdom(ere) membrane is the site of origin of the electrical response has come from the squid retina, where receptor current is confined only to the region illuminated (Hagins et al., 1962) which is similar to the situation in vertebrate rods (Hagins and Jennings, 1959). Furthermore, both the receptor potential and the early receptor potential show the same decay characteristics along squid rods (Hagins and McGaughy, 1968b), with the early receptor potential being attributed to changes in charge distribution in rhodopsin molecules aligned in the rhabdomere (Hagins and McGaughy, 1968a). This suggests that they both have a similar origin, in or near the rhabdomeric membranes. Indisputable proof came with the elegant experiments of Lasansky and Fuortes (1969) on leech photoreceptors. By recording visual responses intracellularly, and comparing them with simultaneous extracellular recordings made adjacent to the microvilli, they found that as the cell depolarizes, an inward

current penetrates the cell through the microvillar membrane.

The magnitude of the transient peaks was used as a measure of a cell's sensitivity to off-axial light (angle of acceptance) and this is related to visual acuity. The movement of a vertical striped pattern in front of a whole eye has been the most common method of determining acuity in arthropods, with acuity defined as the angle subtended by the repeat distance of the narrowest stripes which elicit an optomotor response (Horridge, 1968). Taking this to the single cell level, the total stimulus at any moment due to the moving stripes at the cell is a summation of the black and white areas distributed over the acceptance angle cone, and one would expect to find a modulation of the receptor potential as the stripes move. This has been shown in locust (Tunstall and Horridge, 1967).

For a fixed angle of acceptance, the receptor potential modulation decreases for decreasing stripe widths. A corollary of this phenomenon is that the narrower the acceptance angle, the narrower the stripe width can be to maintain a constant modulation. The speed of stripe movement also affects the degree of modulation. Increasingly faster speeds decrease the effect until no modulation is apparent (flicker fusion). The discussion is confined to constant speeds slow enough for the receptor response lag to cope.

Tunstall and Horridge (1967) related this receptor potential modulation or "contrast transfer" to Götz's (1964) equation for the integrated light intensity of contrasting stripes at a receptor. The equation relates acceptance angle ($\Delta\rho$) (assumed Gaussain), angular stripe repeat period (λ), and light intensity at the receptor (I), by :

$$\text{contrast transfer} = \frac{I_{max} - I_{min}}{I_{max} + I_{min}} = e^{-\frac{\pi^2}{4 \ln 2}\left(\frac{\Delta\rho}{\lambda}\right)^2}$$

Narrow angles of acceptance indicate greater acuity than large ones. Furthermore, the use of these angles of acceptance as acuity indices is close to reality for the animal where each receptor accepts a cone of light, and avoids the problem of artificial windows (Horridge, 1968).

In Periplaneta the horizontal and vertical angles of acceptance for both the light- and dark-adapted states were symmetrical about the visual axis. The averaged values were 2.4° ± 0.8° (LA) and 6.8° ± 1.6° (DA), the difference being about three-fold. Careful consideration of the anatomy showed the palisade in the dark-adapted state as the only noticeable

difference between the two states of adaptation (Fig. 22 cf. Fig. 26) and it is most likely that this is the anatomical basis for the difference in angular sensitivity.

Direct measurements for angular sensitivity in both states of adaptation have been made on only two other insects and yielded somewhat comparable values: Locusta, 3.4° (LA) and 6.6° (DA) (Tunstall and Horridge, 1967); Lethocerus, 3.5° (LA) and 9.0° (DA) (Walcott, 1971b).[6] In each case, the change in angular sensitivity can be attributed to relatively gross morphological changes associated with light- and dark-adaptation.

The locust has a palisade in the dark-adapted state similar to that found in Periplaneta, and this has been regarded as the cause for the angular sensitivity changes. Horridge and Barnard (1965) made some refractive index measurements on dark-adapted locust ommatidia. Although they had to work on fixed tissue, from which the lipids had been disolved, and made relative rather than absolute measurements, they found that the palisade had a lower RI than the rest of the retinula cell

---

[6] Accurate angular sensitivity measurements have been made on many insects in the DA state alone: Calliphora, 3.3° - 5.2° (Washizu, Burkhardt and Streck, 1964); Musca, 2.5° (Scholes, 1969); Epargyreus, 2.1° (Døving and Miller, 1969); Libellula, 1.2° - 1.8° (Horridge, 1969); Apis drone, 2° (Shaw, 1969a) and Apis worker, 2.5° - 2.7° (Laughlin and Horridge, 1971).

cytoplasm and rhabdom. These limited measurements allowed the authors to predict an increase in angular sensitivity of the retinula cells as the relatively low refractive index and large size of the palisade should alter the optical properties of the ommatidium by constraining light within the rhabdom. The prediction was proved true in locust by Tunstall and Horridge (1967), where an increase in the acceptance angle was measured intracellularly upon dark-adaptation.

This theory has been supported by recent work with worker bee ommatidia. Cisternae of the endoplasmic reticulum are present in Apis workers in both the light- and dark-adapted states (Varela and Porter, 1969). Absolute refractive index measurements have been made on worker bee retina (Varela and Wiitanen, 1970) with values of 1.347 (rhabdom), 1.339 (cisternae) and 1.343 (retinula cell cytoplasm). Regardless of the accuracy of the last decimal place, the measurements show that Horridge and Barnard's (1965) finding was generally correct.

Some of the studies which have been done on the open-rhabdomere eye of fly have resulted in conclusions which substantiate Horridge and Barnard's (1965) original suggestion. RI measurements on Calliphora by Seitz (1968) were : 1.349 (rhabdome), 1.336 (inter-rhabdomere space), and 1.340-1.342 (retinula cell cytoplasm), and are remarkably similar to those found in worker bee. Kirschfeld

and Franceschini (1969) explained time-dependent light flux variations observed in Musca rhabdomeres by the influence of the clear zone which appears with dark-adaptation. They envisage this zone as keeping pigment particles away from the rhabdomere and hence removing any influence on electromagnetic propagation down the rhabdomere.

All this evidence supports the general concept that the presence of a palisade tends to keep more light within the rhabdom(ere) where the photopigment is located and would hold true regardless of the actual mode of light transmission within the rhabdom and regardless of the actual mechanism by which this optical effect is achieved.

Ray diagrams are the easiest method of representing the optical phenomena where light is kept within the rhabdom by internal reflections. Although rays bouncing off rhabdom walls is a naïve concept, and will be considered in the general discussion (CHAPTER VI), it can be used usefully here. The palisade effectively reduces the RI of the medium surrounding the rhabdom, and in doing so alters the boundary conditions. The effect of this is to decrease the critical angle and hence increase the amount of light totally reflected internally. During light-adaptation, the palisade disappears and is replaced by the pigment granules and other cytoplasm. This increases the RI of the medium surrounding the rhabdom, alters the optical properties

of the boundary and as a result increases the critical angle. The effect is to frustrate much of the total internal reflection, and to diffract light out of the rhabdom where it is subsequently absorbed or scattered by the pigment particles.

The function of this palisade seems to be to increase the ability to concentrate light in the region of the photopigment in the dark-adapted state and to protect the receptors against strong light when in the light-adapted state. The small amount of light reaching the rhabdom from an off-axial position will be enhanced when the cell is DA, and will be reduced when the cell is LA.

The anatomical studies showed that the palisade formation was the only change observable (with the electron microscope) upon dark-adaptation, and must represent the anatomical basis for the measured changes in angular sensitivity. The increase in acceptance angle upon dark-adaptation in Periplaneta is predictable if the above hypothesis holds and the results did show the expected increase. In Lethocerus, an entirely different mechanism achieves the same results. The retinula cells move distally upon dark-adaptation and proximally upon light-adaptation, resulting in displacements of primary pigment cell pigment particles and the formation of a crystalline tract (Walcott, 1969, 1971a). This may act as a "longitudinal pupil", reducing the amount of light

able to reach the rhabdom in the light-adapted state.

Some of the other eyes mentioned, such as Libellula, form a palisade when dark-adapted, and it is expected that angular sensitivity would decrease in the light-adapted state. Vowles (1966) has correlated a small increase in acceptance angle upon dark-adaptation with pigment movement in Musca, although it is not as large as one would expect from the extent of pigment migration (Kirschfeld and Franceschini, 1969).

The acuity study on Periplaneta is important for comparisons between insects with different living habits. The ratios between LA and DA angles of acceptance are similar to locust (daytime flying insect), and Lethocerus (predacious water bug). Initially, it was expected that cockroach acuity would be very poor, as it tends to be a terrestrial insect, living in shadows and relying on running speed as an escape reflex, rather than visual detection. Even so, the best acuity reached in cockroach (ie. LA) is not as good as the worst (DA) acuity of other flying insects, such as flies, dragonflies and bees.

It is easy to define the completely light-adapted state as that where no palisade exists and pigment particles abutt up against the rhabdom. On the other hand, the completely dark-adapted

state is virtually impossible to define as the actual width of the palisade at any point tends to be probabilistic, although it is generally related to rhabdomere width (see CHAPTER V). This may account for the large standard deviations and spread of the frequency histograms of Figs. 39 and 40.

Regional variations of acceptance angles across the eye were not found for either state of adaptation, although looked for. However, a large degree of variation in interommatidial angles was observed (Figs. 10, 11). The overlapping of the visual field for the LA and DA states for the extreme interommatidial angles (1° and 10°) is shown in Fig. 41. The implication is that there is a regional variation across the eye for movement perception as related to the state of adaptation. Movement perception involves the sequential excitation of receptors in adjacent ommatidia.

Consider the extreme interommatidial angle of 1°. When an eye is LA, a point source on-axis for one ommatidium excites its adjacent neighbours to only 50%, whereas in the DA eye, on-axis light for one ommatidium excites adjacent neighbours to about 90%. To get a 50% modulation (approx.) of the receptor response in any one ommatidium, a movement of only 1.1° is required for the LA eye, but 3.4° for the DA eye. For movement perception,

it is the differential modulation between ommatidia which is relevant and this would be greater in the LA than DA case, for any amount of movement.

At the other interommatidial angle extreme, 10°, intra-ommatidial modulation remains as above for LA and DA states. A point stimulus initially on-axis for one ommatidium would have to move 9° in a LA eye to excite the adjacent ommatidium to 50 per cent of its receptor sensitivity, whereas the same effect would occur in the DA state with a movement of just 6.6°. This shows that motion perception in Periplaneta ought to be sharpest in regions of small interommatidial angles when LA, and in regions of large interommatidial angles when DA. The nett effect may be to weight, differentially, information about movement anteriorly in the horizontal plane and posteriorly in the vertical plane when LA (see Fig. 11) and to reduce this differential favouritism when DA. This is not a new phenomenon, as the crab Carcinus has different areas of the eye differentially sensitive to movement (von Buddenbrock and Freidrich, 1933).

Absolute sensitivity changes are obvious between the LA and DA state (Figs. 42, 43). In the LA state with constant low level background illumination, the retinula cell membrane is slightly more depolarized than when DA, and this may be a prime reason for the

smaller responses from LA cells (Naka and Kishida, 1966).

It is not unreasonable to assume that the magnitude of the response is somehow geared to the amount of photopigment available to do the job. Some speculative ideas into what might be occurring in the insect retina can be gleaned by considering a somewhat similar situation in the vertebrate retina. Rushton and Cohen (1954) showed that for dark-adapted vertebrate rods, a retinal illuminance x time which would bleach only 3 per cent of a film of rhodopsin (assuming the fraction of rhodopsin bleached to be independent of the amount present), raised the increment threshold (ΔI) fifty-fold. Although the comparative relationship between ΔI and retinula cell sensitivity is unknown, the important point here is that an enormous desensitization of rods is correlated with a small amount of bleaching.

To explain this, Wald (1954) proposed a compartment theory for rods in which rhodopsin molecules in the rods are contained in compartmental units. Each compartment can cause a response by the bleaching of one rhodopsin molecule into retinene and opsin when conditions within the compartment are suitable. A single quantum will cause the compartment to initiate a response if and only if the compartment in which it is absorbed is completely

dark-adapted (all rhodopsin regenerated). Absorption by a compartment which is not completely DA will prolong the time until it can respond again. Thus, threshold is doubled not when half the molecules have caught a quantum, but when half the compartments have done so. With many molecules to a compartment, desensitization is rapid.

Such a system may apply, at least conceptually, to the insect retina. If so, then another observation by Rushton (1963) on rods and cones may also be applicable; that is, for light-adapted eyes, the increment threshold ΔI (somehow related to sensitivity) depends on the intensity of background illumination, and is independent of the state of rhodopsin regeneration. This could be important for insects active during the daytime, as a mechanism to keep cells responding in their dynamic range.

The variation in absolute sensitivity from one cell to the next in the same state of adaptation is also obvious (Figs. 42, 43). The reasons for this are probably due to the expected normal distribution of maximal responses from a population of cells. Most of the cells studied were considered healthy, giving observable responses down to 2 - 3 log units below maximal response. Relative insensitivity was regarded as a symptom of a cell in poor condition, and results from these were not used.

Tunstall and Horridge (1967) showed in a series

of experiments on a single cell that the increase in absolute sensitivity of a dark-adapting cell (occuring within the first 2 min of DA) preceeds the increase in angular sensitivity (occuring after 2 min of DA). This implies that if angular and absolute sensitivities are related in a dark-adapting cell and are not coincidental, then angular sensitivity changes would be a consequence of absolute sensitivity changes. It is possible that each is an independent mechanism to achieve a different effect and some evidence for this lies in the above analogy with vertebrate rods and cones, where the level of background illumination can largely determine sensitivity. Furthermore, pigment particle migration (and subsequent palisade formation) can occur without light, due to the application of factors which partially depolarize the cell, such as CO_2 (Kirschfeld and Franceschini, 1969). Neither of these examples demonstrate, unequivocally, the lack of a relationship between angular and absolute sensitivity, but neither do they contradict the findings of Tunstall and Horridge (1967).

The increase in absolute sensitivity when a light-adapted unit dark adapts may be either a consequence of the biochemistry of the photopigment or a consequence of the anatomical changes that occur (ie. ommatidium with palisade accepts a wider

cone of light, making more available to the rhabdom), or both. How the animal uses this increased sensitivity to its advantage is rather difficult to sort out, but two possibilities exist. The first, and most probable, is that as dim light in a dark environment produces relatively greater responses than an equivalent stimulus in a lighted environment, the retinula cells have the advantage of increased sensitivity to offset decreased stimulus intensities. The other alternative, although speculative, is of interest. Thomas and Autrum (1965) demonstrated the absence of a Purkinje shift in bees, with no shift in peak spectral sensitivity as related to the state of adaptation. If this finding is applicable to other insects, then the greater sensitivity of DA cells might be used to offset the lack of the Purkinje shift and enhance the effect of the shorter wavelengths which predominate from twilight onwards (ie. blues, violets).

The fact that light-adaptation reduces receptor potential amplitude cannot be inferred as a loss of sensory information. This is quite apparent from studies where a 1 mV depolarization in the receptor can cause a behavioural response (Scholes and Reichardt, 1969). Keidel et al. (1969) have suggested that signal amplitude reduction as a result of adaptation can result in a gain of

sensory information in certain sensory systems. Their examples are drawn from data partly taken from the CNS, behind integrating centres, and as such cannot be extrapolated to the peripheral receptors. Nothing concrete can be said about any such gains from my studies on Periplaneta's retinal photoreceptors, but this does not rule out the possibility of this phenomenon existing further up the optic tract.

The results show a polarized-light sensitivity ratio of 5:1 ($I_{max}:I_{min}$) for the cells studied. This result was surprising as poor sensitivity (or complete lack of sensitivity) was initially anticipated, based on considerations of the animal's mode of life. The presence of orthogonal lamellae in the rhabdomeres (Fig. 22) in itself does not indicate polarized light sensitivity, as the precision with which the lamellae are maintained in three dimensions cannot be determined from random electron micrographs. However, the fact that the retinula cells are sensitive to polarized light does not necessarily mean that the animal uses the information available.

The cells studied also fell into two groups with peak sensitivities 90° apart, coinciding with the orthogonal orientation of the rhabdomeric lamellae. These findings fit the current hypothesis which explains polarized-light sensitivity. Wald et al.

(1963) suggested that the dichroism of individual rhodopsin molecules is responsible for the polarized-light effect with this being achieved by the molecules lying between membrane lamellae with their dichroic axes in the same plane. This was based on earlier work with fish and frog retinae where increased bleaching of rhodopsin was observed when receptors were illuminated at right angles to the normal light path, by polarized light with the e-vector across the receptor discs (eg. Denton, 1959). Molecular dichroic axes at right angles to the normal light path explains Denton's (1959) results while the experiments of Hagins and Jennings (1959) which indicate rotational freedom and random arrangement of rhodopsin within the plane of each rod disc can account for the general insensitivity to polarized-light in vertebrates.

The rhabdoms of arthropods are built in such a way as to possess the ability to limit the orientation of the photopigment to one dimension and by the above theory possess the ability to analyse polarized light along the normal light path. Since the lamellae in adjacent pairs of cells in the same ommatidium have orthogonal orientations (see Fig. 22) the dichroic-rhabdomere theory for polarized-light sensitivity requires these cells to have different polarized-light sensitivities, which is the case (Fig. 44).

There are three other possible explanations for the polarized-light response. The first has to do with the physical set-up for experiments where a reflected stimulus becomes partially polarized, or reflected (and refracted) intensities due to polaroid rotation cause intensity changes which are detected by the retinula cells. The second is the possibility of the dioptric apparatus having polarizing properties. The third arises from the suggestion of Menzer and Stockhammer (1951) that open-rhabdomeres have double-refracting properties, which could produce a polarization analyser if one component was refracted out of the rhabdom, leaving behind the oppositely polarized component. Shaw (1968a; 1969a, b) performed experiments which eliminated these last three alternatives. He also combined his polarization studies with experiments to show electrical coupling between cells in the same ommatidium. He demonstrated that drone bee, which has a low measured polarized-light sensitivity ratio has high coupling between cells, a factor which may reduce the measured sensitivity. Locust on the other hand has a higher measured sensitivity than drone bee, but a lower coupling ratio. Perrelet (1970) identifies the tight junctions between adjacent rhabdomeres in drone bee as the site for inter-receptor coupling based on anatomical findings and on Shaw's (1969a)

physiological data. This suggests that coupling between receptors in Periplaneta must also be relatively weak as the sensitivity ratio (5:1) is large (see also CHAPTER V for evidence of poor coupling in Periplaneta).

A further anatomical implication of high PL sensitivity is that the rhabdomere lamellae must be maintained with relatively rigid orientation within each cell over the length of the rhabdom. It would not take much rotation or twisting of the rhabdom to effectively randomize the orientation of photopigment molecules in the rhabdomeres and reduce sensitivity.

Figure 34

Conventional intracellular depolarizing responses for light- and dark-adapted cells (LA and DA) at different stimulus intensities. All LA responses are from the same cell, and all DA responses are from a different cell. In all cases, stimulus duration was 0.5 s.

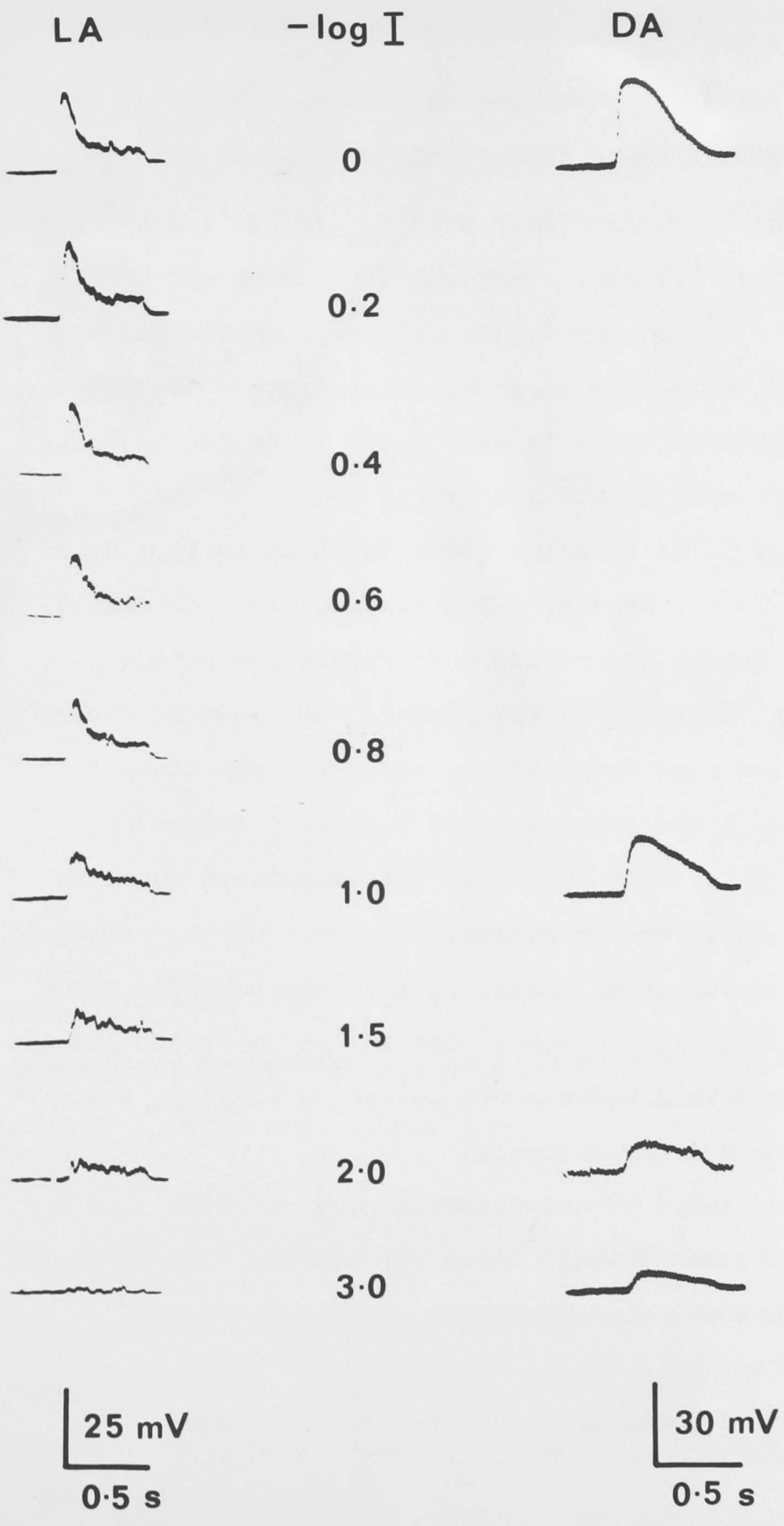
LA
−log I
DA
0
0·2
0·4
0·6
0·8
1·0
1·5
2·0
3·0
25 mV
0·5 s
30 mV
0·5 s

Figure 35

Aspects of physiological adaptation on intracellular depolarizing responses.

The responses (less than $V_{max}/2$) in (a) are for 50 ms stimulus durations with intervals of 5 s. The decreasing amplitudes are a manifestation of rapid physiological adaptation in the cell. Baseline drift is only about 2 mV, and response attenuation would be very small. In (b), the 50 ms stimulus (same log I as in (a)) have a 10 s interval, which is sufficient to permit recovery and remove this adaptation effect. In (a) and (b), the records were made on a very slow time base and the vertical excursions of the trace represent the laterally compressed depolarizing response, with amplitude equal to that of the transient.

The series of traces in (c) show how this rapid adaptation is emphasized in the transient phase. Intervals between traces are 10 s, 10 s, 2 s and 4 s, respectively.

The angle of acceptance in (d) was made with a constant intense light surrounding the stimulus pinhole. All responses are subject to the adaptation described above. The angle is as normal, but the responses are very small.

continued next page

Figure 35, continued
Fig. 35e has nothing to do with physiological adaptation, and was included here for spatial reasons. It shows the curious double peaks which some cells produce when acceptance angles are being measured.

Calibrations. a-e, 10 mV

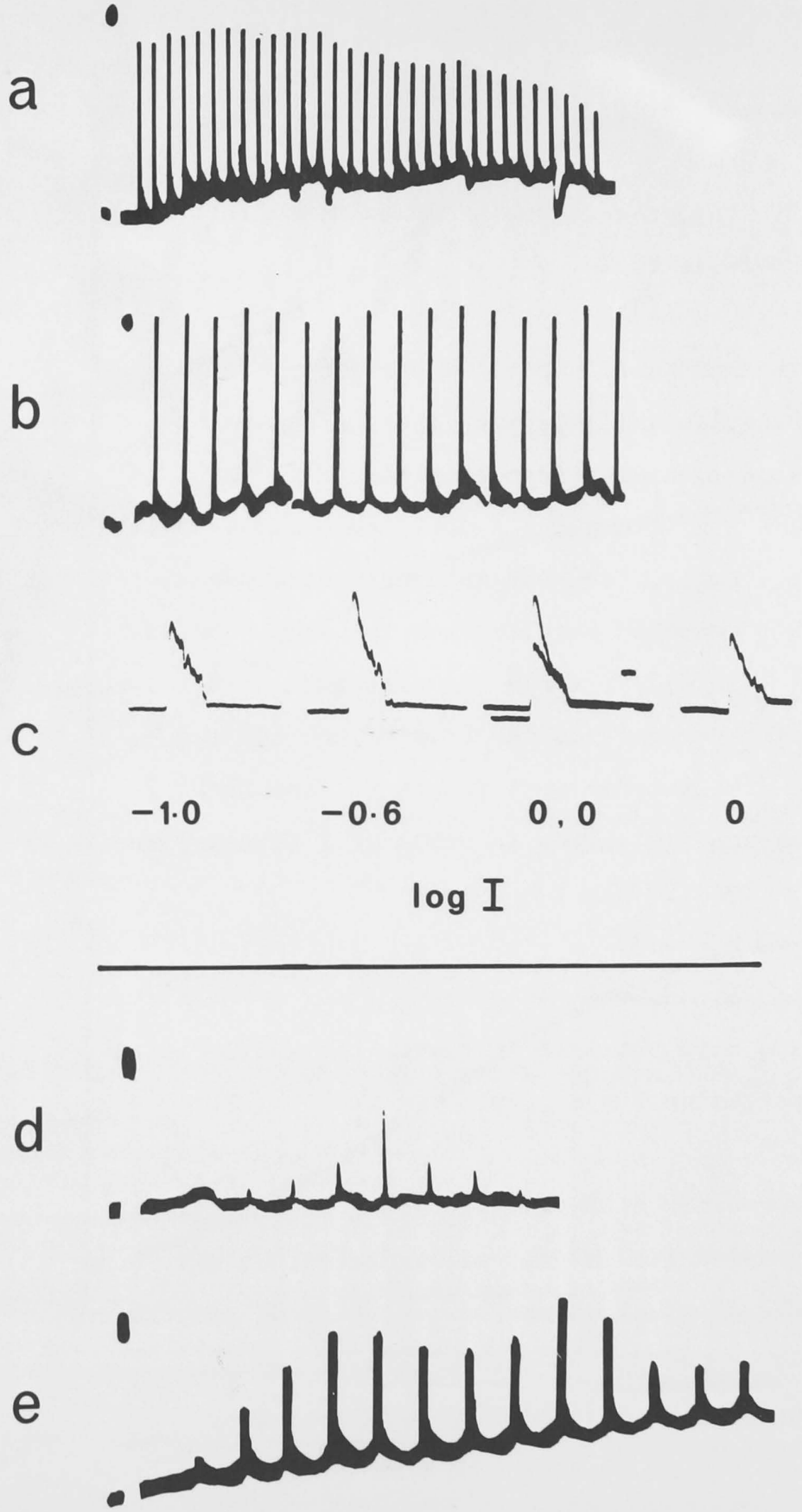
a
b
c
−1·0
−0·6
0,0
0
log I
d
e

Figure 36

The response-intensity relationships for retinula cells.

In each case, the solid curve represents the function $I/(I+k)$, with k being determined experimentally from each set.

a. Averaged results are from 5 light-adapted cells, for peak transient responses.

b. Averaged results from the same 5 cells in (a), but for the plateaus.

c. Averaged results from 4 dark-adapted cells, for peak transient responses.

Averaged k values in units of I (linear) are:

a. 0.03

b. 0.01

c. 0.04

and were obtained by taking the antilog of I for which $V = V_{max}/2$.

A greater difference in absolute sensitivity between (a) and (c) was expected, but not found. Histological checks on the state of adaptation were made on the method as an independent assessment of the state of adaptation.

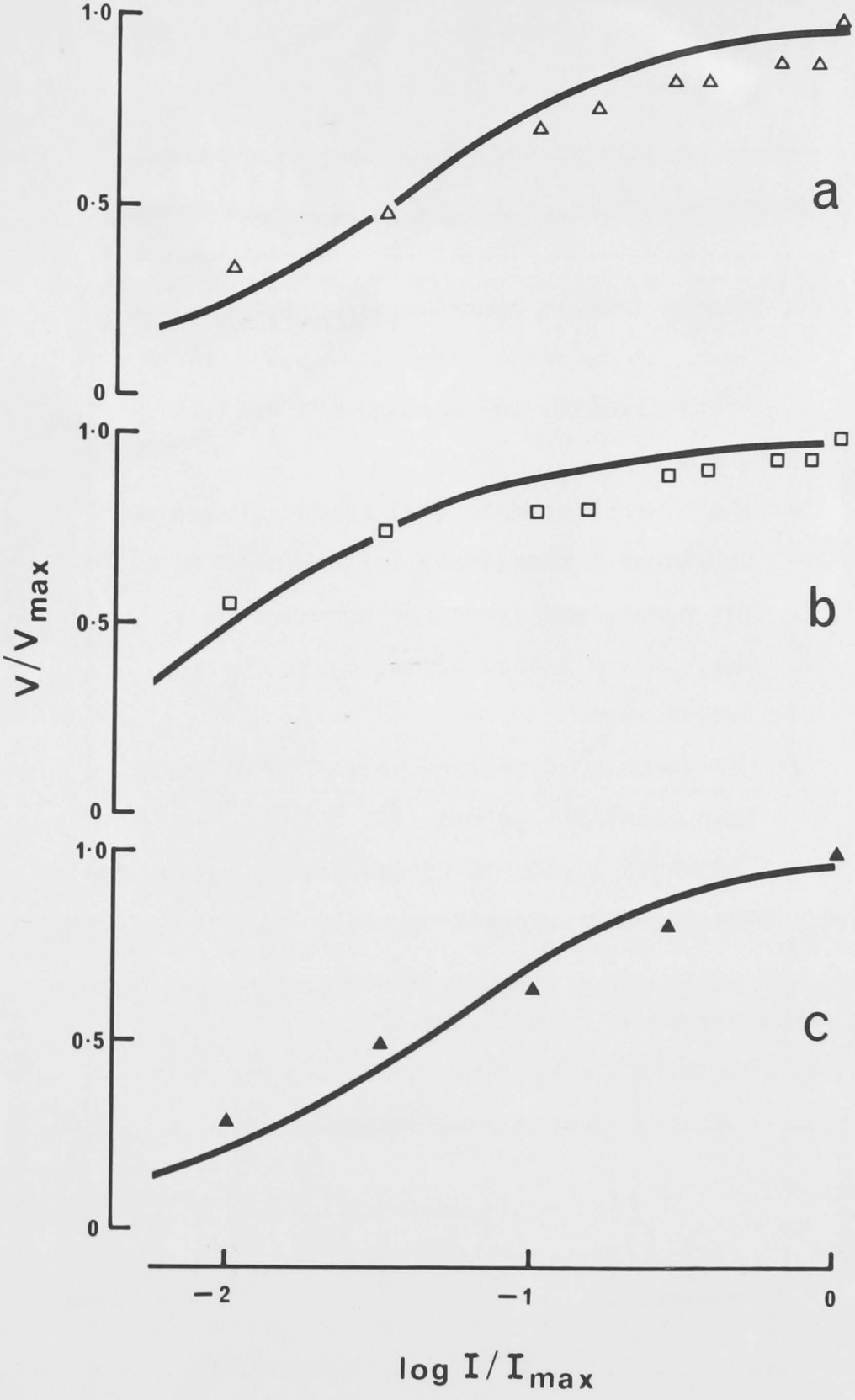
1·0
0·5
0
a
b
c
V/V max
−2
−1
0
log I/I max

Figure 37

Angles of acceptance. Light-adapted state. Horizontal field.

A. Record from an experimental run, with the lamp (at constant intensity) moved in 1° steps (inclination through the visual axis).
B. The neutral density (ND) series (responses to graded intensities) for the cell in A.
C. The normalized curve for the cell in A.
D. The V - log I sensitivity curve for the series in B.
E. The normalized average curve for 20 cells. Each point is the mean ± 1 SD.
F. Frequency histogram of acceptance angles for the 20 units averaged in E.

Calibrations. A and B, 10 mV
A, anterior; P, posterior; $\Delta\rho$, angle of acceptance at 50 per cent sensitivity

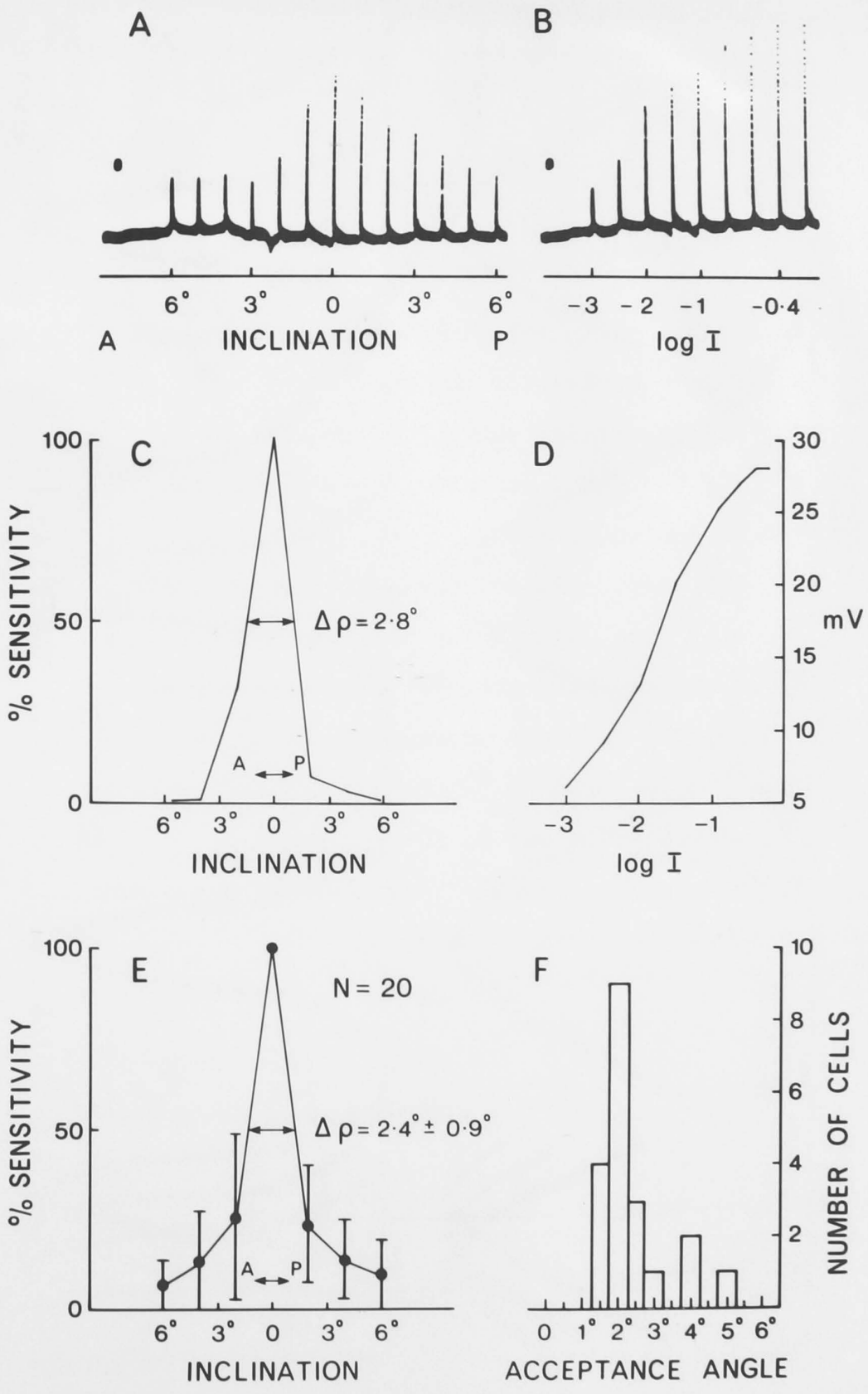
A
B
6° 3° 0 3° 6°
A INCLINATION P
-3 -2 -1 -0·4
log I
C
100
50
0
% SENSITIVITY
Δρ = 2·8°
A P
6° 3° 0 3° 6°
INCLINATION
D
30
25
20
15
10
5
mV
-3 -2 -1
log I
E
N = 20
Δρ = 2·4° ± 0·9°
A P
6° 3° 0 3° 6°
INCLINATION
F
10
8
6
4
2
NUMBER OF CELLS
0 1° 2° 3° 4° 5° 6°
ACCEPTANCE ANGLE

Figure 38

Angles of acceptance. Light-adapted state. Vertical field.

A. Record of an experimental run (in 1° steps).

B. The ND series for the cell in A.

C. The normalized curve for the cell in A.

D. The V - log I sensitivity curve for the ND series in B.

E. The normalized average curve for 16 cells, with each point being the mean ± 1 SD.

F. Frequency histogram of acceptance angles for the 16 units averaged in E.

Calibrations. A and B, 10 mV

D, dorsal; V, ventral; $\Delta\rho$, angle of acceptance at 50 per cent sensitivity

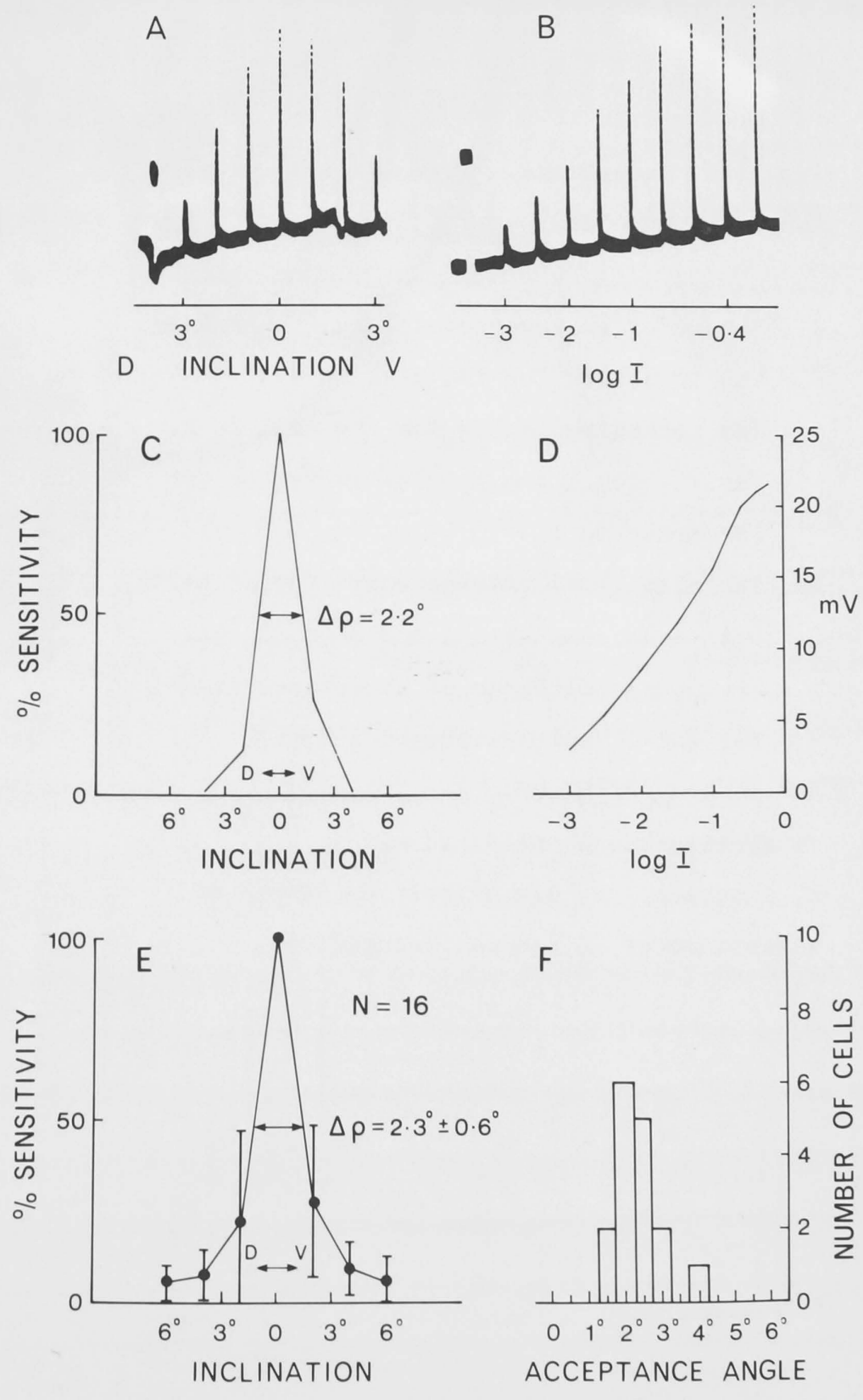
A
B
3°
0
3°
D INCLINATION V
-3
-2
-1
-0·4
log I
C
100
50
0
% SENSITIVITY
Δρ = 2·2°
D ↔ V
6°
3°
0
3°
6°
INCLINATION
D
25
20
15
10
5
0
mV
-3
-2
-1
0
log I
E
N = 16
Δρ = 2·3° ± 0·6°
F
NUMBER OF CELLS
0
1°
2°
3°
4°
5°
6°
ACCEPTANCE ANGLE

Figure 39

Angles of acceptance. Dark-adapted state. Horizontal field.

A. Record of an experimental run (1° steps).
B. The ND series for the cell in A.
C. The normalized curve for the cell in A.
D. The V - log I sensitivity curve for the ND series in B.
E. The normalized average curve for 17 cells with each point being the mean ± 1 SD.
F. Frequency histogram of acceptance angles for the 17 units averaged in E.

Calibrations. A and B, 10 mV
A, anterior; P, posterior; $\Delta\rho$, angle of acceptance of 50 per cent sensitivity

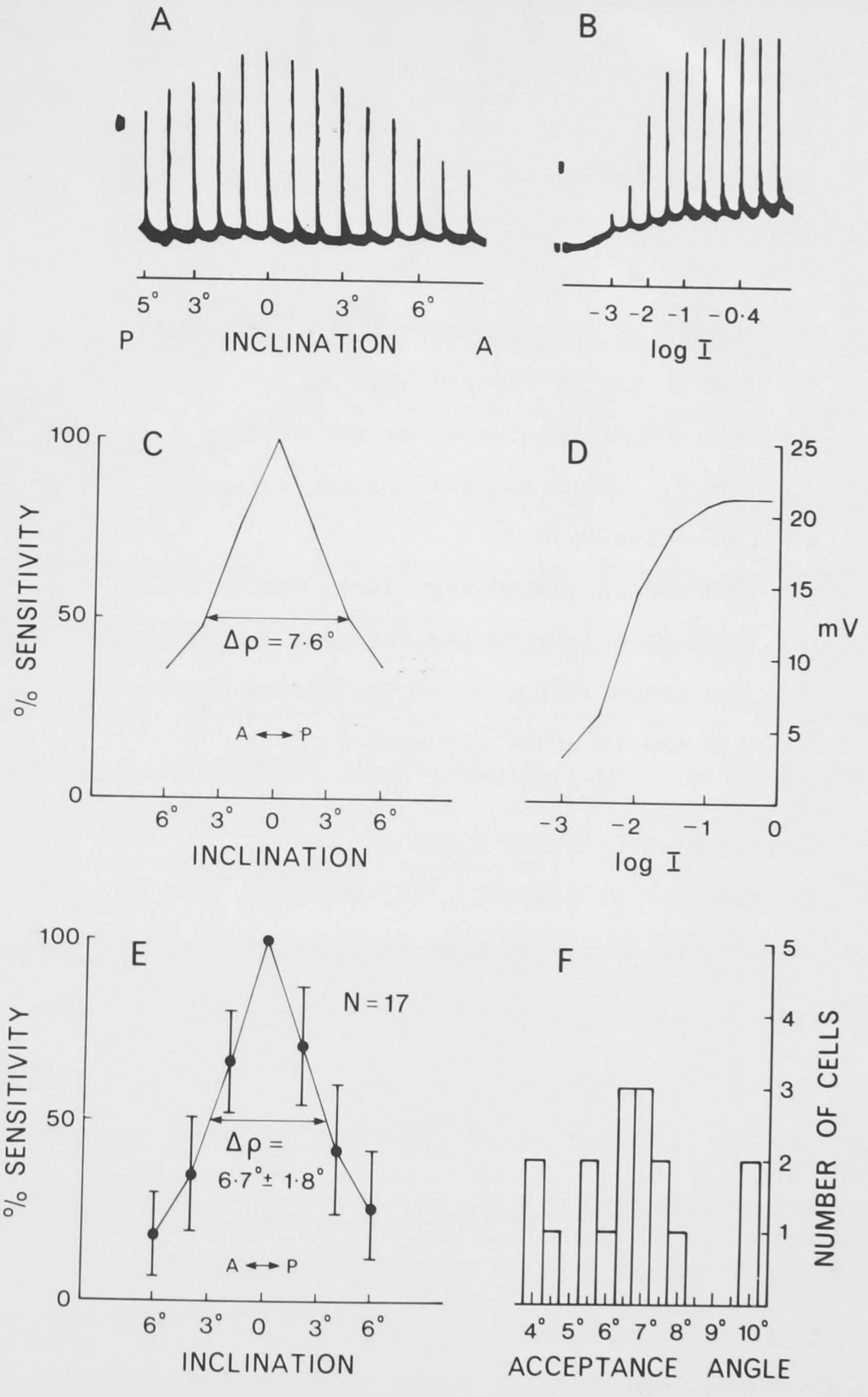
A
5° 3° 0 3° 6°
P INCLINATION A
B
-3 -2 -1 -0·4
log I
C
100
50
0
% SENSITIVITY
Δρ = 7·6°
A ↔ P
6° 3° 0 3° 6°
INCLINATION
D
25
20
15
10
5
mV
-3 -2 -1 0
log I
E
100
50
0
% SENSITIVITY
N = 17
Δρ =
6·7° ± 1·8°
A ↔ P
6° 3° 0 3° 6°
INCLINATION
F
5
4
3
2
1
NUMBER OF CELLS
4° 5° 6° 7° 8° 9° 10°
ACCEPTANCE ANGLE

Figure 40

Angles of acceptance. Dark-adapted state. Vertical field.

A. Record of an experimental run (2° steps).
B. The ND series for the cell in A.
C. The normalized curve for the cell in A.
D. The V - log I sensitivity curve for the ND series in B.
E. The normalized average curve for 14 cells with each point being the mean ± 1 SD.
F. Frequency histogram of acceptance angles for the 14 units averaged in E.

Calibrations. A and B, 10 mV
D, dorsal; V, ventral; $\Delta\rho$, angle of acceptance at 50 per cent sensitivity

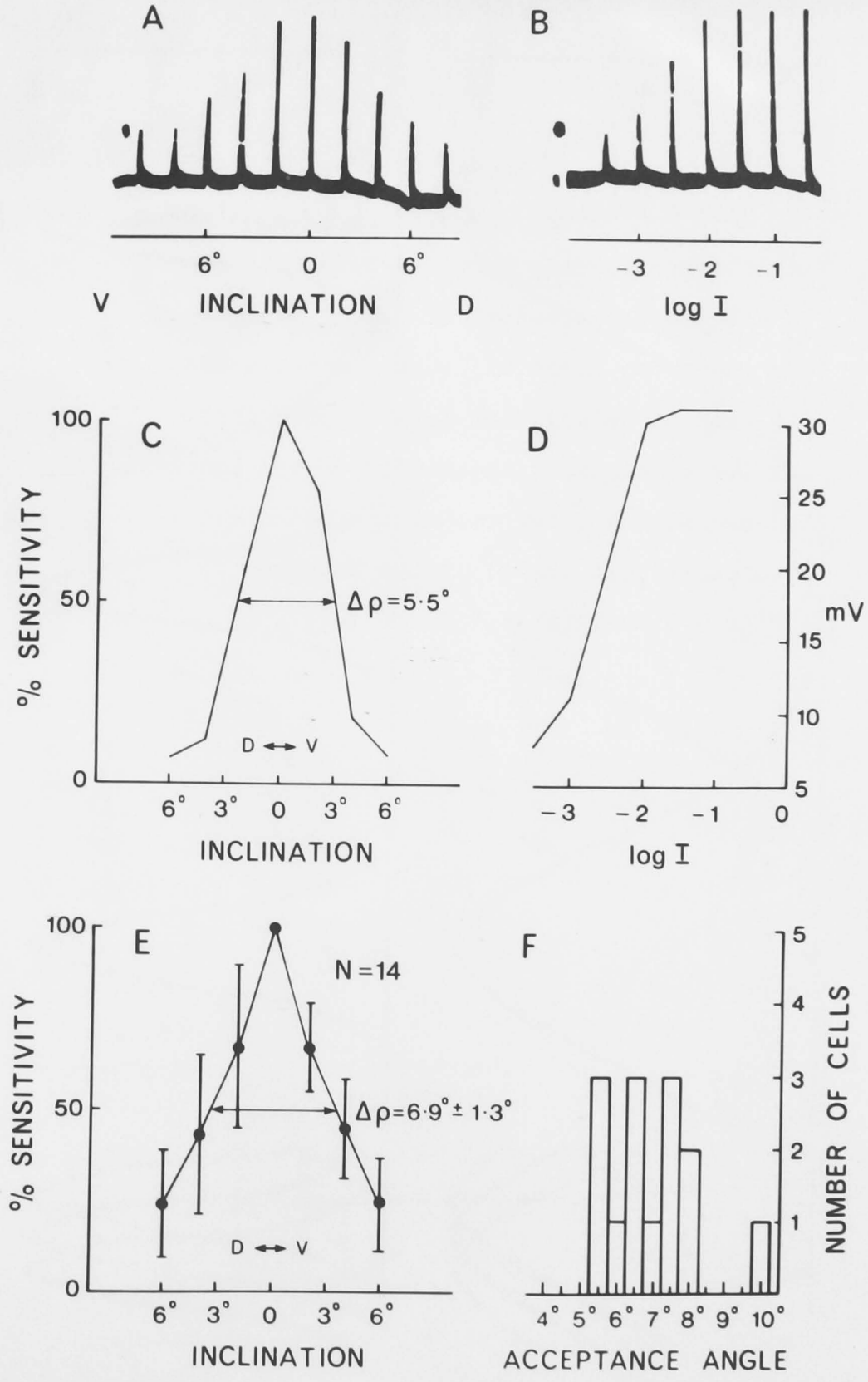
A
6°
0
6°
V
INCLINATION
D
B
-3
-2
-1
log I
C
100
50
0
% SENSITIVITY
Δρ=5·5°
D ↔ V
6°
3°
0
3°
6°
INCLINATION
D
30
25
20
15
10
5
mV
-3
-2
-1
0
log I
E
100
50
0
% SENSITIVITY
N=14
Δρ=6·9° ± 1·3°
D ↔ V
6°
3°
0
3°
6°
INCLINATION
F
5
4
3
2
1
NUMBER OF CELLS
4°
5°
6°
7°
8°
9°
10°
ACCEPTANCE ANGLE

Figure 41

Overlapping of the visual fields.

Normalized Gaussian curves arbitrarily chosen to fit the experimental angles of acceptance are shown for three adjacent light-adapted (LA) and three adjacent dark-adapted (DA) ommatidia. Lateral separation of the curves is determined by the values of the interommatidial angles at the extreme limits of their range (1° and 10°).

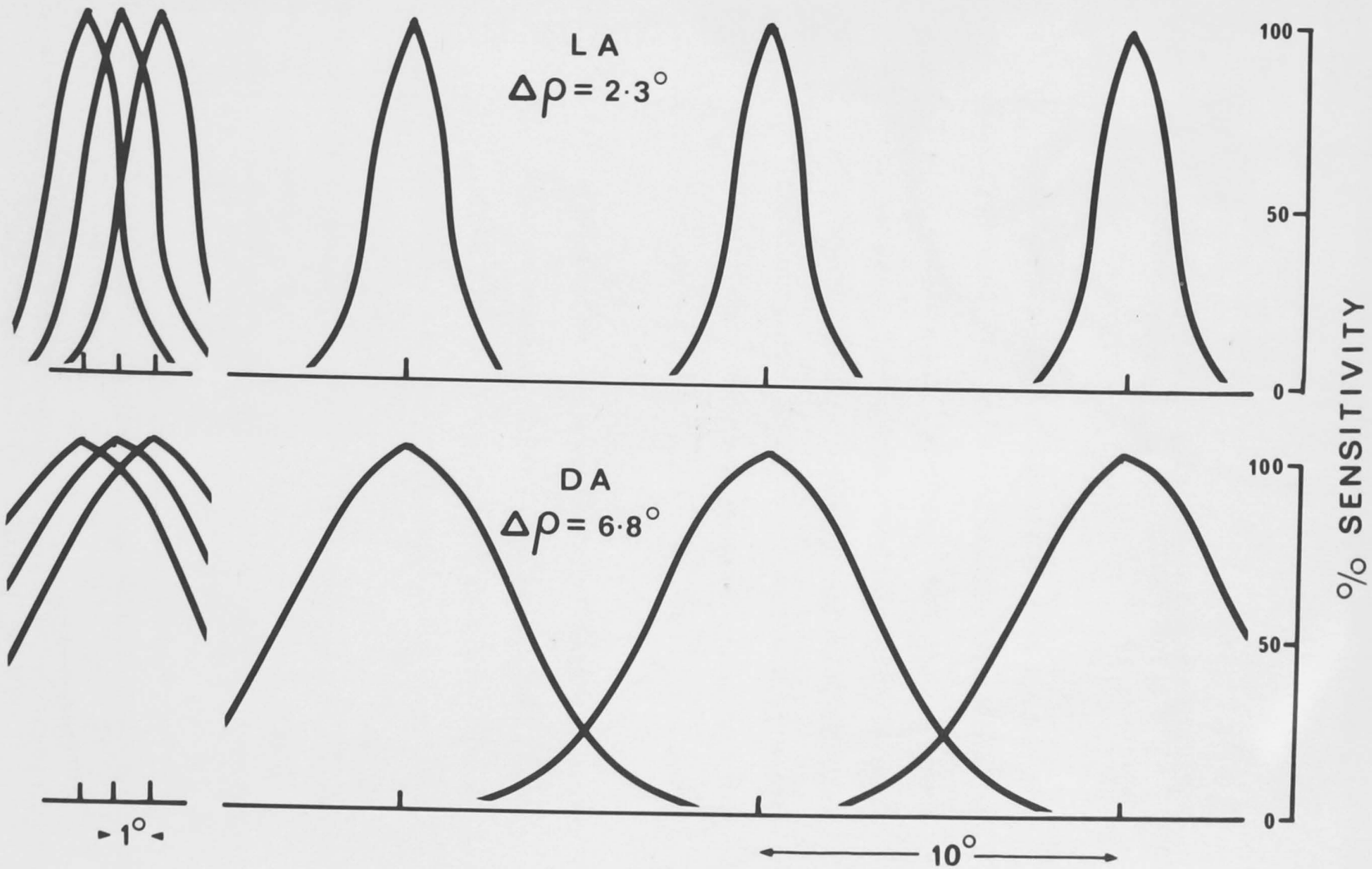
LA
Δρ = 2·3°
100
50
0
DA
Δρ = 6·8°
100
50
0
% SENSITIVITY
1°
10°

Figure 42

Differences in sensitivity between light- and dark-adapted cells.

The angles of acceptance for ten light- and ten dark-adapted cells (each with peak responses about $V_{max}/2$ for that cell) are plotted on a logarithmic relative sensitivity scale against angular position of the stimulus. They clearly fall into two groups with the dark-adapted cells forming the most sensitive group.

Note the individual variations in symmetry about the visual axis which is more evident in the dark-adapted group. One unit with a dual peak was included in the light-adapted group.

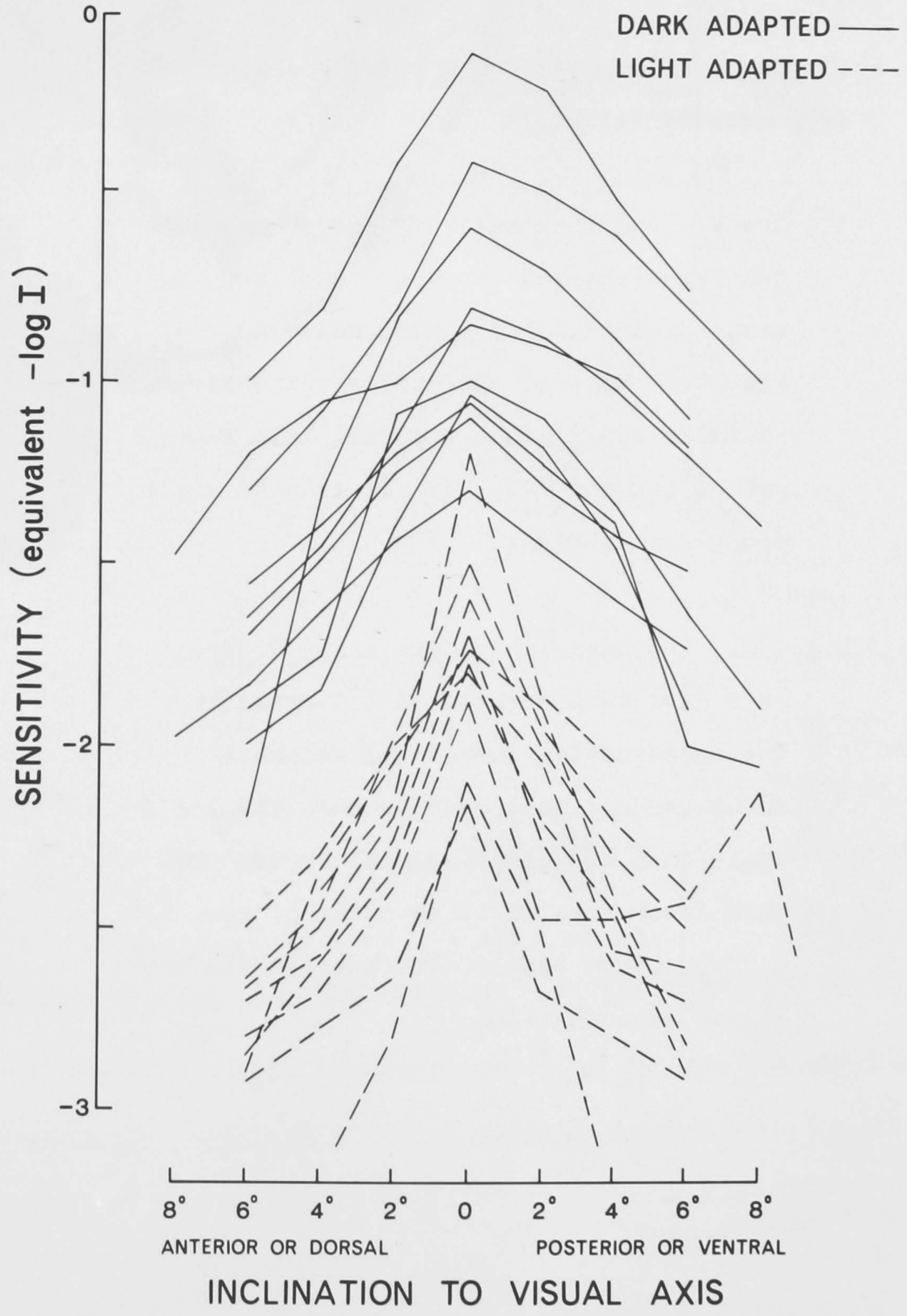
DARK ADAPTED
LIGHT ADAPTED
SENSITIVITY (equivalent -log I)
0
-1
-2
-3
8° 6° 4° 2° 0 2° 4° 6° 8°
ANTERIOR OR DORSAL
POSTERIOR OR VENTRAL
INCLINATION TO VISUAL AXIS

Figure 43

Differences in sensitivity between light- and dark-adapted cells.

A. The V - log I sensitivity curves for all the light-adapted (broken lines) and dark-adapted (solid lines) cells in Fig. 42. Most of the curves are saturated at their upper limit and fall into two groups (LA and DA), without lateral shift along the abscissa.

B and C. The dark- and light-adapted curves of A have been normalized and replotted. The dark-adapted curves (B) saturate about one log unit further down the log I scale than the light-adapted curves (C). This lateral shift is an index of the difference in sensitivity between the two states of adaptation.

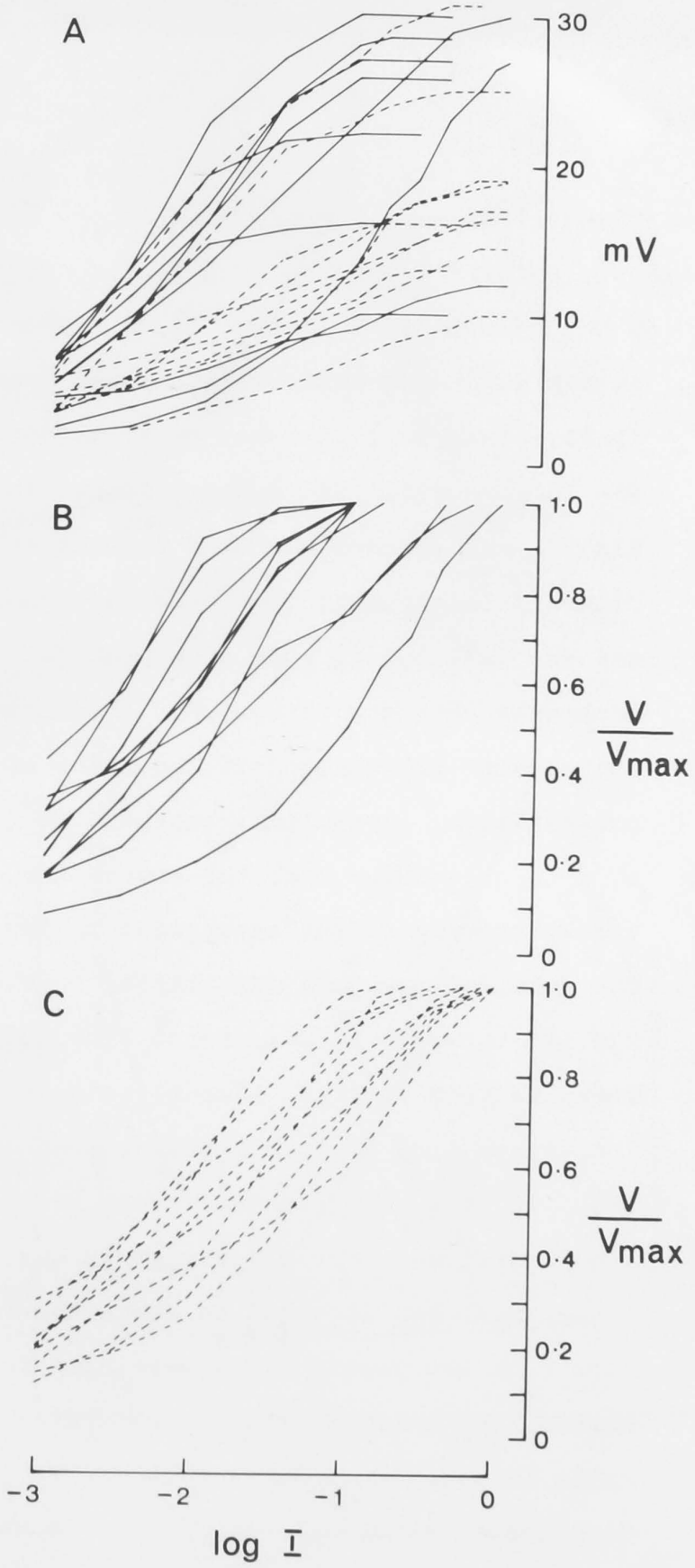
A
30
20
10
0
mV
B
1·0
0·8
0·6
0·4
0·2
0
V
Vmax
C
1·0
0·8
0·6
0·4
0·2
0
V
Vmax
−3
−2
−1
0
log I

Figure 44

Polarized light sensitivity.

a and b. Records of polarized light responses in two different cells whose maxima are 90° apart. Each cell is shown with its own V - log I curve. The final response in each PL run (arrow) was made without the polaroid interrupting the stimulus beam, and was included to show that peak PL responses were not saturated. $\psi°$ denotes the angular orientation of the plane of polarization. Note that responses in (a) tend to be smaller near the end of the trace, showing slight adaptation in the cell.

c. The averaged per cent sensitivity curves for the two types of PL responses. The solid curve is from 4 cells, like the one in (a). The broken line is from 5 cells, such as (b). In each case, the means are shown with 1 SD indicated. For clarity, only half the SD bar has been inserted in cases where error bars from two points would overlap. For both curves, the maximum: minimum sensitivity ratio is 5:1.

Rhabdomere orthogonal tubules lie in the same planes as peak sensitivity.

Calibration. a and b, 10 mV

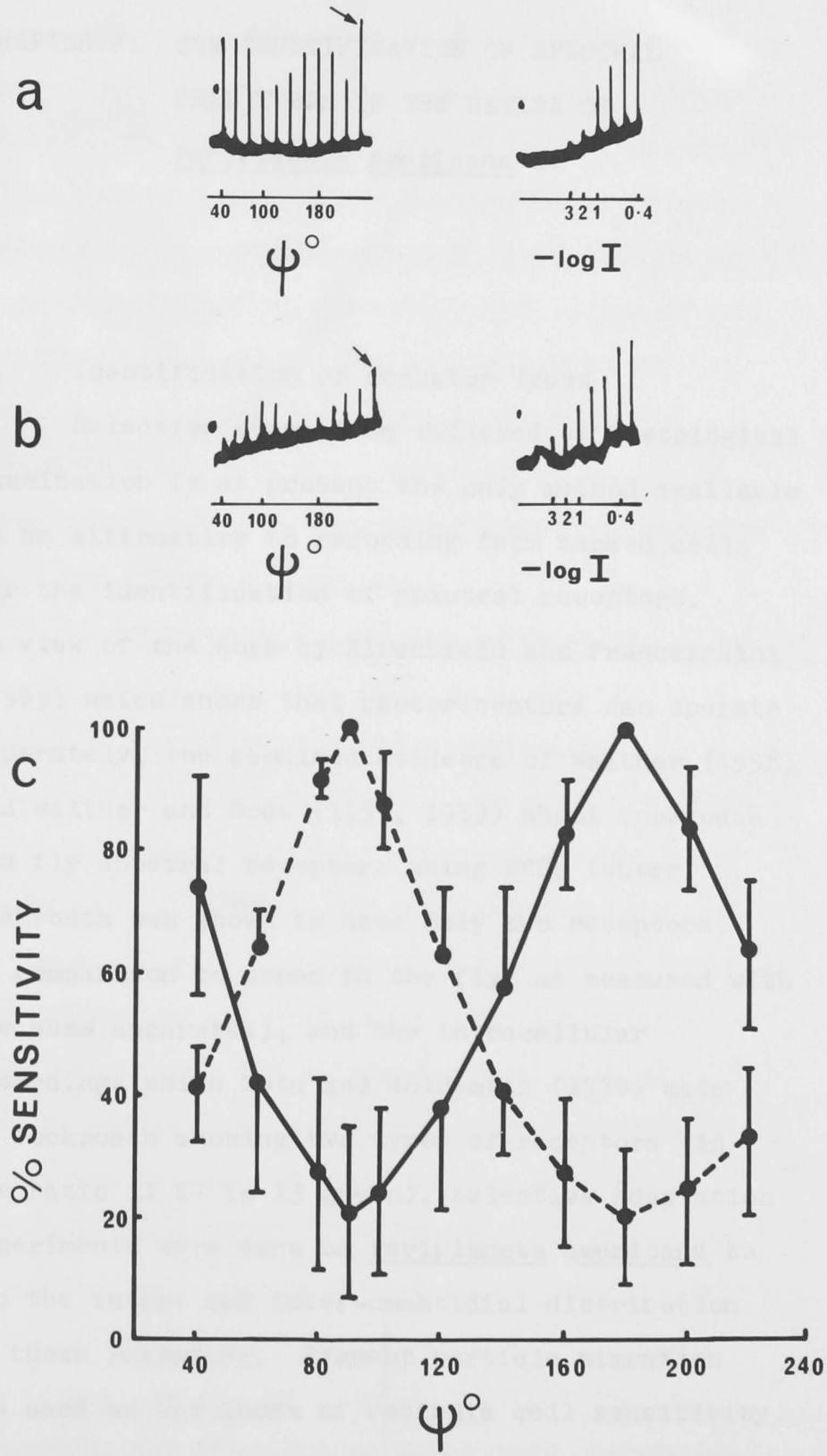
a
40 100 180
ψ°
3 2 1 0·4
−log I
b
40 100 180
ψ°
3 2 1 0·4
−log I
c
% SENSITIVITY
100
80
60
40
20
0
40 80 120 160 200 240
ψ°

CHAPTER V: THE IDENTIFICATION OF SPECTRAL CELL TYPES IN THE RETINA OF *Periplaneta americana* L.

A. Identification of Receptor Types

Selective adaptation followed by histological examination is at present the only method available as an alternative to recording from marked cells for the identification of spectral receptors. In view of the work by Kirschfeld and Franceschini (1969) which shows that photoreceptors can operate separately, the combined evidence of Walther (1958) and Walther and Dodt (1957, 1959) about cockroach and fly spectral receptors using ERGs (where cockroach was shown to have only two receptors in comparison to three in the fly, as measured with the same apparatus), and the intracellular recordings which Mote and Goldsmith (1970) made on cockroach showing two types of receptors (in the ratio 11 UV to 13 green), selective adaptation experiments were done on *Periplaneta americana* to map the intra- and inter-ommatidial distribution of these receptors. Pigment particle migration was used as the index of retinula cell sensitivity.

When a light-adapted ommatidium from Periplaneta is dark-adapted, the pigment moves away from its position adjacent to the rhabdom. The maximum movement is limited by the maximum width (up to 1 μm) of the palisade (see below). The extent of movement after a fixed time is some function of the intensity and colour of the light. The crucial point is the length of time one leaves the eye in light of an intensity which is convenient to use for selective adaptation. Preliminary tests showed that 3 min with the filter was adequate.

A measure of the movement was obtained in the following way (Fig.45): each cell's contribution to twenty-five rhabdoms was determined in photographs. Half-way along each soma-rhabdomere boundary the width of the rhabdomere (b in Fig.45c) was measured perpendicular to the general trend of the boundary. Measurements were made under a dissecting microscope with any ultrastructural changes due to boiling being disregarded. Palisade width was measured at its maximum from the same boundary point (a in Fig.45c). The ratio $a/a + b$, which ranges from 0 to 1, was calculated for each cell. The ratio was selected because it is most sensitive when a is small. The cell numbers used correspond to those used in CHAPTER III.

1. Ultraviolet (UV) Receptors

Cells 1, 5 and 7 are UV sensitive. Fig. 46 shows a typical section from the ventral portion of a left eye selectively adapted by 311 nm light. Very few of the cells are completely light-adapted by the selected wavelengths, showing that they are not saturated. However, in each ommatidium, cells 1, 5 and 7 are more light adapted than cells 2, 3, 4, 6 and 8. Incomplete light-adaptation was the rule, and conveniently avoids the problem of complete saturation. With increasing depth in the retina one sees decreasing degrees of light-adaptation after a dark-adapted eye is illuminated for short periods (see Section C, below). To avoid variability due to differing depths, all ratios for all experiments were taken from a 10 μm deep band at a 180 - 190 μm depth from the corneal surface in the retina, except as otherwise stated. Average ratios from all cells of 25 different ommatidia were plotted as histograms for dorsal (Fig.48a) and ventral (Fig.48c) portions in left eyes selectively adapted with 311 nm light. In each case the results are all the same with cells 1, 5, and 7 forming one most sensitive set. Cells 2, 3, 4, 6 and 8 are relatively insensitive.

2. Green Receptors

The converse adaptation experiment was done using 536 nm light. As before, few cells are completely light-adapted (Fig.47). Cells 2, 3, 4, 6 and 8 are more light-adapted within each ommatidium than cells 1, 5 and 7, in both dorsal and ventral regions (Fig.48b, d).

The cells fall into the same two groups as before, except for the expected reversal.

If only two types occur as other work suggests, cells 1, 5 and 7 are the UV receptors and all and only cells 2, 3, 4, 6 and 8 are the green receptors. This receptor pattern is constant, both intra- and inter-ommatidially, across the whole retina (see Fig. 9, CHAPTER III).

B. Inter-Retinal Transfer of Adaptation Effects

Blacked-out right eyes available from the above experiments were fixed, sectioned and photographed as before. Histograms of the ratios (Fig.49) are from eyes on the opposite side to eyes adapted with 311 nm and 536 nm light. The cells do not fall into groups in either case. This confirms the general finding (Day, 1941; Kirschfeld and Franceschini, 1969) that the retinula cells are independent effectors.

C. Implications of the Ratio Method

At the start of each experiment the ratios must all be uniform or the two groups which separate out upon selective adaptation cannot be used to identify two types of receptors. Furthermore, pigment particles must migrate at different rates in different cells or the grouping is invalid. Experiments were done on dark-adapted and partly light-adapted (ND 1.5) eyes to cover these points.

1. Ratios from Dark-Adapted Eyes

The ratios of dark-adapted cells are constant at all depths in the retina (Fig.50). The histograms have an average level between 0.55 and 0.57 indicating that each maximum palisade width is slightly greater than the rhabdomere width of its cell.

2. Ratios from Partly Light-Adapted Eyes

These ratios are fairly constant for all cells at any one depth in the retina but show a trend towards greater values with increasing depth from the corneal surface (Fig.51).

3. Rhabdomere Widths

Average rhabdomere widths (from dark- and partly light-adapted ratios) show a curious depth profile (Fig.52). Width is defined as b

in Fig.45c. Crystalline cones extend down about 100 µm, with rhabdomeres surrounding their proximal tips. Rhabdomeres 1 and 5 are conspicuously wider throughout the entire depth. Generally, the others are of uniform width to the 125 µm depth, after which all rhabdomeres swell to maximum width at 155 µm and then recede, reaching equivalent status with higher levels (say 100 µm) at 185 µm.

D. Statistical Treatment

A rank order test for the difference between two groups (cells 1, 5, 7 versus cells 2, 3, 4, 6, 8) was used (after Edwards, 1967). Results are given in Table 2. The null hypothesis was rejected only for selective adaptation data, confirming that two groups exist.

E. Discussion

Several methods have been used to study the spectral sensitivity of insect compound eye photoreceptors. Spectral sensitivity curves obtained from intracellular recordings are regarded as being the most accurate and meaningful. Although indications have come from some intracellular recordings, information from this source about intra- and inter-ommatidial distributions of different spectral receptors is meagre. Burkhardt (1962) found blue, green, and yellow-green receptors in

TABLE 2

Results of the rank order test for the difference between two groups

Conditions[a]	Region[a]	T or T' values[b]	Null hypothesis
Dark-adapted L(V)	95 µm depth	T = 13	Accept
	125 µm depth	T'= 8	Accept
	155 µm depth	T = 13	Accept
	185 µm depth	T = 10	Accept
Partly light-adapted L(V)	95 µm depth	T'= 10	Accept
	125 µm depth	T'= 7.5	Accept
	155 µm depth	T'= 11	Accept
	185 µm depth	T'= 8.5	Accept
311 nm adapt. of L(D, V)	R(V)	T = 10	Accept
	L(D)	T'= 6	Reject
	L(V)	T'= 6	Reject
536 nm adapt. of L (D, V)	R(V)	T'= 10	Accept
	L(D)	T = 6	Reject
	L(V)	T = 6	Reject

[a] L = left eye; R = right eye; D = dorsal; V = ventral.

[b] T or T' has P = 0.05 whenever T or T' (whichever smallest) ≤ 6 for two groups of $n_1 = 3$ (cells 1, 5, 7) and $n_2 = 5$ (cells 2, 3, 4, 6, 8).

ventral fly eye in the proportions 1:5:1. He related these anatomically to a seven-celled ommatidium by speculating that all three types of receptors may be found in each ommatidium, in the same 1:5:1 proportions. This has not been confirmed by the other methods.

Major differences in spectral behaviour between regions of some insect eyes have long been known, mainly by ERG methods, but these are too crude to study ommatidial differences. At the more informative single cell level, Burkhardt (1962) found the dorsal half of fly eye populated by green receptors while the ventral region contains a mixture of these types. Autrum and von Zwehl (1964) found three receptor types in drone bee: an ultraviolet (UV), a blue and a green. The green receptor was found only in the ventral region of the eye. The anterior (Autrum and von Zwehl, 1964) and central (Shaw, 1969a) areas of drone eye are populated exclusively by UV receptors. In adult dragonflies, Horridge (1969) reports that the dorsal portion of the eye contains mainly violet receptors.

Although marking of recorded cells by dye injection is feasible, and can be used as a check, the electrophysiological mapping of intra- and inter-ommatidial distributions of spectral receptors is tedious.

Intra-ommatidial mapping of receptors by microspectrophotometry (Langer and Thorell, 1966) on the fly partially agrees with Burkhardt's above results. The peripheral six cells are green and a central one is blue. However, this method is only applicable to open rhabdomere eyes.

Many kinds of structural changes in compound eyes can occur under the influence of light. The only ones that are relevant to this work are those occurring in the retinula cells as these are the primary receptors, and the changes are cell specific. Some of these intra-cellular changes are at the ultrastructural level and can only be identified by using the electron microscope (EM). Others such as screening pigment particle migration and palisade formation are gross, are readily seen across large numbers of ommatidia under the light microscope, and generally are not influenced by fixation artifacts. In worker bee, Gribakin (1969) found differences at the ultrastructural level between three types of cells which respond differently to different coloured lights. It is not clear to what extent the fixation procedure contributed to the morphological differences. The use of an EM limits the survey area.

Early ERG studies on Periplaneta indicated only two receptor types, UV and green (Walther, 1958; Walther and Dodt, 1957, 1959). This was confirmed by Mote and Goldsmith (1970) who showed that individual

receptors had single peaks at 365 nm (UV) and 507 nm (green).

The histological results substantiate the two-receptor system of cockroach but contradict some aspects of previous work. Walther (1958) found two dorsal receptor types, but only one (green) ventral. Mote and Goldsmith (1970) reported dorsal receptor types in about equal numbers. I found a 3 (UV): 5 (green) ratio within each ommatidium which is absolutely constant across the retina. Furthermore, the positions of receptor types are fixed and constant among all ommatidia. The receptor pattern is mirror-imaged about the dorsal-ventral axis in the opposite eye. This fixed receptor pattern may be functionally important if dichromatic vision is realized centrally.

Any coupling between individual units must be relatively small. Receptors of one type respond quite independently of the others (cf. Kirschfeld and Franceschini, 1969). That converse units were partly light-adapted (cf. Fig.46 and47) can be attributed to small potentials arising from stimulation by the adapting light. This agrees with the conclusions of the polarized light sensitivity studies (CHAPTER IV D).

The inter-retinal transfer experiments confirmed the existence of independent effectors. Evaluation of the data from experiments on dark- and partly light-adapted eyes yields more subtle evidence, showing just how localized effects can be. The extent of the

palisade at any given depth in dark-adapted cells is directly related to the amount of rhabdomere immediately adjacent. The ratios of dark-adapted cells (Fig.50) are relatively flat and equal at all levels. Rhabdomere widths vary with retinal depth (Fig.52), showing that the palisade must also vary with depth in order to keep the ratios equal. Screening pigment migration is related to photopigment excitation (i.e., depolarization). Fig.51 implies that this migration is a very localized phenomenon within the cell. The histograms are fairly flat at each depth indicating uniform adaptation at that level, but there is a gradation towards greater dark-adaptation with increasing depth in the retina. This applies for all cells, showing that each is capable of being simultaneously light-adapted distally and dark-adapted proximally, with a graded continuum between.

Uniform adaptation in white light yields intuitive information about the velocity of pigment particle migration in individual cells. The rate of this migration is also related to the amount of rhabdomere. Rhabdomeres 3 and 6 are consistently smaller than 1 and 5 (Fig.52) and their palisades are also smaller when dark-adapted. During light-adaptation the ratios of all cells are equal (Fig.51). Therefore, pigment particles must be moving at different rates in individual cells in order to maintain equal ratios. The relation between

rhabdomere volume and degree of receptor depolarization is unknown, so any correlation between quantity and/or quality of light and adaptation rates is impossible to determine.

After this study was completed and was in press, Mote and Goldsmith (1971) published a short paper in which they also showed two receptor types within a single ommatidium of Periplaneta. They made simultaneous intracellular recordings from green and UV cells and injected two types of dye to identify the units. Their drawings show no detail of ommatidial anatomy or spatial geometry, but do confirm that the two receptors do occur together in one ommatidium.

Figure 45

a. Photomicrograph (Zeiss Planapochromat X 100/1.3 oil immersion objective) of a left ventral ommatidium after selective adaptation with 311 nm light. Cells 1, 5, 7 (UV receptors) are completely light-adapted, the rest only partly.

b. Drawing of (a).

c. Drawing of (a) to show explanation of measurements. pal palisade; rh rhabdom; A anterior; D dorsal.

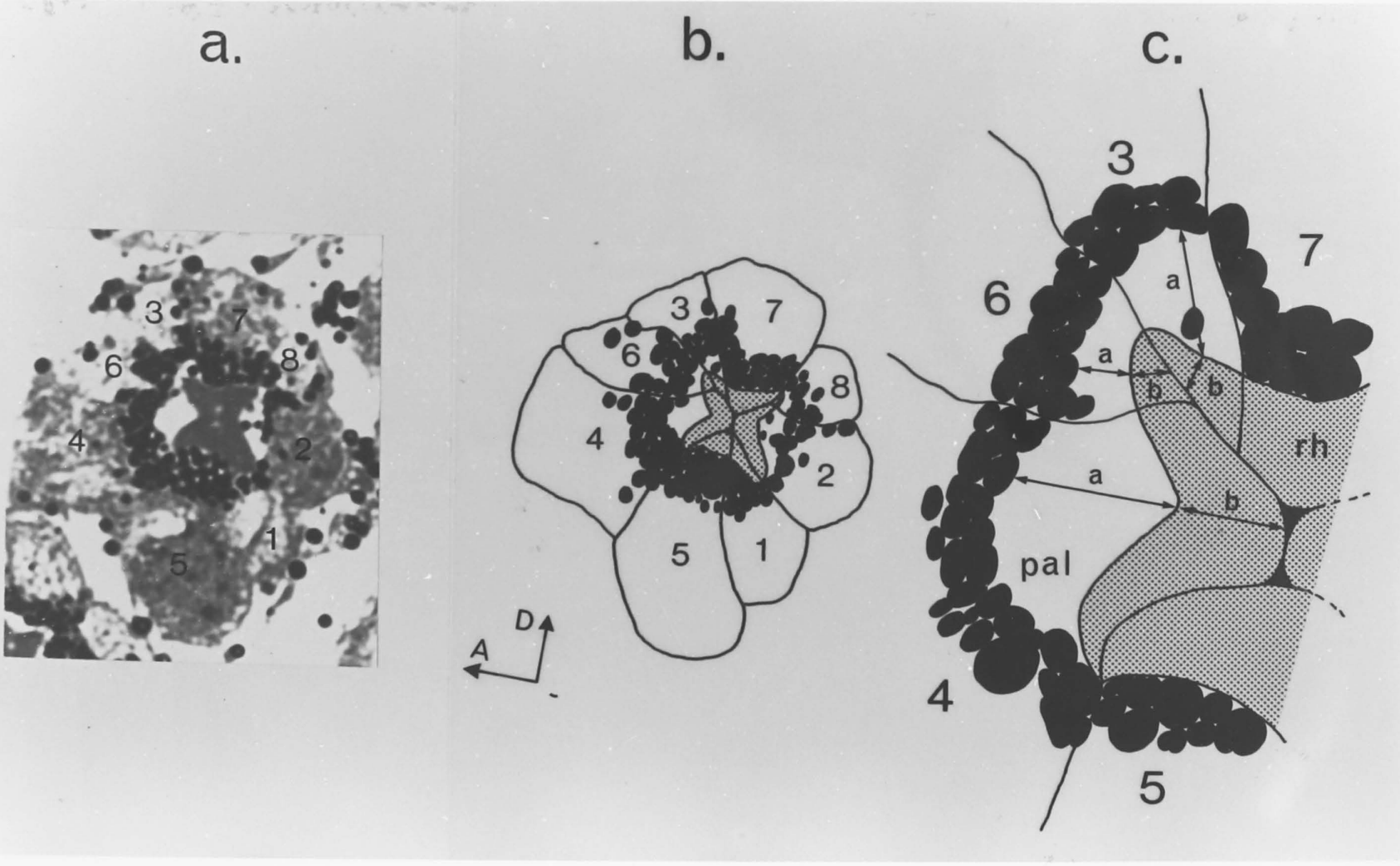
a.
b.
c.
3
7
6
8
4
2
5
1
D
A
a
b
rh
pal

Figure 46

Photomicrograph (Zeiss Planapo x 100 oil) of ommatidia in left ventral eye selectively adapted with 311 nm light. Cells 1, 5, 7 are more light-adapted than the others and are the UV receptors. A anterior; D dorsal.

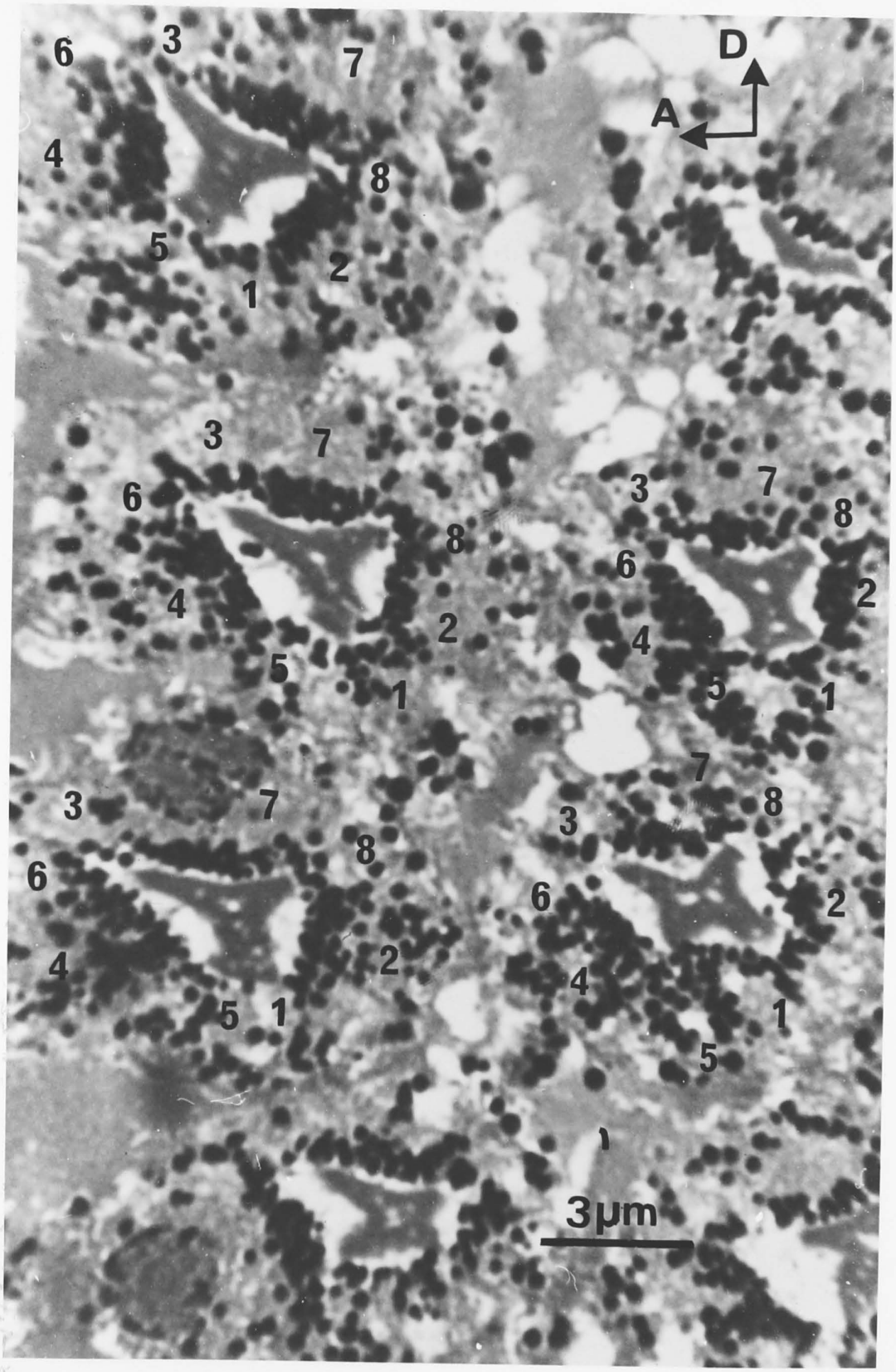
D
A
3µm

Figure 47

Photomicrograph (Zeiss Planapo x 100 oil) of ommatidia in left ventral eye selectively adapted with 536 nm light. Cells 2, 3, 4, 6, 8 are the green receptors and are more light-adapted than the others. A anterior; D dorsal.

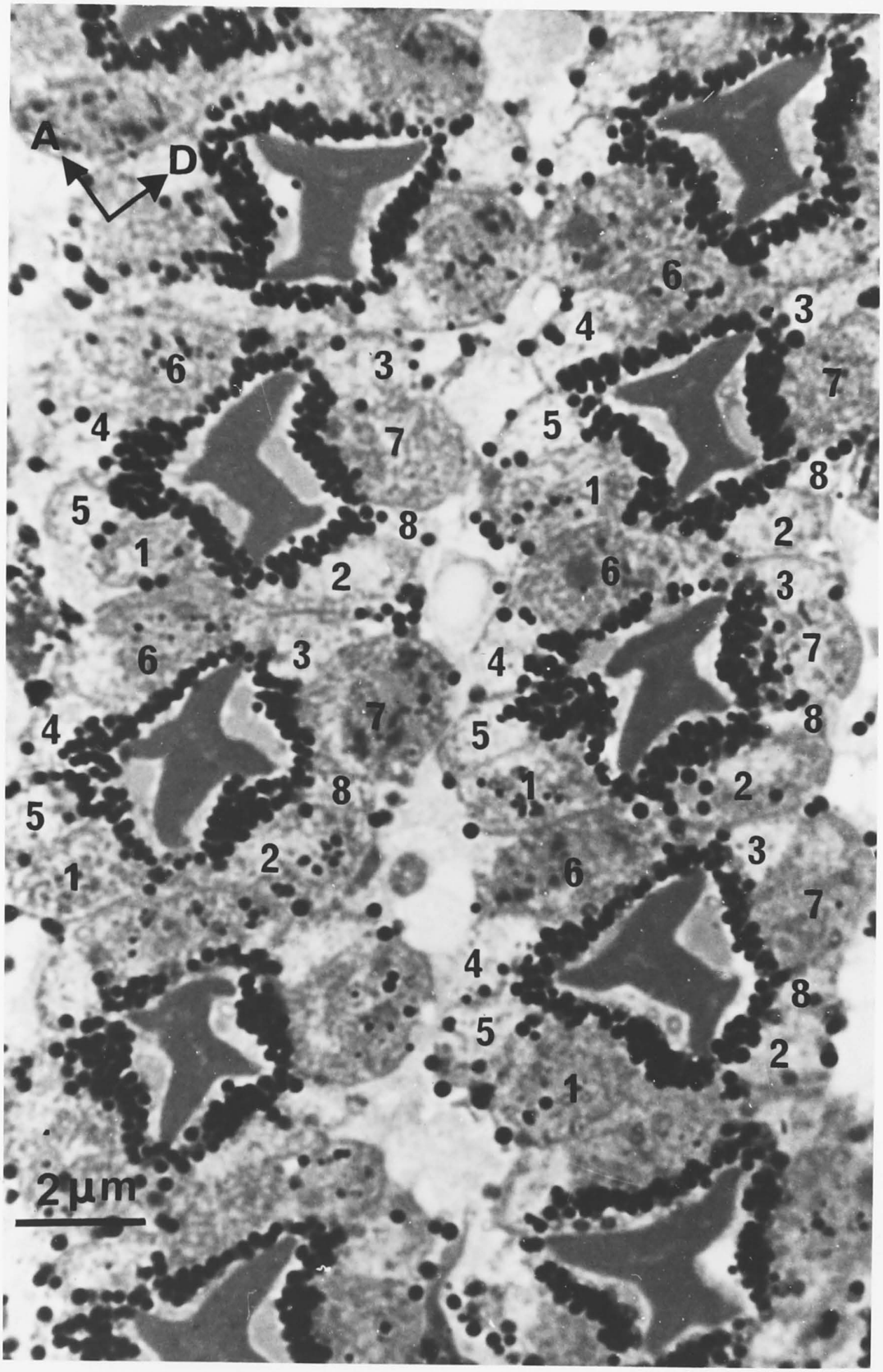
A
D
2µm

Figure 48

Histograms of averaged ratios from left dorsal (a) and ventral (c) ommatidia selectively adapted with 311 nm light; and from left dorsal (b) and ventral (d) ommatidia selectively adapted with 536 nm light. The lower the ratio (palisade/ palisade + rhabdom) value, the more sensitive the cell.

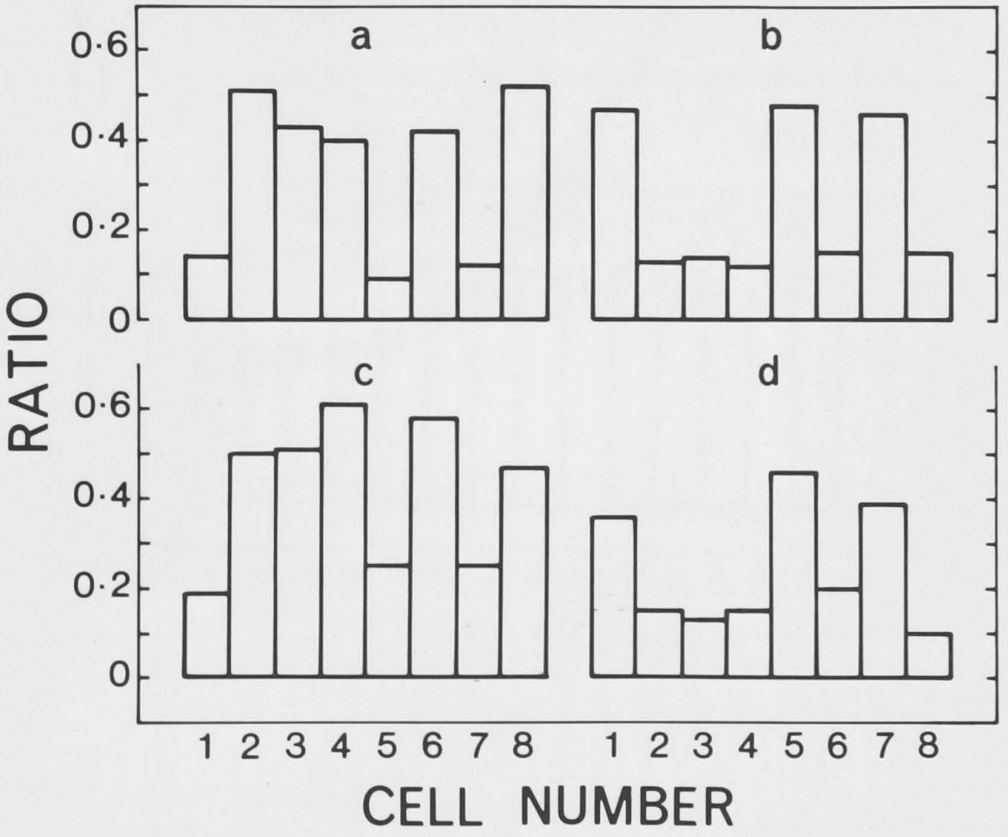
a
b
c
d
0·6
0·4
0·2
0
RATIO
1 2 3 4 5 6 7 8
1 2 3 4 5 6 7 8
CELL NUMBER

Figure 49

Histograms of inter-retinal transfer effects from right ventral eyes whose counterpart was selectively adapted with (a) 311 nm and (b) 536 nm light.

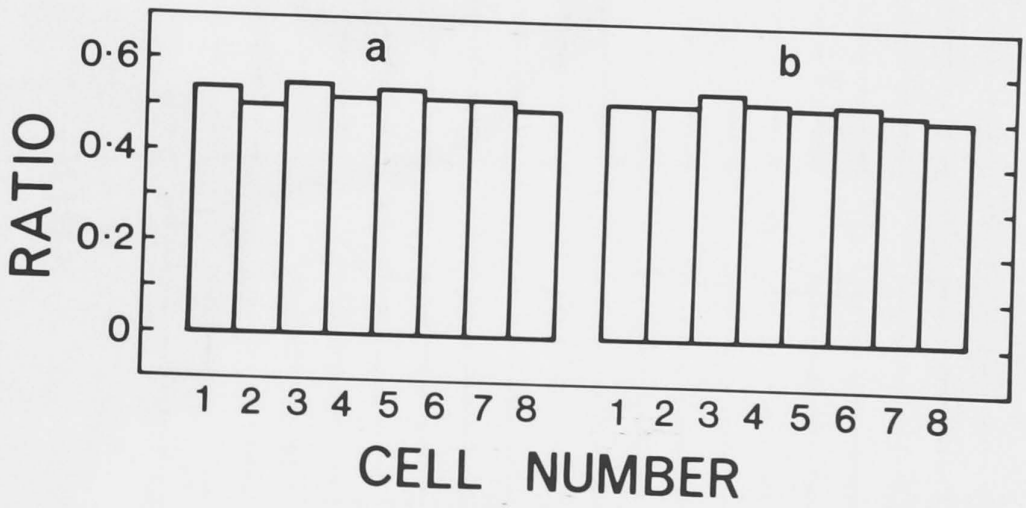
a
b
0·6
0·4
0·2
0
RATIO
1 2 3 4 5 6 7 8
1 2 3 4 5 6 7 8
CELL NUMBER

Figure 50

Histograms of averaged ratios of dark-adapted left ventral ommatidia at four depths from the corneal surface. (a) 95 μm; (b) 125 μm; (c) 155 μm; (d) 185 μm.

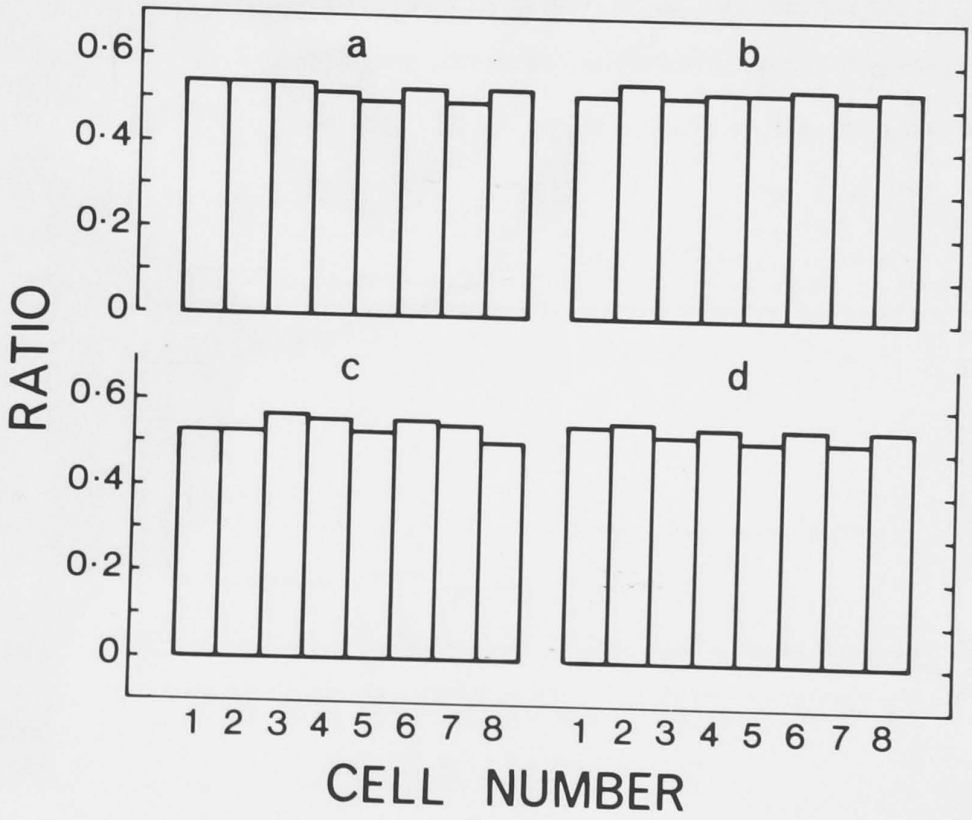
a
b
c
d
0·6
0·4
0·2
0
RATIO
1 2 3 4 5 6 7 8
1 2 3 4 5 6 7 8
CELL NUMBER

Figure 51

Histograms of averaged ratios of partly light-adapted left ventral ommatidia, at four depths from the corneal surface.
(a) 95 µm; (b) 125 µm; (c) 155 µm;
(d) 185 µm.

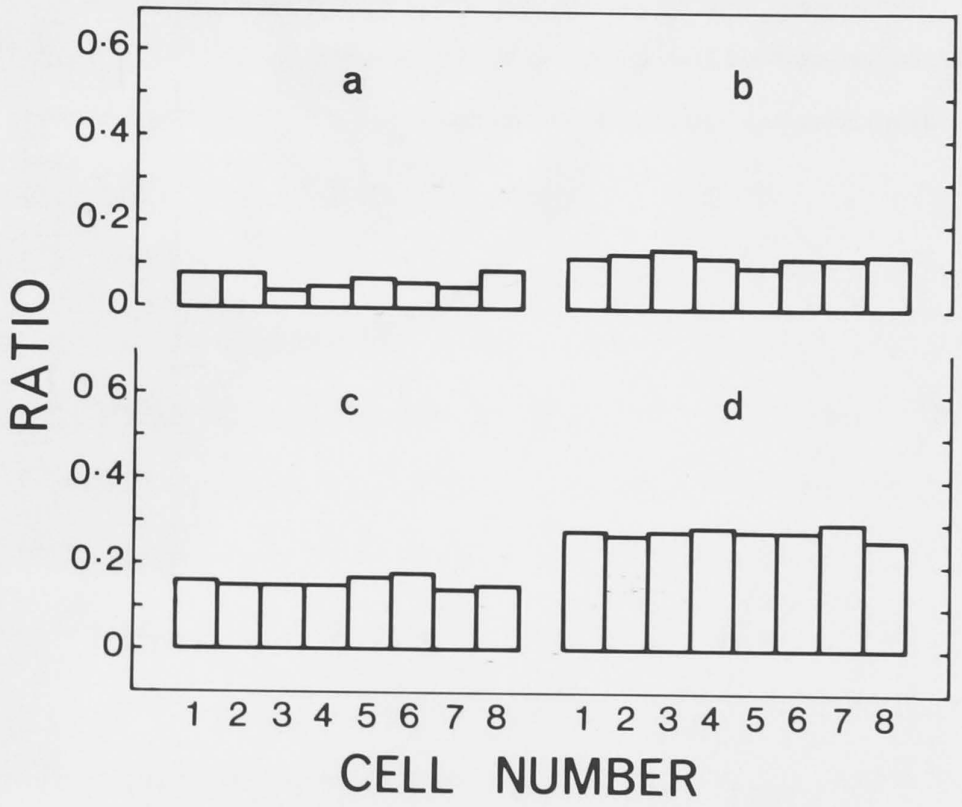
0·6
0·4
0·2
0
a
b
RATIO
0 6
0·4
0·2
0
c
d
1 2 3 4 5 6 7 8
1 2 3 4 5 6 7 8
CELL NUMBER

Figure 52

Averaged rhabdomere (1 to 8) widths at different depths from the corneal surface. Above and below depth limits shown, all rhabdomeres quickly terminate.

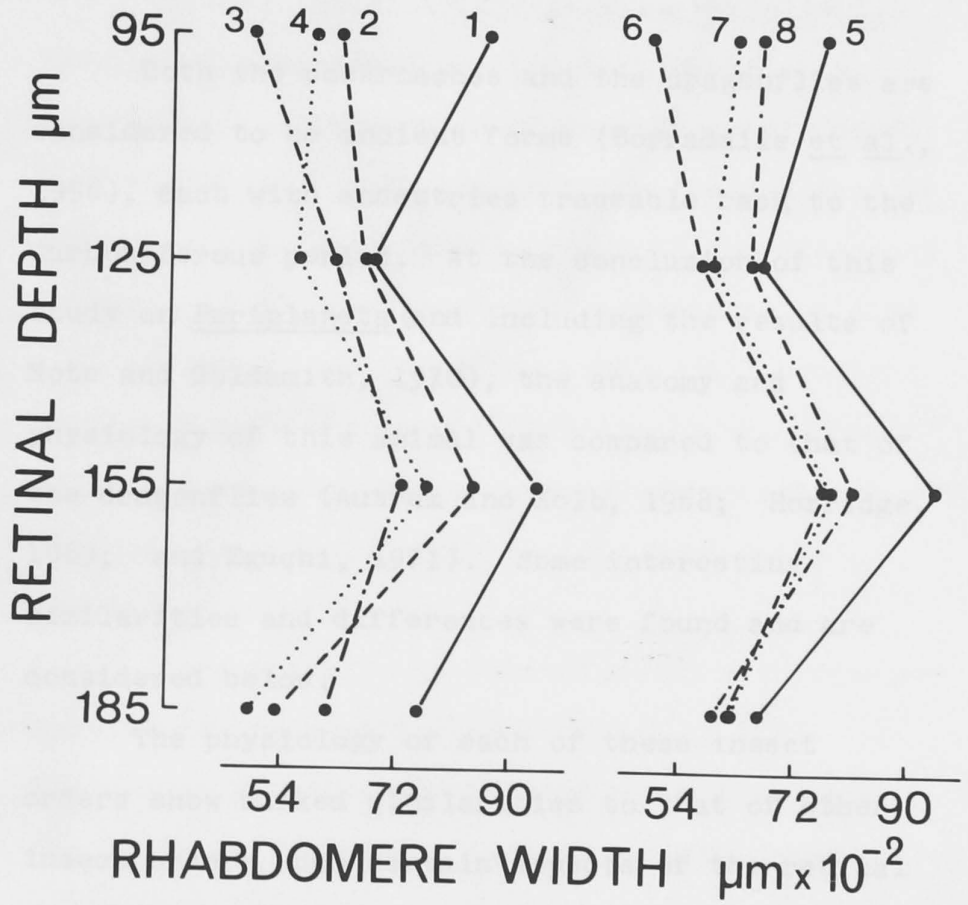
95
125
155
185
RETINAL DEPTH µm
3
4
2
1
6
7
8
5
54
72
90
54
72
90
RHABDOMERE WIDTH µm x 10⁻²

CHAPTER VI: DISCUSSION

Both the cockroaches and the dragonflies are considered to be ancient forms (Borradaile *et al.*, 1958), each with ancestries traceable back to the Carboniferous period. At the conclusion of this study on *Periplaneta* (and including the results of Mote and Goldsmith, 1970), the anatomy and physiology of this animal was compared to that of the dragonflies (Autrum and Kolb, 1968; Horridge, 1969; and Eguchi, 1971). Some interesting similarities and differences were found and are considered below.

The physiology of each of these insect orders show marked similarities to that of other insect orders when certain aspects of the retinal anatomy are very similar. In dragonflies, the rhabdom abuts up against the apex of the crystalline cone (Horridge, 1969; Eguchi, 1971) and the angle of acceptance for the dark-adapted state is 1.5° (specifically for *Libellula*; Horridge, 1969). When the rhabdom-cone configuration as found in dragonfly appears in other insects (eg. *Apis* drone (Perrelet, 1970) and *Apis* worker (Varela and Porter, 1969)), a small dark-adapted angle of acceptance is also found (2° for *Apis* drone (Shaw, 1969a) and

2.5° - 2.7° for Apis worker (Laughlin and Horridge, 1971)).

The anatomical arrangement in Periplaneta has the rhabdom engulfing and infiltrating the cone apex, and the angles of acceptance are about 6.8° (DA). In locust, the rhabdom forms a smaller but similar cup around the cone apex (Horridge and Barnard, 1965), with angles of acceptance of 6.6° (DA) (Tunstall and Horridge, 1967). All species mentioned here have a palisade when dark-adapted and hence results can be compared as no other obvious anatomical factor is influencing the results.

There seems to be a trend here, with angular sensitivity related to the intimacy of the anatomical relationship between rhabdom and cone. The study on Lethocerus (Walcott, 1971a, b) also bears this out. In the dark-adapted state the rhabdom moves distally to the cone and has an acceptance angle of 9.0°. Upon light-adaptation the rhabdom moves proximally and is separated from the cone by a crystalline thread, and for this configuration the acceptance angle about three-fold smaller. This trend may hopefully lead to the situation where some aspects of retinal physiology can be predicted with reasonable confidence from a knowledge of the anatomy. However, joint studies on the anatomy and physiology

of a number of other species must be done to ensure that this is indeed a trend and not merely coincidental.

The basic structure of the ommatidia of Periplaneta and dragonflies seem quite different, as the dragonflies have a tiered arrangement of retinula cells (with considerable variation between species (Horridge, 1969 cf. Eguchi, 1971). The depth profiles of retinula cells in Periplaneta, however, show that four cells are larger distally (1, 2, 3, 4) and three are larger proximally (5, 6, 7) with cell 8 always small and all extend over the depth of the retina. This basic arrangement is very similar to the tiered Aeschna ommatidium (Eguchi, 1971) which has four distal, three proximal and one rudimentary cell. Nowikoff (1932) considered Periplaneta's retina to be an intermediate form between tiered and columnar types and this may very well be the case.

A positive relation between the cockroach and dragonfly retinae is also suggested by studies on spectral cell types. Two types of cells (UV and green) have been identified in Periplaneta (CHAPTER V; Mote and Goldsmith, 1970) with cells 1, 5 and 7 being the UV group. In the dorsal region of Aeschna compound eye, UV and green receptors are also found and are assumed to occur in the

same ommatidium (Eguchi, 1971). On the basis of careful positioning of the electrode, Eguchi speculates that the cells of the distal tier are the green receptors with the proximal tier containing the UV cells. If the cockroach ommatidium has evolved from an original tiered type, similar to dragonfly, or vice-versa, then it is not surprising that at least two of the three UV cells (5 and 7) are from the group which are larger proximally, and three of the five green cells (2, 3 and 4) belong to the group which are larger distally. It should be noted, however, that there is a regional variation of spectral cell types across the retina of dragonflies (Autrum and Kolb, 1968; Horridge, 1969), and these bear little or no relation at all to Periplaneta.

I would now like to consider a purely speculative idea regarding the optical functioning of the rhabdom.

The possibility of retinal receptors possessing optical characteristics was first noted in 1843 by Brücke (cited by O'Brien, 1946) who related the high refractive index of vertebrate retinal receptors to the possibility of total internal reflection effects. Exner (1891) used

classical optics in a further development of Müller's theory of mosaic vision and also suggested that the rhabdom of the insect photoreceptor could act as a light trap through total internal reflection.

Diagrams based on ray optics have been the most common method of illustrating conceptural ideas of optical phenomena in photoreceptor cells (eg. Exner, 1891; O'Brien, 1946; Shaw, 1969b). However, all the laws of conventional ray optics, when applied to propagation inside photoreceptors, cease to hold good even as a first approximation, as the receptors are of the order of magnitude of a few wavelengths. Toraldo di Francia (1949) was the first to suggest that retinal receptors act as dielectric waveguides, as an alternative to the use of geometrical optics. Studies on vertebrate photoreceptors (Enoch, 1963) and insect rhabdoms (Varela and Wiitanen, 1970), have confirmed the existence of waveguide interference patterns (modes) in retinal photoreceptors, which compare favourably with the results of more theoretical treatments of waveguide effects in fibre optics (Kapany and Burke, 1961). These modal patterns are the observed light energy emergingfrom the cut ends of the receptors, and represent the field pattern of the propagated energy (Enoch, 1963). The factors which influence these patterns are the configuration and diameter of the rhabdom; the

refractive index of the rhabdom and the surrounding medium; and the wavelength and angle of incidence of the incident light (Enoch, 1963).

There is little evidence to suggest how such guided modes are supported in a biological structure such as the rhabdom, which is a relatively complex and highly ordered structure composed of triple-layered (protein outer and inner layer with a lipid bilayer in the centre) photoreceptor membranes (Worthington, 1971). If the rhabdom is considered, conceptually at least, as being composed of stratified dielectric layers, then a speculative idea can be advanced that the propagated modes may be supported either in or on the lipid component of the membrane.

The idea of modes supported <u>in</u> the lipid bilayer can be considered since a theoretical treatment of the subject (Kane and Osterberg, 1964) has shown that propagating modes can be supported by stratified dielectrics. However, there is a discrete set of dielectric thicknesses which can support the modes, and these are much thicker than the lipid bilayer.

A more likely explanation is that the light flux is flowing <u>on</u> the lipid bilayer as surface waves. This phenomenon has been treated both theoretically and experimentally (Osterberg and Smith, 1964a, b), and is, of course, independent

of the thickness of the dielectric.

In order to transfer light from the crystalline cone to the surface of the lipid component, the incident light would have to be at or very near to the critical angle (Ic). The extensive infiltration of the cone by rhabdom in Periplaneta create innumerable chances for the incident light flux to meet this requirement. For the cases where the rhabdom abuts up against the cone apex (eg. dragonflies and bees), only a small portion of the incident flux from the cone would be able to achieve the Ic conditions. This in turn would originate from a narrow segment of the total flux at the cornea. Thus, a narrower angle of acceptance would be predicted from this type of arrangement than from Periplaneta, and this is exactly what has been shown physiologically. This may be an invalid confirmation of a prediction, as Shaw (1968a) demonstrated spectral independence of angles of acceptance, and guiding surfaces are known to be highly selective with respect to the wavelength that it will transmit at a given angle of incidence (Osterberg and Smith, 1964b).

If surface-guided waves on the lipid component of the membrane are the way in which optical transmission is supported, the modes would still be visible from the (cut) ends of receptors as surface waves re-radiate (endfire) at the end of the surface.

There is some important evidence, however, which appears to be inconsistent with the concept of surface waves as the mechanism by which optical transmission is supported in the rhabdom. It is known that when a lens (eg. dioptric apparatus) produces an image of a point source, a three-dimensional diffraction pattern results which is related to the lens aperture (McCutchen, 1964). Kuiper (1966) reports that intensity measurements made both along and across the optical axis of an ommatidium in Calliphora also show a three-dimensional distribution. Probably a similar thing occurs in Periplaneta, and it may be that the variation in rhabdomere widths with retinal depth (Fig. 52) is the anatomical adaptation to accommodate such effects. However, Osterberg and Smith (1964b) have shown that surface-guided waves can carry images, and hence intensity variations.

REFERENCES

Adrian, R.H. 1956. The effect of internal and external potassium concentration on the membrane potential of frog muscle. J. Physiol. 133: 631-658.

Alder, H.L. and E.B. Roessler. 1964. Introduction to probability and statistics. 3rd edn. W.H. Freeman, San Francisco. pp 82-91.

Autrum, H. and G. Kolb. 1968. Spektrale Empfindlichkeit einzelner Sehzellen der Aeschniden. Z. vergl. Physiol. 60: 450-477.

Autrum, H. and V. von Zwehl. 1962a. Die Sehzellen der Insekten als Analysatoren fur polarisiertes Licht. Z. vergl. Physiol. 46: 1-7.

Autrum, H. and V. von Zwehl. 1962b. Zur spektralen Empfindlichkeit einzelner Sehzellen der Drohne (Apis mellifica ♂). Z. vergl. Physiol. 46: 8-12.

Autrum, H. and V. von Zwehl. 1964. Die spektrale Empfindlichkeit einzelner Sehzellen des Bienenauges. Z. vergl. Physiol. 48: 357-384.

Barrós Pita, J.C. and H. Maldonado. 1970. A fovea in the praying mantis eye. II. Some morphological characteristics. Z. vergl. Physiol. 67: 79-92.

Baumann, F. 1968. Slow and spike potentials recorded from retinula cells of the honeybee drone in response to light. J. gen. Physiol. 52: 855-875.

Bäumgartner, H. 1928. Der Formensinn und die Sehschärfe der Bienen. Z. vergl. Physiol. 7: 56-143.

Baylor, D.A. and M.G.F. Fuortes. 1970. Electrical responses of single cones in the retina of the turtle. J. Physiol. 207: 77-92.

Benolken, R.M. 1961. Reversal of photoreceptor polarity recorded during the graded receptor potential response to light in the eye of Limulus. Biophys. J. 1: 551-564.

Berkowitz, L.R., O. Fiorello, L. Kruger and D.S. Maxwell. 1968. Selective staining of nervous tissue for light microscopy following preparation for electron microscopy. J. Histochem. Cytochem. 16: 808-814.

Bernhard, C.G., G. Gemne and J. Sällström. 1970. Comparative ultrastructure of corneal surface topography in insects with aspects on phylogenesis and function. Z. vergl. Physiol. 67: 1-25.

Blest, A.D. 1961. Some modifications of Holme's silver nitrate method for insect central nervous system. Q. Jl. microsc. Sci. 102: 413-417.

Borradaile, L.A., F.A. Potts, L.E.S. Eastham and J.T. Saunders. 1958. The Invertebrata. 3rd edn. Cambridge Univ. Press, Cambridge. p. 472.

Bownds, D. and A.C. Gaide-Huguenin. 1970. Rhodopsin content of frog photoreceptor outer segments. Nature 225: 870-872.

Brown, E.B. 1965. Modern Optics. Reinhold, New York. 645 pp.

Brown, H.M., S. Hagiwara, H. Koike and R.M. Meech. 1970. Membrane properties of a barnacle photoreceptor examined by the voltage clamp technique. J. Physiol. 208: 385-413.

Buddenbrock, W. von and H. Friedrich. 1933. Neue Beobachtungen über die Kompensatorischen Augenbewegungen und den Farbensinn der Taschkrabben Carcinus maenes. Z. vergl. Physiol. 19: 747-761.

Bullock, T.H. and G.A. Horridge. 1965. Structure and Function in the Nervous System of Invertebrates. W.H. Freeman, San Francisco. pp. 1064-1097.

Burkhardt, D. 1962. Spectral sensitivity and other response characteristics of single visual cells. Symp. Soc. exp. Biol. 16: 86-109.

Burkhardt, D. and H. Autrum. 1960. Die Belichtungspotentiale einzelner Sehzellen von Calliphora erythrocephala Meig. Z. Naturf. 15 B: 612-616.

Burkhardt, D. and L. Wendler. 1960. Ein direkter Beweis für die fähigkeit einzelner Sehzellen des Insektauges, die Schwirgungsrichtung polarisierten Lichtes zu analysieren. Z. vergl. Physiol. 43: 687-692.

Burtt, E.T. and W.T. Catton. 1954. Visual perception of movement in the locust. J. Physiol. 125: 566-580.

Burtt, E.T. and W.T. Catton. 1956. Electrical responses to visual stimulation in the optic lobes of the locust and certain other insects. J. Physiol. 133: 68-88.

Burtt, E.T. and W.T. Catton. 1959. Transmission of visual responses in the nervous system of the locust. J. Physiol. 146: 492-515.

Burtt, E.T. and W.T. Catton. 1962. Resolving power of the compound eye. Symp. Soc. exp. Biol. 16: 72-85.

Burtt, E.T. and W.T. Catton. 1962. A diffraction theory of insect vision. I. An experimental investigation of visual acuity and image formation in the compound eyes of three species of insects. Proc. Roy. Soc. B 157: 53-82.

Bush, B.M.H. and A. Roberts. 1968. Resistance reflexes from crab muscle receptors without impulses. Nature 218: 1171-1173.

Butler, L., R. Roppel and J. Zeigler. 1970. Post emergence maturation of the eye of the adult black carpet beetle, Attagenus megatoma (Fab.): An electron microscope study. J. Morph. 130: 103-127.

Butler, R. 1971a. The identification and mapping of spectral cell types in the retina of Periplaneta americana. Z. vergl. Physiol. 72: 67-80.

Butler, R. 1971b. Very rapid selective silver (Golgi) impregnations and embedding of invertebrate nervous tissue. Brain Research 33: 540-544.

Davenport, H.A. 1960. Histological and Histochemical Technics. W.B. Saunders Co., Philadelphia. pp. 166-167.

Day, M.F. 1941. Pigment migration in the eyes of the moth, Ephestia kuehniella Zeller. Biol. Bull. mar. biol. Lab. (Woods Hole) 80: 275-291.

Del Portillo, J. 1936. Beziehungen zurischen den Öffnungswinkel der Ommatidien, Krümmung und Gestalt der Insektenauge und ihrer funktionellen Aufgabe. Z. vergl. Physiol. 23: 100. Cited from: Wiitanen, W. and F.G. Varela. 1971. Analysis of the organization and overlap of the visual fields in the compound eye of the honeybee (Apis mellifera). J. gen. Physiol. 57: 303-325.

Denton, E.J. 1959. The contributions of the oriented photosensitive and other molecules to the absorption of whole retina. Proc. Roy. Soc. B 150: 78-94.

Dewey, M.M., P.K. Davis, J.K. Blasie and L. Barr. 1969. Localization of rhodopsin antibody in the retina of the frog. J. Molec. Biol. 39: 395-405.

Dietrich, W. 1909. Die Facettenaugen der Dipteren. Z. wiss. Zool. 92: 465-539.

Døving, K.B. and W.H. Miller. 1969. Function of insect compound eyes containing crystalline tracts. J. gen. Physiol. 54: 250-267.

Edwards, A.L. 1967. Statistical Methods. 2nd edn. Holt, Rinehart and Winston, Inc. New York. 462 pp.

Eguchi, E. 1971. Fine structure and spectral sensitivities of retinular cells in the dorsal sector of compound eyes in the dragonfly Aeschna. Z. vergl. Physiol. 71: 201-218.

Enoch, J.M. 1963. Optical properties of the retinal receptors. J. opt. Soc. Am. 53: 71-85.

Exner, S. 1891. Die Physiologie der facettirten Augen von Krebsen und Insecten. Leipzig. 206 pp.

Fahrenbach, W.H. 1969. The morphology of the eyes of Limulus. II. Ommatidia of the compound eye. Z. Zellforsch. 93: 451-483.

Fernández-Morán, H. 1956. Fine structure of the insect retinula as revealed by electron microscopy. Nature 177: 742-743.

Fernández-Morán, H. 1958. Fine structure of the light receptors in the compound eyes of insects. Expl Cell Res. Suppl. 5: 586-644.

Fuortes, M.G.F. 1959. Initiation of impulses in visual cells of Limulus. J. Physiol. 148: 14-28.

Fuortes, M.G.F. 1963. Visual responses in the eye of the dragonfly. Science 142: 69-70.

Gemperlein, R. 1969. Grundlagen zur genauen Beschreibung von Komplexaugen. Z. vergl. Physiol. 65: 428-444.

Gier, H.T. 1947. Growth rate in the cockroach Periplaneta americana (Linn). Ann. ent. Soc. Am. 40: 303-317.

Goldsmith, T.H. 1964. The visual system of insects. In: The Physiology of Insecta, ed. by M. Rockstein. Academic Press, New York. pp. 397-462.

Goldsmith, T.H. and D.E. Philpott. 1957. The microstructure of the compound eye of insects. J. biophys. biochem. Cytol. 3: 429-440.

Gordon, G.B., L.R. Miller and K.G. Bensch. 1965. Studies on the intracellular digestive process in mammalian tissue culture cells. J. Cell Biol. 25: 41-55.

Götz, K.G. 1964. Optomotorische Untersuchungen des visuellen Systems einiger Augenmutanten der Fruchtfliege Drosophila. Kybernetik 2: 77-92.

Götz, K.G. 1965. Die optischen Übertragungseigenschaften der Komplexaugen von Drosophila. Kybernetik 2: 215-221.

Grenacher, H. 1879. Untersuchungen über die Sehorgane der Arthropoden, insbesondere der Spinnen, Insecten und Crustaceen. Vandenhoek and Ruprecht. Göttingen. 188 pp.

Gribakin, F.G. 1969. Cellular basis of colour vision in the honey bee. Nature (Lond.) 223: 639-641.

Guthrie, D.M. and A.R. Tindall. 1968. The Biology of the Cockroach. William Clowes and Sons, London. 408 pp.

Hagins, W.A. and W.H. Jennings. 1959. Radiationless migration of electronic excitation in retinal rods. Discuss. Faraday Soc. 27: 180-190.

Hagins, W.A. and R.E. McGaughy. 1968a. Membrane origin of the fast photovoltage of squid retina. Science 159: 213-215.

Hagins, W.A. and R.E. McGaughy. 1968b. Fast photovoltages, receptor currents and electrical cable constants in squid photoreceptors. Biophys. J. 8: A158.

Hagins, W.A., H.V. Zonana and R.G. Adams. 1962. Local membrane current in the outer segments of squid photoreceptors. Nature 194: 844-846.

Harper, E., S. Seifter and B. Scharrer. 1967. Electron microscopic and biochemical characteristics of collagen in blattarian insects. J. Cell Biol. 33: 385-393.

Hecht, S. and E. Wolf. 1929. The visual acuity of the honeybee. J. gen. Physiol. 12: 727-760.

Hesse, R. 1901. Untersuchungen über die Organe der Lichtempfindung bei niederen Thieren. VII. Von den Arthropoden-Augen. Z. wiss. Zool. 70: 347-473.

Horridge, G.A. 1966. The retina of the locust. In: C.G. Bernhard (Ed.) The Functional Organization of the Compound Eye. Pergamon, Oxford. pp. 513-541.

Horridge, G.A. 1968. Interneurons. W.H. Freeman, San Francisco. pp. 145-194.

Horridge, G.A. 1969. Unit studies on the retina of dragonflies. Z. vergl. Physiol. 62: 1-37.

Horridge, G.A. 1971. Further observations on the clear zone eye of Ephestia. Submitted to Proc. Roy. Soc. B.

Horridge, G.A. and P.B.T. Barnard. 1965. Movement of palisade in locust retinula cells when illuminated. Quart. J. micr. Sci. 106: 131-135.

Horridge, G.A. and I.A. Meinertzhagen. 1970a. The accuracy of the patterns of connexions of the first- and second-order neurons of the visual system of Calliphora. Proc. Roy. Soc. Lond. B 175: 69-82.

Horridge, G.A. and I.A. Meinertzhagen. 1970b. The exact neural projection of the visual fields upon the first and second ganglia of the insect eye. Z. vergl. Physiol. 66: 369-378.

Horridge, G.A., B. Walcott and A.C. Ioannides. 1970. The tiered retina of Dytiscus: a new type of compound eye. Proc. Roy. Soc. Lond. B. 175: 83-94.

Ioannides, A.C. 1971. Personal communication.

Ioannides, A.C. and B. Walcott. 1971. Graded illumination potentials from retinula cell axons in the bug Lethocerus. Z. vergl. Physiol. 71: 315-325.

Jörschke, H. 1914. Die Facettenaugen der Orthoptern und Termiten. Zeitschrift f. wissensch. Zoologie 111: 153-280.

Kane, J. and H. Osterberg. 1964. Optical characteristics of planar guided modes. J. opt. Soc. Am. 54: 347-352.

Kapany, N.S. and J.J. Burke. 1961. Fiber optics. IX. Wave-guide effects. J. opt. Soc. Am. 51: 1067-1078.

Keidel, W.D., V.O. Keidel and M.E. Wigand. 1961. Adaptation: loss or gain of sensory information? In: W.A. Rosenblith (Ed.), Sensory Communication. M.I.T. Press, Cambridge, Mass. pp. 319-338.

Kennedy, D. 1964. The photoreceptor porcess in lower animals. In: A.C. Giese (Ed.), Photophysiology. Volume II. Academic Press, New York. pp. 79-123.

Kirschfeld, K. 1969. Absorption properties of photopigments in single rods, cones and rhabdomeres. Proc. Internat. School of Physcis "Enrico Fermi" 43: 116-136.

Kirschfeld, K. and N. Franceschini. 1969. Ein Mechanismus zur Steuerung des Lichtflusses in den Rhabdomeren des Komplexauges von Musca. Kybernetik 6: 13-22.

Kostyuk, P.G. 1965. Intrinsic potentials of glass microelectrodes. Fed. Proc. (Transl. Suppl.) 24: T329-T332.

Kuiper, J.W. 1966. On the image formation in a single ommatidium of the compound eye in Diptera. In: C.G. Bernhard (Ed.), The Functional Organization of the Compound Eye. Pergamon, Oxford. pp. 35-50.

Langer, H. 1967. Über die Pigmentgranula im Facettenauge von Calliphora erythrocephala. Z. vergl. Physiol. 55: 354-377.

Langer, H. and C. Hoffmann. 1966. Elektro- und stoffwechselphysiologische Untersuchungen über den Einfluss von Ommochromen und Pteridinen auf die Funktion des Facettenauges von Calliphora erythrocephala. J. Insect Physiol. 12: 357-387.

Langer, H. and B. Thorell. 1966. Microspectrophotometry of single rhabdomeres in the insect eye. Exp. Cell Res. 41: 673-677.

Lasansky, A. 1967. Cell junctions in ommatidia of Limulus. J. Cell Biol. 33: 365-384.

Lasansky, A. and M.G.F. Fuortes. 1969. The site of origin of electrical responses in the visual cells of the leech, Hirudo medicinalis. J. Cell Biol. 42: 241-252.

Laughlin, S.B. and G.A. Horridge. 1971. Angular sensitivity of the retinula cells of dark-adapted worker bee. Z. vergl. Physiol. 74: 329-339.

Levin, L. and H. Maldonado. 1970. A fovea in the praying mantis eye. III. The centring of the prey. Z. vergl. Physiol. 67: 93-101.

Locke, M. 1964. The structure and formation of the integument in insects. In: M. Rockstein (Ed.) The Physiology of Insecta. Academic Press, New York. pp. 379-470.

Luft, J.H. 1959. The use of acrolein as a fixative for light and electron microscopy. Anat. Rec. 133: 305.

Maldonado, H. and J.C. Barrós Pita. 1970. A fovea in the praying mantis eye. I. Estimation of the catching distance. Z. vergl. Physiol. 67: 58-78.

Maldonado, H., M. Benko and M. Isern. 1970. Study of the role of the binocular vision in mantids to estimate long distances, using the deimatic reaction as experimental situation. Z. vergl. Physiol. 68: 72-83.

Maldonado, H. and L. Levin. 1967. Distance estimation and the monocular cleaning reflex in praying mantis. Z. vergl. Physiol. 56: 258-267.

Maldonado, H., L. Levin and J.C. Barrós Pita. 1967. Hit distance and the predatory strike of the praying mantis. Z. vergl. Physiol. 56: 237-257.

Martin, A.R. and G. Pilar. 1964. Quantal components of the synaptic potential in the ciliary ganglion of the chick. J. Physiol. 175: 1-16.

McCann, G.D. and G.F. MacGinitie. 1965. Optomotor response studies of insect vision. Proc. Roy. Soc. B 163: 369-401.

McCutchen, C.W. 1964. Generalized aperature and the three-dimensional diffraction image. J. opt. Soc. Am. 54: 240-244.

Meinertzhagen, I.A. 1971. The First and Second Neural Projections of the Insect Eye. Ph.D. thesis. University of St. Andrews.

Menzer, G. and K. Stockhammer. 1951. Die polarisationsoptik der Facettenaugen von Insekten. Naturwissenschaften 38: 190-191.

Miall, L.C. and A. Denny. 1886. The Structure and Life-History of the Cockroach (Periplaneta orientalis). Rovell Reeve, London. 224 pp.

Millecchia, R. and A. Mauro. 1969a. The ventral photoreceptor cells of Limulus. II. The basic photoresponse. J. gen. Physiol. 54: 310-330.

Millecchia, R. and A. Mauro. 1969b. The ventral photoreceptor cells of Limulus. III. A voltage-clamp study. J. gen. Physiol. 54: 331-351.

Miller, W.H. 1957. Morphology of the ommatidia of the compound eye of Limulus. J. biophys. biochem. Cytol. 3: 421-428.

Millonig, G. 1961. Advantages of a phosphate buffer for OsO_4 solutions in fixation. Proc. Electron Microscope Soc. Amer. J. appl. Phys. 32: 1637.

Moon, P. 1948. A table of Planckian radiation. J. opt. Soc. Am. 38: 291-294.

Mote, M.I. and T.H. Goldsmith. 1970. Spectral sensitivities of color receptors in the compound eye of the cockroach Periplaneta. J. exp. Zool. 173: 137-146.

Mote, M.I. and T.H. Goldsmith. 1971. Compound eyes: localization of two color receptors in the same ommatidium. Science 171: 1254-1255.

Naka, K.-I. 1961. Recording of retinal action potentials from single cells in the insect compound eye. J. gen. Physiol. 44: 571-584.

Naka, K.-I. and E. Eguchi. 1962. Spike potentials recorded from the insect photoreceptor. J. gen. Physiol. 45: 663-680.

Naka, K.-I. and K. Kishida. 1966. Retinal action potentials during dark and light adaptation. In: C.G. Bernhard (Ed.), The Functional Organization of the Compound Eye. Pergamon, Oxford. pp. 251-266.

Nowikoff, M. 1931. Untersuchungen über die Komplexaugen von Lepidopteren nebst einigen Bemerkungen über die Rhabdome der Arthropoden im allgemeinen. Z. wiss. Zool. 138: 1-67.

Nowikoff, M. 1932. Über den Bau der Komplexaugen von Periplaneta (Stylopyga) orientalis L. Jena. Z. Naturw. 67: 58-69.

O'Brien, B. 1946. A theory of the Stiles and Crawford effect. J. opt. Soc. Am. 36: 506-509.

Osterberg, H. and L.W. Smith. 1964a. Transmission of optical energy along surfaces: Part I, homogeneous media. J. opt. Soc. Am. 54: 1073-1078.

Osterberg, H. and L.W. Smith. 1964b. Transmission of optical energy along surfaces: Part II, inhomogeneous media. J. opt. Soc. Am. 54: 1078-1084.

Pantin, C.F.A. 1946. Notes on Microscopical Technique for Zoologists. Cambridge University Press, London. 76 pp.

Patat, U. 1965. Über das Pterinmuster der Facettenaugen von Calliphora erythrocephala. Ein Beitrag zur Funktion und Stabilität der Pterine. Z. vergl. Physiol. 51: 103-134.

Perrelet, A. 1970. The fine structure of the retina of the honey bee drone. An electron microscopical study. Z. Zellforsch. 108: 530-562.

Perrelet, A. and F. Baumann. 1969. Evidence for extracellular space in the rhabdom of the honey bee drone eye. J. Cell Biol. 40: 825-830.

Reynolds, E.S. 1963. The use of lead citrate at high pH as electron opaque stain in electron microscopy. J. Cell Biol. 17: 208-212.

Ripley, S.H., B.M.H. Bush and A. Roberts. 1968. Crab muscle receptor which responds without impulses. Nature 218: 1170-1171.

Rogers, G.L. 1962. A diffraction theory of insect vision. II. Theory and experiments with a simple model eye. Proc. Roy. Soc. B 157: 83-98.

Ruck, P. 1964. On photoreceptor mechanisms of retinula cells. Biol. Bull. 123: 618-634.

Rushton, W.A.H. 1959. A theoretical treatment of Fuortes' observations upon eccentric cell activity in Limulus. J. Physiol. 148: 29-38.

Rushton, W.A.H. 1963. Increment threshold and dark adaptation. J. opt. Soc. Am. 53: 104-109.

Rushton, W.A.H. and R.D. Cohen. 1954. Visual purple level and the course of dark adaptation. Nature 173: 301-302.

Sabatini, D.D., K.G. Bensch and R.J. Barrnett. 1963. Cytochemistry and electron microscopy. The preservation of cellular ultrastructure and enzymatic activity by aldehyde fixation. J. Cell Biol. 17: 19-58.

Sanchez, D.S. 1920. Sobre la existencia de un aparato tactil en los ojos compuestos de los abejas. Trab. Lab. Invest. biol. Univ. Madrid 18: 207-244.

Scholes, J.H. 1964. Discrete subthreshold potentials from the dimly lit insect eye. Nature 202: 572-573.

Scholes, J.H. 1965a. A Discontinuous Excitation Process in Visual Receptor Cells. Ph.D. thesis. University of St. Andrews.

Scholes, J.H. 1965b. Discontinuity of the excitation process in locust visual cells. Cold Spring Harb. Symp. quant. Biol. 30: 517-527.

Scholes, J. 1969. The electrical responses of the retinal receptors and the lamina in the visual system of the fly Musca. Kybernetik 6: 149-162.

Scholes, J. and W. Reichardt. 1969. The quantal content of optomotor stimuli and the electrical responses of receptors in the compound eye of the fly Musca. Kybernetik 6: 74-80.

Seitz, G. 1968. Der Strahlengang im Appositionsauge von Calliphora erythrocephala (Meig.). Z. vergl. Physiol. 59: 205-231.

Seitz, G. 1969. Untersuchungen am dioptrischen Apparat des Leuchtkäferauges. Z. vergl. Physiol. 62: 61-74.

Shaw, S.R. 1966. Polarized light responses from crab retinula cells. Nature 211: 92-93.

Shaw, S.R. 1967. Simultaneous recording from two cells in the locust retina. Z. vergl. Physiol. 55: 183-194.

Shaw, S.R. 1968a. Polarized-light Detection and Receptor Interaction in the Arthropod Eye. Ph.D. thesis. University of St. Andrews.

Shaw, S.R. 1968b. Organization of the locust retina. Symp. Zool. Soc. Lond. No. 23: 135-163.

Shaw, S.R. 1969a. Interreceptor coupling in ommatidia of drone honeybee and locust compound eyes. Vision Res. 9: 999-1029.

Shaw, S.R. 1969b. Sense-cell structure and interspecies comparisons of polarized-light absorption in arthropod compound eyes. Vision Res. 9: 1031-1040.

Shearer, A.C.I. 1969. Morphology of the isolated pigment particle of the eye by scanning electron microscopy. Expl Eye Res. 8: 122-126.

Smith, D.S. 1968. Insect Cells. Their Structure and Function. Oliver and Boyd, Edinburgh. 372 pp.

Snodgrass, R.E. 1935. Principles of Insect Morphology. McGraw-Hill, New York. 667 pp.

Stratten, W.P. and T.E. Ogden. 1971. Spectral sensitivity of the barnacle, Balanus amphitrite. J. gen. Physiol. 57: 435-447.

Tasaki, K., Y. Tsukahara, S. Ito, M.J. Wayner and W.Y. Yu. 1968. A simple, direct and rapid method for filling microelectrodes. Physiology and Behavior 3: 1009-1010.

Thomas, I. and H. Autrum. 1965. Die Empfindlichkeit der Dunkel - und Hell - Adaptierten Biene (Apis mellifica) für Spektrale Farben: Zum Purkinje - Phänomen der Insekten. Z. vergl. Physiol. 51: 204-218.

Tomita, T. 1969. Single and coaxial microelectrodes in the study of the retina. In: M. Lavellée, O.F. Schanne and N.C. Hébert (Eds), Glass Microelectrodes. John Wiley and Sons, New York. pp. 124-153.

Toraldo di Francia, G. 1949. Retina cones as dielectric antennas. J. opt. Soc. Am. 39: 324.

Trujillo-Cenóz, O. and J. Melamed. 1971. Spatial distribution of photoreceptor cells in the ommatidia of Periplaneta americana. J. Ultrastruct. Res. 34: 397-400.

Trump, B.F., E.A. Smuckler and E.P. Benditt. 1961. A method for staining epoxy sections for light microscopy. J. Ultrastruct. Res. 5: 343-348.

Tunstall, J. and G.A. Horridge. 1967. Electrophysiological investigation of the optics of the locust retina. Z. vergl. Physiol. 55: 167-182.

Varela, F.G. and K.R. Porter. 1969. Fine structure of the visual system of the honeybee (Apis mellifera). I. The retina. J. Ultrastruct. Res. 29: 236-259.

Varela, F.G. and W. Wiitanen. 1970. The optics of the compound eye of the honeybee (Apis mellifera). J. gen. Physiol. 55: 336-358.

Vowles, D.M. 1966. The receptive fields of cells in the retina of the housefly (Musca domestica). Proc. Roy. Soc. B 164: 552-576.

Walcott, B. 1969. Movement of retinula cells in insect eyes on light-adaptation. Nature 223: 971-972.

Walcott, B. 1971a. Cell movement on light-adaptation in the retina of Lethocerus (Belostomatidae, Hemiptera). Z. vergl. Physiol. 74: 1-16.

Walcott, B. 1971b. Unit studies on receptor movement in the retina of Lethocerus (Belostomatidae, Hemiptera). Z. vergl. Physiol. 74: 17-25.

Wald, G. 1954. On the mechanism of the visual threshold and visual adaptation. Science 119: 887-892.

Wald, G. 1968. Single and multiple visual systems in Arthropods. J. gen. Physiol. 51: 125-156.

Wald, G., P.K. Brown and I.R. Gibbons. 1963. The problem of visual excitation. J. opt. Soc. Am. 53: 20-35.

Walther, J.B. 1958. Changes induced in spectral sensitivity and form of retinal action potential of the cockroach eye by selective adaptation. J. Insect Physiol. 2: 142-151.

Walther, J.B. and E. Dodt. 1957. Elektrophysiologische Untersuchungen über die Ultraviolettempfindlichkeit von Insektenaugen. Experientia (Basel) 13: 333-334.

Walther, J.B. and E. Dodt. 1959. Die Spektralsensitivität von Insekten-Komplexaugen im Ultraviolett bis 290 mμ. Z. Naturforsch. 14 b: 273-278.

Washizu, Y. 1964. Electrical activity of single retinula cells in the compound eye of the blowfly, Calliphora erythrocephala Meig. Comp. Biochem. Physiol. 12: 369-387.

Washizu, Y., D. Burkhardt and P. Streck. 1964. Visual field of single retinula cells and interommatidial inclination in the compound eye of the blowfly Calliphora erythrocephala. Z. vergl. Physiol. 48: 413-428.

Wiitanen, W. and F.G. Varela. 1971. Analysis of the organization and overlap of the visual fields in the compound eye of the honeybee (Apis mellifera). J. gen. Physiol. 57: 303-325.

Wolken, J.J. and P.D. Gupta. 1961. Photoreceptor structures. The retinal cells of the cockroach eye. IV. Periplaneta americana and Blaberus giganteus. J. biophys. biochem. Cytol. 9: 720-724.

Worthington, C.R. 1971. Structure of photoreceptor membranes. Fed. Proc. 30: 57-63.

Yagi, N. and N. Koyama. 1963. The Compound Eye of Lepidoptera. Approach from Organic Evolution. Shinkyo-Press, Tokyo. 319 pp.

Yamasaki, T. and T. Narahashi. 1959. The effects of potassium and sodium ions on the resting and action potentials of the cockraoch giant axon. J. Insect Physiol. 3: 146-158.